

**DEVELOPMENT OF A SCAFFOLD INCORPORATING
ZINC-OXIDE NANO-PARTICLES FOR CARTILAGE TISSUE
ENGINEERING UNDER PHYSIOLOGICAL CONDITIONS**

ERAJ HUMAYUN MIRZA

**FACULTY OF ENGINEERING
UNIVERSITY OF MALAYA
KUALA LUMPUR**

2016

DEVELOPMENT OF A SCAFFOLD INCORPORATING
ZINC-OXIDE NANO-PARTICLES FOR CARTILAGE
TISSUE ENGINEERING UNDER PHYSIOLOGICAL
CONDITIONS

ERAJ HUMAYUN MIRZA

THESIS SUBMITTED IN FULFILMENT OF THE
REQUIREMENTS FOR THE DEGREE OF DOCTOR OF
PHILOSOPHY

FACULTY OF ENGINEERING
UNIVERSITY OF MALAYA
KUALA LUMPUR

2016

UNIVERSITY OF MALAYA
ORIGINAL LITERARY WORK DECLARATION

Name of Candidate: Eraj Humayun Mirza

Matric No: KHA110058

Name of Degree: Doctor of Philosophy

Title of Thesis: The Development of a Scaffold incorporating Zinc-Oxide Nano-particles for Cartilage Tissue Engineering under Physiological Conditions

Field of Study: Biomaterials and Tissue Engineering

I do solemnly and sincerely declare that:

- (1) I am the sole author/writer of this Work;
- (2) This Work is original;
- (3) Any use of any work in which copyright exists was done by way of fair dealing and for permitted purposes and any excerpt or extract from, or reference to or reproduction of any copyright work has been disclosed expressly and sufficiently and the title of the Work and its authorship have been acknowledged in this Work;
- (4) I do not have any actual knowledge nor do I ought reasonably to know that the making of this work constitutes an infringement of any copyright work;
- (5) I hereby assign all and every rights in the copyright to this Work to the University of Malaya ("UM"), who henceforth shall be owner of the copyright in this Work and that any reproduction or use in any form or by any means whatsoever is prohibited without the written consent of UM having been first had and obtained;
- (6) I am fully aware that if in the course of making this Work I have infringed any copyright whether intentionally or otherwise, I may be subject to legal action or any other action as may be determined by UM.

Candidate's Signature

Date: 22nd August 2016

Subscribed and solemnly declared before,

Witness's Signature

Date: 22nd August 2016

Name:

Designation:

Abstract

Cartilage tissue is among the most complex of all in the human body. Degeneration of cartilage, lack of repair and various traumatic and pathological conditions among individuals increase joint pain and disability. Researchers have been trying to repair cartilage damage for decades, but have failed to achieve an optimal repair strategy. Cartilage tissue is adapted to low oxygen environments and this condition appears to be a key factor in the growth, regulation, and survival of chondrocytes; which are the only cells present in cartilage tissue. The present thesis defines the fabrication and characterisation of an antibacterial biomaterial for cartilage tissue repair. Furthermore, this thesis promotes the use of Zinc Oxide (ZnO) nanoparticles (NP) for better growth of cartilage cells and survival of cartilage tissue as a whole.

Composite scaffolds and thin films of polyoctanediol citrate (POC) polyester elastomer, with varying concentrations (1wt%, 3wt% and 5wt%) of ZnO were fabricated by a solvent-casting/particulate-leaching and mould casting technique respectively. It was observed that material properties can be successfully controlled by simple variation of NP concentration within the composite. The ion release kinetics from ZnO-POC scaffolds are strongly dependent on NP concentration and degradation of pure POC matrix. All the composite scaffolds showed strong antibacterial characteristics. However, cell culture studies demonstrated that 1% ZnO incorporation in POC polymer is the optimal concentration for chondrocyte cells.

Moreover, the effect of 1% ZnONP on chondrocyte proliferation and matrix synthesis cultured under normoxia (21% O₂) and hypoxia (5% O₂) demonstrated upregulation of chondrocyte proliferation and sulphated glycosaminoglycan (S-GAG) in hypoxic culture. A synergistic effect of oxygen concentration and 1% ZnONP in up-regulation of anabolic gene expression (Type II collagen (*COL2A1*) and aggrecan (*ACAN*)), and a down regulation of catabolic (*MMP-13*) gene expression was observed. Furthermore,

production of transcription factor hypoxia-inducible factor 1A (*HIF-1A*) in response to hypoxic condition to regulate chondrocyte survival under hypoxia was not affected by the presence of 1% ZnONP. Lastly this thesis discusses the physiological adaptations of cartilage tissue in a dynamic mechanical loading and hypoxic condition to yield benefits of combined bio-factors for cartilage tissue engineering applications. The results indicate that the combination of dynamic loading is compatible with the nanoparticle addition. Furthermore, dynamic loading suppresses *MMP-13*, and increase the expression of *COL2A1* and *ACAN* with an increase in cell viability, and promotion of rounded cell morphology (a phenotypic marker).

It was concluded that POC-ZnONP scaffolds are of major importance in the development of multifunctional scaffolds based on biodegradable polyesters for cartilage tissue engineering and presence of 1% ZnONP appears to preserve homeostasis of cartilage in its hypoxic environment. While 1% ZnONP should be considered for beneficial incorporation into 3D hypoxic culture systems in the presence of mechanical stimulation. Further studies must focus on determining the use of 1% ZnONP in different polymers for use in various tissue engineering applications.

Abstrak

Tisu rawan adalah antara tisu yang paling kompleks di dalam badan manusia. Kemerosotan rawan, kurang pembaikan dan pelbagai trauma dan keadaan patologi di kalangan individu meningkatkan kesakitan pada sendi dan kecacatan. Penyelidik telah berusaha untuk memperbaiki kerosakan rawan selama bertahun-tahun, tetapi telah gagal mencapai strategi optimum pembaikan. Tisu rawan disuaidirikan kepada persekitaran rendah oksigen dan keadaan ini menjadi satu faktor kepada pertumbuhan, peraturan dan kebertahanan kondrosit; iaitu satu-satunya jenis sel yang ada di dalam tisu rawan. Tesis ini menentukan fabrikasi dan pencirian biobahan antibakteria untuk pembaikan tisu rawan. Tambahan pula, tesis ini menggalakkan penggunaan nano-partikel (NP) Zink Oksida (ZnO) untuk pertumbuhan yang lebih baik bagi sel-sel rawan dan kebertahanan tisu rawan secara keseluruhannya.

Perancah komposit dan filem nipis daripada elastomer polyester polyoctanediol sitrat (POC), dengan kepekatan (1wt%, 3wt% and 5wt%) ZnO yang berbeza telah difabrikasikan masing –masing dengan menggunakan teknik pelarut-pemutus/larutresap-zarahan dan pemutus acuan. Daripada pemerhatian, didapati sifat-sifat material telah berjaya terkawal oleh perubahan mudah kepekatan NP di dalam komposit itu. Kinetik pembebasan ion daripada perancah ZnO-POC bergantung secara kuat kepada kepekatan NP dan degradasi matriks tulen POC. Semua perancah komposit telah menunjukkan sifat-sifat antibakteria yang kuat. Walau bagaimanapun, kajian sel kultur mendapati gabungan 1% ZnO di dalam polimer POC adalah kepekatan yang optimum untuk sel-sel kondrosit. Tambahan lagi, kesan 1% ZnONP terhadap pertumbuhan kondrosit dan sintesis matriks yang dikultur di bawah keadaan normoksia (21% O²) dan hipoksia (5% O²) telah menunjukkan pengawalan-atas pertumbuhan kondrosit dan sulfat-glycosaminoglycan (S-GAG) di dalam kultur hipoksia. Satu kesan sinergi kepekatan oksigen dan 1% ZnONP di dalam pernyataan gen pengawalan-atas anabolic (Kolagen Type II (*COL2A1*)) dan

aggrekan (*ACAN*)), dan pernyataan gen pengawalan-bawah katabolic (*MMP-13*) telah diperhatikan. Tambahan pula, pengeluaran hipoksia transkripsi faktor-dorongan factor 1A (*HIF-1A*) di dalam tindakbalasnya terhadap keadaan hipoksia untuk mengawal kewujudan kondrosit tidak dipengaruhi dengan kehadiran 1% ZnONP. Akhir sekali, tesis ini membincangkan tentang penyesuaian fisiologi tisu rawan di dalam pemuatan mekanikal dinamik dan keadaan hipoksia untuk menghasilkan manfaat biofaktor yang digabungkan untuk penggunaan kejuruteraan tisu rawan. Keputusan menunjukkan gabungan pemuatan dinamik adalah serasi dengan penambahan nano-partikel. Tambahan pula, pemuatan dinamik menyekat *MMP-13* dan meningkatkan pernyataan *COL2A1* dan *ACAN* dengan peningkatan pertumbuhan sel dan morfologi sel bulat (satu penanda fenotip).

Ini dapat disimpulkan bahawa perancah POC-ZnONP sangat penting di dalam penambahbaikan pelbagai fungsi perancah berasaskan polyester biodegradasi untuk kejuruteraan tisu rawan dan kehadiran 1% ZnONP telah memelihara homeostasis rawan di dalam persekitaran hipoksia. Manakala 1% ZnONP perlu dipertimbangkan untuk gabungan bermanfaat kepada system 3D kultur hipoksia dengan kehadiran rangsangan mekanikal. Kajian lanjut fokus kepada penentuan penggunaan 1% ZnONP di dalam polimer yang berbeza untuk kegunaan pelbagai aplikasi kejuruteraan tisu.

I dedicate this thesis to Ammi and Baba

University of Malaya

ACKNOWLEDGEMENT

First of all I would like to praise ALLAH who blessed me with the strength to accomplish my dream.

I would like to explicitly thank my supervisors Dr. Belinda Pingguan – Murphy and Dr. Wan Mohd Azhar bin Wan Ibrahim, for their unconditional support, vast knowledge, precious time and critical feedback. I am especially grateful to Dr. Belinda Pingguan– Murphy for her patience with me and her critical review which allowed me to enhance the quality of my articles and my thesis. Moreover, I sincerely acknowledge my ustad, Dr. Ali Moradi, from whom I have learnt not only cell culture techniques and scaffold fabrication but also to help everyone. I would like to extend my appreciation to my friends, my lab mates and my colleagues; Adel Al-Halawani, Yasser Al-Saffar, Haris Akram, Salfarina Ezrina, Kar Wey, Poon Chi-Tat, Janu Ru, Dr. Chong Pan-Pan, Dr. Eleanor Parker, Syed Shahabuddin, Shahid Mehmood, Kashan Pirzada, Forough Ataollahi, Adel Dalilottojari and all those who supported me knowing or unknowingly.

I like to thank Dr. Wan Safwani and Dr. Farina to provide me with their valuable suggestions during candidature defence.

I admire the support from Dr. Adib, Dr. Ahmad Khairi, Liyana bint Abu, Kakak Enas naeem, Mr. Hanafi, Mr Adhli and all the staff at biomedical engineering administration.

I would also like to thank all the laboratory technical staff throughout University of Malaya.

I would like to acknowledge the scholarship from MOHE without which I would have never had enough financial support to continue my PhD. Furthermore, I would like to thank University of Malaya for providing IPPP and HIR grant to fulfil my research needs.

I would like to thank Ammi and Baba for their unconditional love, support and long conversations to calm down my anxiety. A sincere thanks to my brothers. My gratitude and love to my wife who loves me and care for me.

TABLE OF CONTENTS

LIST OF FIGURES	xv
LIST OF TABLES	xx
LIST OF ABBREVIATIONS	xxi
CHAPTER 1: INTRODUCTION	1
1.1 Thesis Overview	1
1.1 Background	1
1.2 Problem Statement	3
1.3 Objectives	4
1.4 Hypotheses	5
CHAPTER 2: LITERATURE REVIEW	6
2.1 Introduction	6
2.2 Cartilage	6
2.2.1 Composition of articular cartilage	7
2.2.1.1 Chondrocytes	7
2.2.1.2 Extracellular Matrix	8
2.2.1.3 Water	8
2.2.1.4 Collagens	9
2.2.1.5 Proteoglycans	9
2.2.1.6 Non-Collagenous proteins and Glycoproteins	10
2.2.2 Zonal arrangement in articular cartilage	10
2.3 Chondrogenesis and chondrocyte differentiation	12
2.4 Articular Cartilage Disease and Injury	12
2.5 Treatment Options for Cartilage Injury	14
2.5.1 Marrow Stimulation Technique	14
2.5.2 Osteochondral Grafting	15

2.5.3	Autologous Chondrocyte Transplantation	16
2.6	Cartilage Tissue Engineering	17
2.6.1	Cell Sources	18
2.6.2	Cell Signalling Strategies	19
2.6.2.1	Mechanical stimulus	20
2.6.2.2	Oxygen Tension/Hypoxia	22
2.6.3	Tissue Engineering Scaffolds	23
2.7	Poly Octanediol Citrate (POC)	25
2.7.1	POC, its structure, synthesis, and form	25
2.7.2	POC as a biomaterial	26
2.7.3	POC in cartilage tissue engineering	27
2.8	Infection and Anti-bacterial scaffolds	28
2.9	Antibacterial activity of ZnO	32
2.10	Motivation for current study	33
	CHAPTER 3: MATERIALS AND METHODS	36
3.1	Introduction	36
3.2	Preparation of POC pre-polymer	36
3.3	Fabrication of POC and ZnO-POC composites	38
3.4	Chondrocyte Isolation	40
3.4.1	Chondrocyte Culture Medium	42
3.4.2	Cartilage ECM digestion	42
3.4.2.1	Protease preparation	43
3.4.2.2	Collagenous preparation	43
3.4.3	Cell Viability	43
3.5	Cell proliferation assay	44
3.6	DNA Biochemical Assay	44

3.6.1	Lysis of BACs	45
3.6.2	DNA quantification	45
3.6.2.1	DNA Standard	46
3.7	Sulphated Glycosaminoglycan (S-GAG) quantification assays	47
3.8	Quantitative Polymerase Chain Reaction (q-PCR)	48
3.8.1	RNA Isolation	48
3.8.2	cDNA synthesis	49
3.8.3	Gene Expression	49
3.9	Scanning Electron Microscopy (SEM) for cell adhesion	50
3.10	Live/Dead Assay	51
3.11	Statistical Analysis	51
CHAPTER 4: CHARACTERISATION OF POLYOCTANEDIOL		
CITRATE-ZINC OXIDE NANO-COMPOSITE SCAFFOLD		
		52
4.1	Introduction	52
4.2	Materials and Methods	54
4.2.1	Surface and elemental properties	54
4.2.2	Zinc oxide nanoparticles distribution within POC	54
4.2.3	Surface wettability test	55
4.2.4	Mechanical property and porosity	55
4.2.5	Swelling test	56
4.2.6	Fourier transform infrared spectroscopy (FTIR) analysis	56
4.2.7	Thermal analysis	56
4.2.8	Degradation analysis	57
4.2.9	ZnO NPs release kinetics in physiological conditions	57
4.2.10	Anti-bacterial properties	58
4.2.11	In vitro tests with chondrocyte cell culture	58

4.3	Results	59
4.3.1	Surface morphology	59
4.3.2	Influence of ZnO-NPs on relative hydrophilicity	60
4.3.3	Physical properties of scaffolds	62
4.3.4	Swelling and cross-linking density	63
4.3.5	Chemical composition	63
4.3.6	Thermal stability	64
4.3.7	Degradation	65
4.3.8	ZnO release kinetics	66
4.3.9	Anti-bacterial properties of ZnO-POC scaffolds	68
4.3.10	Cytotoxic effects of ZnO NPs on primary chondrocytes	70
4.4	Discussion	71
4.4.1	Surface morphology	71
4.4.2	Influence of ZnO-NPs on relative hydrophilicity	71
4.4.3	Physical properties of ZnO-POC scaffolds: porosity and elasticity	72
4.4.4	Swelling and cross-linking density	73
4.4.5	Chemical composition	73
4.4.6	Thermal stability	74
4.4.7	Degradation	75
4.4.8	ZnO release kinetics	75
4.4.9	Anti-bacterial properties of ZnO-POC composite scaffolds	76
4.4.10	Cytotoxic effects of ZnO NPs on primary chondrocytes	77

CHAPTER 5: EFFECT OF HYPOXIA ON BOVINE ARTICULAR	79
CHONDROCYTES	79
5.1 Introduction	80
5.2 Materials and Methods	81
5.2.1 Experimental Design	81
5.2.2 Cell Proliferation Assays	81
5.2.3 Sulphated glycosaminoglycan (S-GAG) quantification assays	81
5.2.4 Quantitative Polymerase Chain Reaction (q-PCR)	82
5.2.5 Statistical Analysis	82
5.3 Results	82
5.3.1 Cell proliferation	83
5.3.2 Proteoglycan Synthesis	87
5.3.3 Gene expression	88
5.4 Discussion	89
5.4.1 Cell proliferation	90
5.4.2 Proteoglycan Synthesis	91
5.4.3 Gene expression	91
CHAPTER 6: EFFECT OF DYNAMIC MECHANICAL	
COMPRESSION ON BOVINE ARTICULAR CHONDROCYTES	95
6.1 Introduction	95
6.2 Materials and Methods	97
6.2.1 Experimental Design	97
6.2.2 Application of dynamic compression	98
6.2.3 Cell Proliferation Assay	99

6.2.4 Sulphated glycosaminoglycan (S-GAG) quantification	
assays	100
6.2.5 Quantitative Polymerase Chain Reaction (q-PCR)	100
6.3 Results	100
6.3.1 Cell proliferation and morphology	100
6.3.2 Proteoglycan synthesis	105
6.3.3 Gene Expression	106
6.4 Discussion	107
6.4.1 Cell proliferation and morphology	108
6.4.2 Proteoglycan synthesis	109
6.4.3 Gene Expression	109
CHAPTER 7: CONCLUSIONS AND FUTURE DIRECTIONS	111
7.1 Conclusions	111
7.2 Future directions	115
REFERENCES	116
PUBLICATIONS	149
APPENDIX I	153
APPENDIX II	154

LIST OF FIGURES

Figure 2.1: Zones of Articular cartilage, modified from (Bhosale & Richardson, 2008).....	11
Figure 2.2: Wurtzite structure of ZnO crystal	32
Figure 2.3: Chondrocytes cultured in a T-75 flask losing their morphology and turning flat only after 24 hours of culture	34
Figure 3.1: (A) The reaction scheme of POC pre-polymer fabrication via the polycondensation reaction in a two necked round bottom flask with a nitrogen purge to remove excess water content. (B) Synthesis scheme of monomers reacting to form POC polymer	37
Figure 3.2: Steps involved in fabrication of (A) Pure-POC and (B) POC-ZnONP scaffolds, films and coatings prior to curing	39
Figure 3.3: A custom-designed rack placed under water to categorise Pure-POC scaffolds from ZnO-POC scaffolds and to leach out the salt from scaffolds	40
Figure 3.4: Procedure of isolation of primary chondrocytes from cow legs. (A) Removal of hide from cow leg insert shows completely removed hide, (B) Opening of joint by removing ligament, (C) Cutting of cartilage and (D) Complete shaved cartilage joint and explants placed in sterile container	41
Figure 4.1: FESEM images of POC (control) and 1%, 3% and 5% ZnO-POC composite scaffolds; (A) POC, (B) 1% ZnO-POC, (C) 3% ZnO-POC and (D) 5% ZnO-POC; inserts show representative magnified surfaces of pore walls within scaffolds (inserts: A and B bars = 1 μm ; C and D bars = 2 μm)	60

Figure 4.2: Optical microscopy images of Pure-POC and ZnO-POC surfaces developed by spin-coating technique at a magnification of 100X; (A) POC, (B) 1% ZnO-POC, (C) 3% ZnO-POC and (D) 5% ZnO-POC	61
Figure 4.3: Water-in-air contact angle results measured for thin films of Pure-POC and 1%, 3% and 5% ZnO-POC produced by spin-coating technique	62
Figure 4.4: Percentage swelling in water for Pure-POC (control) and 1%, 3% and 5% ZnO-POC composite films	63
Figure 4.5: Representative ATR-FTIR spectra of POC and 5% ZnO-POC scaffolds ...	64
Figure 4.6: Thermal degradation curves of Pure-POC and (1%, 3% & 5%) ZnO-POC scaffolds measured by TGA	65
Figure 4.7: Weight loss of Pure-POC, 1%, 3% and 5% ZnO-POC scaffolds over the period of 20 weeks in Phosphate Buffered Saline (PBS)	66
Figure 4.8: In-vitro Release kinetics profile of ZnO (Zn^{2+}) from ZnO-POC scaffolds in PBS at 37°C; M_t = mass of ZnO released at time intervals; M_∞ = total mass of ZnO within the scaffold (all M_t / M_∞ ratios are the mean values for five samples measured with AAS).....	67
Figure 4.9: Zn-ions released over the period of 28 days calculated in ppm via AAS. Where * shows a significant difference between the number of days, $p < 0.05$	68
Figure 4.10: Growth rates of E. coli and S. Aureus in LB broth inoculated with 50 μ l of 10^{4-5} CFU/ml for Pure-POC (positive control), LB Broth (negative control) and 1%, 3% and 5% ZnO-POC scaffolds (optical density at 595 nm was measured in microplate reader and is proportional to bacterial growth)	69

Figure 4.11: (A) Resazurin reduction (%) for Pure-POC (control) and 1%, 3% and 5% ZnO-POC scaffolds after 24 and after 72 hours. FESEM images of scaffolds after 72 hours in chondrocyte culture: **(B)** Pure-POC; and **(C)** 1% ZnO-POC (bar = 10 μm).....**70**

Figure 5.1: Summary of experimental design**81**

Figure 5.2: Cell vitality determined via resazurin reduction assay, of chondrocytes, seeded on Pure-POC and 1% ZnO-POC in normoxic (21%O₂) & hypoxic (5%O₂) conditions. Where * shows a significant difference between O₂ tension. 5 ≤ N ≤ 6, p < 0.05.....**83**

Figure 5.3 (A – L): Live/Dead assay of Chondrocytes seeded on the scaffold at day 1, 7 and 14 under normoxic and hypoxic conditions. Outer images are at 10X magnification with a scale bar of 300 μm and their respective inserts are at 40X magnification with a scale bar of 100 μm **84**

Figure 5.4: Cell quantification through DNA Hoechst fluorescence assay method, of chondrocytes, seeded on Pure-POC and 1% ZnO-POC in normoxic (21%O₂) & hypoxic (5%O₂) conditions. Where + shows significant differences between groups and * shows a significant difference between O₂ tension. 5 ≤ N ≤ 6, p < 0.05**85**

Figure 5.5 (A – L): SEM images showing the morphologies of Chondrocytes seeded on the scaffold at day 1, 7 and 14 under normoxic and hypoxic conditions. Outer images are at 1000X magnification with a scale bar of 10 μm and their respective inserts are at 3000X magnification with a scale bar of 2 μm **86**

Figure 5.6: (A) Total S-GAG, measured in digested scaffolds and **(B)** S-GAG measured in medium via DMMB assay for chondrocytes seeded on Pure-POC and 1% ZnO-POC in normoxic (21%O₂) & hypoxic (5%O₂) conditions. Where + shows significant

differences between groups and * shows a significant difference between O ₂ tension. 5 ≤ N ≤ 6, p < 0.05.....	87
Figure 5.7 (A, B, C & D): mRNA expression of <i>COL2A1</i> , <i>ACAN</i> , <i>MMP – 13</i> and <i>HIF – 1A</i> respectively normalized to GAPDH with respect to Pure-POC on day 1. Where + shows significant differences between groups and * shows a significant difference between O ₂ tension. 3 ≤ N ≤ 5, p < 0.05.....	89
Figure 5.8: Schematic of divalent ion involvement in binding COMP with collagens with a selective preference of Zn ⁺² binding phenomenon within synovial fluid.....	92
Figure 5.9: FESEM image at 5K magnification of 1% ZnO-POC in hypoxia at day 14. Set of red arrows points to visible fibrils in ECM.....	93
Figure 6.1: Illustration summarizing all experimental groups with respect to culture conditions and oxygen tensions	98
Figure 6.2: Bose ElectroForce® 5500 USA. (A) Bose Bioreactor setup with 24-well plate fixture in a 5% CO ₂ incubator. (B) 24-well plate with compression platens in a box chamber	98
Figure 6.3: Schematic illustration of the intermittent dynamic compression profile of cell culture regimes.....	99
Figure 6.4: Cell quantification through DNA Hoechst fluorescence assay for chondrocytes seeded on pure-POC and 1% ZnO-POC in normoxic (21% O ₂) & hypoxic (5% O ₂) conditions, under static and dynamic culture regimes. Where ^ shows a significant difference between due to the presence of ZnONP, * shows a significant difference between O ₂ tension and + shows a significant difference between static and dynamic culture. p < 0.05.....	101

Figure 6.5: Confocal imaging of Chondrocytes (A-H) seeded on Pure-POC and 1% ZnO-POC scaffolds in normoxic (21%O₂) & hypoxic (5%O₂) conditions, under static and dynamic culture regimes. Outer images are at 10X with a scale bar of 300 μm and their respective inserts are at 40X magnification with a scale bar of 100 μm.....102

Figure 6.6: SEM imaging of Chondrocytes (A-H) seeded on Pure-POC and 1% ZnO-POC scaffolds in normoxic (21%O₂) & hypoxic (5%O₂) conditions, under static and dynamic culture regimes. Outer images are taken at 1000X magnification, it has a scale bar of 10 μm. Corresponding images in inserts were taken at 3000X magnification having a scale bar of 2 μm.....104

Figure 6.7: DMMB assay for glycosaminoglycans (A) Total S-GAG, measured in digested scaffolds and (B) S-GAG measured in medium via DMMB assay for chondrocytes seeded on pure-POC and 1% ZnO-POC in normoxic (21%O₂) & hypoxic (5%O₂) conditions, under static and dynamic culture regimes. Where ^ shows a significant difference between due to the presence of ZnONP, * shows a significant difference between O₂ tension and + shows a significant difference between static and dynamic culture. p<0.05.....105

Figure 6.8: (A) *COL2A1*, (B) *ACAN*, (C) *MMP-13* and (D) *HIF-1A*, for chondrocytes seeded on pure-POC and 1% ZnO-POC in normoxic (21%O₂) & hypoxic (5%O₂) conditions, under static and dynamic culture regimes. Where ^ shows a significant difference between due to the presence of ZnONP, * shows a significant difference between O₂ tension and + shows a significant difference between static and dynamic culture. p<0.05.....107

Figure 6.9: Schematic of the possible pathway by which hypoxia inducible factor controls cartilage destruction with the help of its 2 major genes that are up-regulated in hypoxic conditions.110

LIST OF TABLES

Table 2.1: Constituents of articular cartilage with their respective composition.....	8
Table 3.1: Ingredients to prepare chondrocyte culture medium.....	42
Table 3.2: Ingredients to prepare papain digest buffer.....	45
Table 3.3: Ingredients used in preparation of DMMB solution for DMMB assay.....	47
Table 3.4: Gene identities and their respective amplicon length from LifeTechnologies.....	50
Table 4.1 Compression properties and porosities of ZnO-POC scaffolds.....	62

University of Malaya

List of Abbreviations

3D	three dimensional
AAS	atomic emission spectroscopy
ACAN	Aggrecan gene
ACI	Autologous Chondrocyte Implantation
ANOVA	Analysis of Variance
ATCC	American Type Culture Collection
BAC	Bovine Articular Chondrocytes
BMPs	Bone Morphogenic Proteins
CA	Citric Acid
cDNA	complimentary Deoxyribonucleic acid
CLSM	confocal laser scanning microscopy
COL2A1	Collagen Type II – Alpha 1 gene
COLX	Collagen Type X gene
COMP	Cartilage Oligomeric Protein
DMEM	Dulbecco's Modified Eagle's Medium
DMMB	Dimethyl Methylene Blue
DNA	Deoxyribonucleic acid
ECM	Extra Cellular Matrix
EDTA	Ethylenediaminetetraacetic acid
EDX	Energy Dispersive X-ray
em	emission
EPS	equilibrium percentage swelling
ex	excitation
FBS	Foetal bovine serum
FDA	Food and Drug Administration

FESEM	Field Emission Scanning Electron microscope
FTIR	Fourier transform infrared spectroscopy
GAGs	Glycosaminoglycans
GAPDH	Glyceraldehyde-3-phosphate dehydrogenase gene
GRAS	Generally Regarded as Safe
HA	Hydroxyapatite
HCl	Hydrochloride
HEPES	<i>4-(2-hydroxyethyl)-1-piperazineethanesulfonic acid</i>
HIF-1A	Hypoxia Inducible Factor-1 alpha gene
HNMR	Hydrogen nuclear magnetic resonance
LB-Broth	Luria-Bertani broth
MALDI-TOF	Matrix-assisted laser desorption ionization- Time of Flight
min	minutes
MMP-13	Matrix Metalloproteinases – 13 gene
MP-AES	microwave plasma-atomic emission spectrophotometer
N ₂	Nitrogen
NaCl	Sodium Chloride
NaOH	Sodium Hydroxide
NP	Nanoparticles
O ₂	Oxygen
OD	1, 8 Octanediol
PBS	Phosphate Buffered Saline
PCL	Polycaprolactone
PEG	Poly Ethylene Glycol
PGA	Poly Glycolic Acid
PGS	Poly (glycerol sebacate)

PLA	Poly _{D,L} – Lactic acid
PLGA	Poly _{D,L} – Lactic acid-co-glycolic acid
PLLA	Poly-L- Lactic acid
POC	Poly 1, 8 Octanediol Citrate
PPLG	Poly γ -propargyl-l-glutamate
Ppm	parts per million
PVP	polyvinylpyrrolidone
q-PCR	Quantitative Polymerase Chain Reaction
RA	Rheumatoid Arthritis
RNA	ribonucleic acid
ROS	reactive oxygen species
SEM	Scanning Electron Microscopy
S-GAG	Sulphated Glycosaminoglycan
SOX9	SRY-box 9
SRTR	Scientific Registry of Transplant Recipients
SSC	Saline Sodium Citrate
TCP	Tricalcium Phosphate
TE	Tissue Engineeirng
TGA	thermo gravimetric analysis
UNOS	United Network for Organ Sharing
w/v	weight by volume ratio
w/w	weight by weight ratio
WACA	Water-in-air contact angle
ZnO	Zinc Oxide
ZnONP	Zinc Oxide Nanoparticles
β -TCP	Beta Tricalcium Phosphate

CHAPTER 1: INTRODUCTION

1.1 Thesis Overview

This thesis comprises 7 chapters. Chapter 1 describes the background of the research and the research problem, followed by objectives and hypothesis. The second chapter discusses the related literature in depth, and lastly, the motivation to perform the research is included. A complete methodology and list of materials used is provided in chapter 3 so the reader can repeat the experiment if they want to. Finally, chapter 4, 5 and 6 are divided according to the objectives, and each chapter includes the results and discussion for the defined objectives. Chapter 7 is the last chapter in this thesis and provides the essence of the thesis in the form of a conclusion, and future direction for related research.

1.2 Background

As per 17 May 2012, data provided by Organ Procurement and Transplantation Network/Scientific Registry of Transplant Recipients (SRTR)/ glyco (UNOS) shows, there are more than 114,000 people in the queue for organ transplants. Every 10 minutes a new patient is added to the queue and 18 people die each day due to organ shortages (Network, 2012). Each year, more than one million people are in need of heart valves, corneas, skin cardiovascular tissue, and bone tissue (Network, 2012).

The facts and figures mentioned above only represent the United States of America. The rest of the world population, especially the third world countries where quality of life is poor and organ donations are scarce, are also affected. There is an urgent need for biocompatible, efficacious, and cost-effective engineered tissues and organs, and this need only increases with advances in quality of life and life expectancy.

Articular cartilage is by far one of the most essential and yet functionally complex tissues that scientists are trying to repair, yet minimal success has been for decades. A major cause of disability is the joint pain that cartilage disease produces, which is not only

limited to older people but found in middle aged persons as well. The cause of joint pain is degeneration of articular cartilage due to primary osteoarthritis or trauma (Temenoff & Mikos, 2000). Cartilage is a tissue with limited self-repair capabilities, and hence any kind of injury to the cartilage tissue which is sustained for a substantial time eventually leads to further detrimental effects (O'Driscoll, 1998; Steinert et al., 2007; Temenoff & Mikos, 2000). Different approaches are adopted by clinicians to address the issue of cartilage repair depending upon the nature of cartilage damage. However current treatment options fail to secure a permanent solution. Furthermore, infection and inflammation may lead to treatment failing. One of the major causes of biomaterial infections is peri-operative contamination and research has shown that tissue engineered implants also pose a risk similar to biomaterial associated infections (Kuijer et al., 2007). Amongst total knee arthroplasty patients, a risk of peri-operative infection of up to 38% has been reported recently (Janz et al., 2015). Matrix-induced Autologous Chondrocyte Implantation has also been reported to cause superficial infection among patients (Bartlett et al., 2005). Additionally, a recent study demonstrated that only the presence of nano surface topography can help reduce bacterial adhesion while increasing cell proliferation due to nanoscale roughness (Liu et al., 2015). This finding adds to the use of nanomaterials, which are already employed in the delivery of drugs (Pi et al., 2015; Shi et al., 2015), fighting of infection (Kalashnikova et al., 2015), enhancing mechanical properties of scaffolds (Pooyan et al., 2015) and increasing cell proliferation (Holmes et al., 2016).

Chondrocytes are the only cell type that is present in cartilage. These cells flourish in a hypoxic environment, while the Extra Cellular Matrix (ECM) in which these cells are embedded undergoes dynamic compression. Current research lack these native physiologic stimuli and other biofactors as required for chondrocytes to flourish.

Tissue engineering provides an alternative approach to address existing problems in an effective and efficient way. Even though cartilage tissue engineering have been adopted by scientist to cure the dilemma of cartilage damage. However, till date there are many problems that are associated directly and indirectly that impede implementation of cartilage repair strategy via tissue engineering approach.

1.3 Problem Statement

Various solutions have been put forward by scientists to successfully implement cartilage tissue engineering clinically. However, the limitations of their proposed techniques exceed their benefits. the use of hydrogels, natural polymers, synthetic polymers, and metal implants has been suggested but they have generally proved unsuitable for clinical use, due to their inferior mechanical properties (Johnstone et al., 2013; Spiller et al., 2011) and lack of recovery of the implanted material to its original level due to creep effect (Shi et al., 2016). Moreover, current cartilage repair strategies have raised a multitude of concerns, including infection (Lichstein et al., 2015; Yeo et al., 2015) implant failure (Hazelwood et al., 2015; Vahdati & Wagner, 2013), lack of native tissue architecture (Chung & Burdick, 2008; Doran, 2015) and absent cell morphology (Hardingham et al., 2002). In order to fight any bacterial infection many antibacterial agents have been studied (Aksoy et al., 2010; Davies, 2003). However, Zinc Oxide stands out as favourable because it also plays a significant role in cartilage synthesis(Kirsch et al., 2000). Current clinical methods include minimally invasive surgery to resurface articular cartilage, arthroscopic lavage, or marrow stimulation techniques. Unfortunately all the aforementioned clinical methods currently used are palliative and for temporary relief only. The most frequently used treatment options for cartilage tissue repair have limitations that hinder their long-term clinical implementation (Marlovits et al., 2006; Portocarrero et al., 2013).

Furthermore, only a handful of studies are present that implement all three components of cartilage tissue engineering: (a) cells, (b) scaffold, and (c) bio factors, together. More recent findings signify the importance of using a three-dimensional environment with dynamic loading for cartilage tissue engineering (Panadero et al., 2016).

A cartilage tissue engineering approach must benefit from a suitable biocompatible and biodegradable scaffold that will provide a micro structure for the chondrocytes to settle and proliferate, while being porous enough to allow cell-cell interaction and exchange of nutrients for uniform tissue formation. Moreover, the newly fabricated scaffold must also be flexible enough to be implanted via minimally invasive techniques, where required (Johnstone et al., 2013).

A successful intervention for a cartilage repair strategy must involve external stimuli that will deliver a physiologic environment to cultured chondrocytes under a 3D structure. Furthermore, to tackle inflammation and infection, a suitable anti-inflammatory and antibacterial mediator must be integrated to assist with diminishing these effects while having no adverse effects on the cells.

In essence, the combination of biocompatible scaffold, physiologic stimuli and facilitation of antibacterial and anti-inflammatory properties bears promise for more effective treatment of cartilage disease.

1.4 Objectives

The objectives of this research are:

1. To develop a biodegradable scaffold with controlled pore size and porosity mimicking the properties of native articular cartilage.
2. To select and optimise the concentration of nano particles that must be biocompatible and having antibacterial effect while showing no toxicity towards chondrocytes.

3. To study the independent and combined effect of Hypoxia and ZnONP on bovine articular chondrocytes seeded on polymer scaffolds.
4. To establish a relationship between dynamic mechanical stimuli, ZnONP and oxygen tension in chondrocyte seeded polymer scaffolds.

1.5 Hypotheses

1. It is hypothesised that chondrocytes will proliferate, secrete more extracellular matrix, and show higher gene expression under a hypoxic environment. Furthermore the incorporation of nanoparticles will deliver an anti-bacterial mechanism to the fabricated scaffold.
2. Furthermore it is hypothesized that scaffolds that will go under dynamic compression with a combination of hypoxia and nanoparticles, will eventually display a more chondrogenic morphology and will help in elevating cartilage specific matrix gene while lowering catabolic gene expression.

CHAPTER 2: LITERATURE REVIEW

2.1 Introduction

In the present study, a novel composite biomaterial for use within cartilage tissue engineering is developed, optimised, and evaluated. The literature which underpins this is therefore reviewed, starting with the current understanding of cartilage as a tissue, followed by cartilage injury, and a review of cartilage repair options. From here, the focus moves to the three components of a tissue engineering strategy as applied to cartilage tissue engineering; first, cell source; second, cell signalling strategy (covering biochemical and biomechanical signalling); and finally, the scaffold material (including a focus on the target material for the present study).

2.2 Cartilage

Cartilage is a tissue that lacks blood vessels, nerves and lymph vessels, and is composed of sparingly distributed chondrocytes (only 1% in humans) (Poole, 1997). There are 3 types of cartilage in the human body, depending upon matrix composition; elastic cartilage, fibrocartilage and hyaline cartilage (Jung, 2014). Elastic cartilage makes up the flexible cartilaginous structures of the nose and ear. It contains elastin as an additional component to ECM. Fibrocartilage contains a higher content of collagen in ECM than in hyaline cartilage and is present in ligaments and tendons that are located in close proximity to bone (Temenoff & Mikos, 2000). Hyaline cartilage is mainly found in the larynx, trachea, ribs, knee and bronchus (Jung, 2014).

Long bones have a covering at their articulating ends known as hyaline cartilage. This type of cartilage is more commonly referred to as articular cartilage. This hyaline cartilage provides a low-friction surface with wear resistant properties (Bhosale & Richardson, 2008).

Hyaline cartilage is made up of water and ECM. Within this ECM, type II collagen is most abundant, followed by proteoglycans that suffice for mechanical properties in vivo (Bhosale & Richardson, 2008). For an articular joint to function optimally, it is critical that engineered cartilage must comply with the properties of native articular cartilage. It must qualify to withstand load-bearing forces, have low friction a coefficient, and have other necessary biological and mechanical properties (Doran, 2015).

2.2.1 Composition of articular cartilage

2.2.1.1 Chondrocytes

Among all the tissues of the human body, articular cartilage has the lowest cellular density, according to volume. Humans have only 1% cellular material in their articular cartilage, namely cells called chondrocytes (Temenoff & Mikos, 2000). Chondrocytes are sparse but extremely important for replacement of degraded matrix molecules in order to maintain homeostasis. At week 5 of gestational, a blastema is formed when few mesenchyme cells form an aggregate. This blastema starts secreting a cartilage matrix which forms the foundation of chondrocytes (Bhosale & Richardson, 2008). It is reported that a cilia extends from surface of some chondrocytes into the ECM that contributes to modifying ECM properties in response to mechanical stimulus (Buckwalter & Mankin, 1997). Chondrocytes pass through various lineages, producing proteins vital for ECM. Chondrocytes in the periphery secrete collagen to form a hyaline cartilage. When chondrocytes mature, they tend to halt their activity, appear circular and are enclosed in a matrix (Buckwalter & Mankin, 1997; Hall, 1994). Table 2.1 summarises the constituents of articular cartilage.

Table 2.1: Constituents of articular cartilage with their respective composition (Jung, 2014; Poole, 1997; Temenoff & Mikos, 2000).

Constituent		Wet weight (%)	Dry weight (%)
Cellular Material	Chondrocytes	-----	1
Extracellular Matrix	Water	80	-----
	Macromolecules	20-40	-----
	Collagen	10-20	50-60
	Proteoglycans	10-20	25-35
	Non-collagenous proteins	-----	15-20

2.2.1.2 Extracellular Matrix

Apart from chondrocytes, articular cartilage comprises a complex mix of water and structural macromolecules in a framework that provides stability to the articular cartilage. A combination of water and macromolecules is called ECM. The majority constituent in ECM of articular cartilage is water, approximately 80% of the weight. However in different regions of cartilage the percentage of water varies from 60% to 80%. The macromolecules comprise collagens, proteoglycans, and non-collagenous proteins. Macromolecules (when combined) account for 20 – 40 % wet weight of articular cartilage (Jung, 2014).

2.2.1.3 Water

In articular cartilage water accounts for majority of the wet weight of the tissue; around 80%. Apart from water tissue fluid contains bulk of cations to neutralise negatively charged GAG's in ECM. Tissue fluid also contains metabolites and gases. The presence of tissue fluid is of vital importance to avascular cartilage as it helps the exchange of nutrients and oxygen (O₂) with synovial fluid. Furthermore, recovery of cartilage and resistance to compression is achieved via the presence of tissue fluid in ECM (Buckwalter & Mankin, 1998b).

2.2.1.4 Collagens

The second-most abundant constituent of ECM is collagen, which accounts for 10% to 20% of the wet weight of articular cartilage (Bhosale & Richardson, 2008) while it equates to 50% to 60% of the dry weight of articular cartilage (Jung, 2014). Collagen types II, VI, IX, X and XI are found in articular cartilage. However, the major role player is type II collagen, which represents 90 – 95% of all the collagens present. Collagen type II also forms the foundation of interlinked fibrils in articular cartilage (Buckwalter & Mankin, 1997). The interlinked fibrils formed by type II collagen not only provide physical strength to the cartilage but also trap other macromolecules (Cohen et al., 1998; Temenoff & Mikos, 2000).

2.2.1.5 Proteoglycans

The third constituent of ECM are the proteoglycans, proteins that give compressive capabilities to the cartilage. However they are only 10 – 20 % of the total wet weight (Bhosale & Richardson, 2008), and they account for 25% to 35% in dry form (Buckwalter & Mankin, 1997). The proteoglycans are composed of polysaccharides and proteins in the ratio of 19 to 1 respectively (Wirth & Rudert, 1996). The protein forms the core, with attachment to one or more glycosaminoglycans (GAGs) chains (Buckwalter & Mankin, 1997; Temenoff & Mikos, 2000). GAGs are from a family of polysaccharides which have a repeating disaccharide unit (Afratis et al., 2012; Anower-E-Khuda & Kimata, 2015). Chondroitin sulfate, dermatan sulfate, keratan sulfate and hyaluronic acid are all GAGs that are present in articular cartilage (Brézillon et al., 2014; Hall, 2012). Proteoglycans are sub-divided into 2 groups: (a) large aggregating proteoglycans and (b) small aggregating proteoglycans. Large aggregating proteoglycans are more commonly referred as Aggrecan (Buckwalter & Mankin, 1997). The Aggrecans are responsible for resilience and distribution of stress in articular cartilage (Temenoff & Mikos, 2000).

2.2.1.6 Non-Collagenous proteins and Glycoproteins

Non-Collagenous proteins and Glycoproteins account for about 15% to 20% of articular cartilage in dry weight. In an articular cartilage there exists wide variety of these molecules. They possess minute quantities of oligosaccharide attached to a protein core. Contrary to proteoglycans and collagens, these non-collagenous proteins and glycoproteins have not been studied extensively. However, they tend to help in maintenance and organization of macromolecular network of ECM (Buckwalter et al., 2005; Gallagher et al., 1983). Among them, cartilage oligomeric protein (COMP) is most abundant. It is concentrated in the matrix of chondrocyte cells and has a binding affinity chondrocytes (Buckwalter & Mankin, 1997; Temenoff & Mikos, 2000); COMP is involved in maintaining the chondrogenic phenotype (Aigner & Fan, 2003).

2.2.2 Zonal arrangement in articular cartilage

Articular cartilage is divided into 4 zones (figure 2.1) according to their structure and function.

1. Superficial zone
2. Transitional zone
3. Deep zone
4. Calcified zone

1. Superficial zone

The superficial zone comprises of flat cells and is the thinnest layer. It is laminated by a specialised layer of synovial fluid called the lamina splendens (*Instructional Course Lectures, The American Academy of Orthopaedic Surgeons - Articular Cartilage. Part I: Tissue Design and Chondrocyte-Matrix Interactions**†, 1997). The lamina splendens is a protein that enhances the low – friction properties of the surface of articular cartilage (Buckwalter & Mankin, 1997; Temenoff & Mikos, 2000).

2. Transitional zone

This zone is dominated by spheroid-shaped cells, although the cell density is lower. Collagen fibres with a higher diameter can be found in this zone, which also has a high content of the proteoglycan aggrecan (Bhosale & Richardson, 2008; Buckwalter & Mankin, 1997).

3. Deep zone

This zone has the lowest of cells densities, with spherical cells distributed throughout the zone. The proteoglycan concentration is the highest in this region (Bhosale & Richardson, 2008; Buckwalter & Mankin, 1997).

4. Calcified zone

Mineralisation is higher in this region of articular cartilage, meaning that cells are embedded in a matrix. The cells in calcified zone synthesise Type X collagen, which is mainly responsible for providing mechanical stability to cartilage, and also assists in absorbing shocks (Buckwalter & Mankin, 1997; Temenoff & Mikos, 2000).

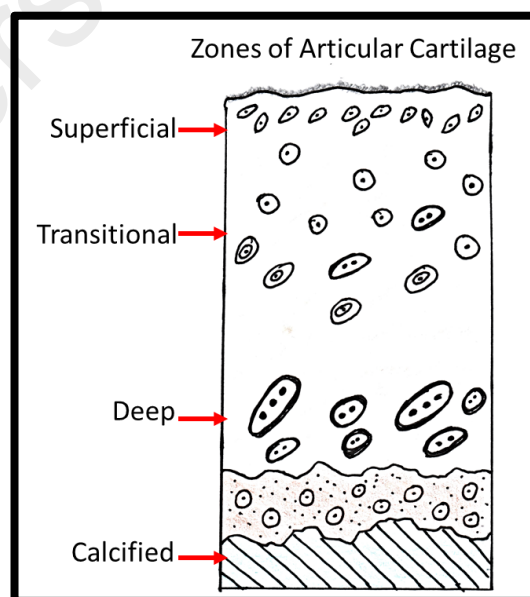


Figure 2.1: Zones of Articular cartilage, modified from (Bhosale & Richardson, 2008).

2.3 Chondrogenesis and chondrocyte differentiation

The process by which cartilage forms is called chondrogenesis. This is a natural process and chondroprogenitor cells are responsible for its initiation. Chondroprogenitor cells are basically mesenchymal cells. Mesenchymal cells come together and form an aggregate and start condensing in one area; this marks the beginning of chondrogenesis. Bone Morphogenic Proteins (BMPs) are responsible for contributing to initiating chondrogenesis by helping in aggregation of loose mesenchymal cells. In the early stages of chondrogenesis, the mesenchymal cells secrete ECM and cell adhesion molecules (Goldring et al., 2006). Among the secreted ECM there are large amounts of type II collagen (Ng et al., 1993), N-cadherin (Oberlender & Tuan, 1994), N-cad (Widelitz et al., 1993) and tenascin (Mackie et al., 1987). Apart from the ECM and cell adhesion molecules, SRY-box 9 (SOX9); a transcription factor, is highly expressed. SOX9 plays a vital role in chondrogenesis and differentiation of chondrocytes.

Differentiation of mesenchymal cells into chondrocytes causes the cells to secrete the ECM that contains large quantities of type II collagen and Aggrecan. After early chondrocyte differentiation, this is the next development stage of cartilage. In this stage the cells proliferate rapidly providing a template for the cartilage. After a certain time old cells draw away from the cell proliferation cycle and enter in to a phase of hypertrophic differentiation. In this process the chondrocytes grow in size, terminally differentiate, mineralize, and eventually undergo apoptosis (Freed et al., 1998; Zuscik et al., 2008). After the death of chondrocytes, they degrade and leave a matrix of their cells that serves as a scaffold for deposition of minerals and formation of bone (Zuscik et al., 2008).

2.4 Articular Cartilage Disease and Injury

Articular cartilage diseases represent the most common cause of joint pain in middle aged and older people (Buckwalter & Mankin, 1998b), and hospital treatment cost for total

knee replacement was reported to be US\$ 28.5 billion in 2009 in the US alone (Murphy & Helmick, 2012). Together with acute injury, such cartilage disorders also result in a substantial reduction in quality of life (Minas, 1999; Murray et al., 2015).

Depending upon the nature of injury, cartilage injury can be subdivided into three major categories; Full thickness defect, partial defect and matrix disruption. A full thickness defect is the most painful and it usually affects entire cartilage thickness while also penetrating deep into the subchondral bone (Temenoff & Mikos, 2000). In this type of injury fibrin clot formation occurs at the site of defect. Blood and bone marrow cells bind to this site and form patches of fibrin clots (Aigner & Fan, 2003). The newly formed tissue lacks the strength of native articular cartilage and has a higher permeability. Lack of strength and excess permeability eventually contribute to degradation and permanent damage to articular cartilage and subchondral bone. An injury of as little as 3mm depth is considered to be a full thickness defect. (Coutts et al., 1997; Fortier et al., 2011; Temenoff & Mikos, 2000).

A secondary injury is a partial thickness defect, resulting in disruption to the surface of cartilage. This damage, unlike a full thickness defect, does not extend to the subchondral bone. In this type of injury the surrounding cells do proliferate but not to an extent which can repair the defect completely (Temenoff & Mikos, 2000). Research over the years has provided evidence against the healing of tissue (Ghadially et al., 1977) or progressive degeneration (Grande et al., 1989) in the case of partial thickness defects. Not only is regeneration limited at the cellular level of cartilage, but also negative charges amongst proteoglycans during injury contribute to the lack of cellular adhesion (Hendrich et al., 2003).

A blunt trauma to cartilage causes matrix disruption injury. This type of injury may occur from a sporting activity or accident. If the extent of injury is not extreme the damage is

reversed by the viable chondrocytes present at the site of injury (Temenoff & Mikos, 2000).

Thus, despite it being such a serious and significant issue, treatment of cartilage problems is severely restricted due to the limited ability of cartilage to self-repair (Lam et al., 2014). This often means that degeneration occurs at a higher rate than repair, causing increasing failure of the degenerative cartilage surface (O'Driscoll, 1998).

2.5 Treatment Options for Cartilage Injury

To provide a sustainable solution to the problem of cartilage damage the primary objective of every clinician is to yield normal function of the joint (Temenoff & Mikos, 2000). Generally there exists three major interventions to restore joint functionality.

2.5.1 Marrow Stimulation Technique

The marrow stimulation technique involves micro-fracture, abrasion arthroplasty, or drilling, and is usually adopted as a primary treatment for cartilage defects up to 2 to 4 cm². This technique involves creating defects that extend to the sub-chondral bone that eventually result in clotting at the site of defect and a natural repair response being induced. This response leads to the formation of fibrocartilage repair tissue. Fibrocartilage tissue is undesirable as it is less resilient than articular cartilage, and mechanically speaking the properties fail to match that of the native cartilage (Buckwalter & Mankin, 1998a; Caplan et al., 1997). Such marrow stimulation techniques are considered to be effective only in younger patients without any prior surgical intervention (Demange et al., 2014; Mithoefer et al., 2009), and the size of the defect that can be treated by marrow stimulation technique is limited to 2 to 4 cm². Further, this technique is ineffective for the femoral condyle region (Gudas et al., 2005; Kreuz et al., 2006).

2.5.2 Osteochondral Grafting

Tissue transplantation of periosteum, perichondrium or osteochondral grafts is used for regeneration of hyaline cartilage (Bouwmeester et al., 1997; Buckwalter & Mankin, 1998a; Hunziker, 2002). The most common approach is to harvest osteochondral cylinders from the donor site and then fit them into holes already drilled in areas of defect. The drilled areas are filled via one or more grafts that range from 5 to 11 mm in diameter while their lengths are 13 to 15 mm (Hangody, 1997). Studies have shown mixed results in cases of osteochondral transplants. Reduced pain and improved function was reported after 6.5 years by Outerbridge et al. (Outerbridge et al., 1995). In two separate studies by Jakob et al. (Jakob et al., 2002), and Hangody et al. (Hangody et al., 2001) improved knee function and good results were reported in more than 90% of patients. In contrast, Laprell and Petersen reported a normal knee in fewer than 50% of patients after a follow up of 6 to 12 years (Laprell & Petersen, 2001). A major limitation of this approach is the availability of tissue where there are large cartilage defects. Further, long term follow up is missing and this technique is reported to be most appropriate for patients less than 35 years of age (Buckwalter & Mankin, 1998a; Caplan et al., 1997; Hunziker, 2002; Insall, 2001). In addition, osteochondral transplantation is associated with some post-operative complications. The accumulation of water (joint effusion), bleeding in joint spaces (hemarthrosis), and persistent swelling have all been reported after osteochondral transplantation (Bobic, 1999; Bös et al., 2000; Hangody et al., 2001; Hunziker, 2002). Researchers have also reported loose bodies, donor site pain, and avascular necrosis as other post-operative complications that emanate due to osteochondral transplantation (Aigner & Fan, 2003).

2.5.3 Autologous Chondrocyte Transplantation

Due to the failure of osteochondral transplantation, autologous chondrocyte transplantation was developed and used since 1994 by Brittberg and coworkers (Brittberg et al., 1994). Autologous chondrocyte implantation (ACI) is considered to be used as the last line of defence when other techniques fail. ACI is considered able to repair full-thickness lesions in cartilage up to 16 cm². This technique involves isolation of a patient's own cells grown in-vitro then implanted at the site of the defect. The follow up results of ACI after 2 to 9 years have reported a failure in more than 30% patients after treatment of multiple lesions. Furthermore, patients with patella lesion treatment demonstrated more than 30% failure, but isolated cartilage lesion treatment displayed less than 10% failure (Peterson et al., 2000). Another long-term follow up study by Harris J. D. et al. sought to determine if current literature supports ACI over other interventions. They observed that ACI can only be helpful over other interventions if the size of defect is greater than 4 cm². ACI or micro fracture or osteochondral transplants, in summary, only provide short term success. (Harris et al., 2010) A study by Niemeyer P and co-workers reported that complications like graft failure, delamination, chondromalacia (softening of cartilage) and hypertrophy can arise after ACI (Niemeyer et al., 2008). More recent reports by Harris J. D et al. have reported decreased failure rates (up to 7.5 %) for ACI, however there are other reports that continue to demonstrate inconsistent outcomes of ACI without any clear recommendation. Furthermore, it was also reported that the differences between various treatments were so small that their clinical significance is questionable, beyond mere statistical significance (Vavken & Samartzis, 2010). Lately it was reported that ACI improves movement significantly after at least 24 months (von Keudell et al., 2016).

2.6 Cartilage Tissue Engineering

Current treatment options, like ACI, Osteochondral transplants and marrow stimulation have demonstrated variable success rates, however more long-term results are not satisfactory (Kreuz et al., 2006; Niemeyer et al., 2008; Redman et al., 2005; Vavken & Samartzis, 2010). The major limitation that arises due to the use of the aforementioned therapeutic techniques for cartilage repair is the lack of mechanical properties of newly formed tissue compared to native articular cartilage tissue. Due to these inferior mechanical properties, the newly formed tissue is prone to failure (Hunziker, 2009). Cartilage tissue engineering strategies contribute to a durable and functional replacement option, beyond any other surgical intervention or technique (Kock et al., 2012).

Tissue engineering is a 3 tier based approach, involving the combination of living cells, a cell signalling strategy, and a scaffold (Hendrich et al., 2003). Cartilage tissue engineering allows researchers a great deal of flexibility in combining various techniques independently and in combination to address the issue of cartilage repair. Cartilage tissue engineering also allows the selection of various cell types to be implemented in-vitro for a better understanding of cartilage repair. Moreover, researchers have shown positive effect of signalling molecules in enhancing anabolic effects and increased ECM synthesis (Elder & Athanasiou, 2009; Seifarth et al., 2009). Further, a widely researched area for better fabrication of cartilage tissue is external mechanical stimuli. Direct dynamic compression has been demonstrated to increase ECM production while improving the compressive properties of the engineered tissue (Bian et al., 2010; Chen et al., 2015; Luo et al., 2015). Another leverage given by a cartilage tissue engineering strategy to the researchers is modification of the properties of scaffolds. Scaffolds provide a temporary frame for the cells to attach to and proliferate while the tissue is being formed and the scaffold is being degraded. Recent publications have shown enhanced mechanical and biological properties of newly fabricated tissue using polymeric scaffolds (Camarero-

Espinosa et al., 2016; Schulze-Tanzil, 2015). Various cartilage tissue engineering studies have been undertaken to engineer a tissue with native sGAG content. However, they have failed to achieve the collagen content present in native articular cartilage, and which gives the cartilage its tensile properties (Eyrich et al., 2007; Kock et al., 2012). Though there are many advantages to cartilage tissue engineering, nevertheless finding optimal cell source is the first issue, followed by choice of scaffold material, the role and the effect of biochemical and mechanical stimulus and lastly tackling any infection that might occur due to surgical intervention, amongst others are pitfalls that need to be addressed (Bhattacharjee et al., 2015; Kock et al., 2012). Gaut C. and Sugaya K. recently suggested that in order to obtain a clinically effective solution for cartilage tissue engineering; a combination of factors is required, such as; cell signalling, scaffold material, mechanical and biological stimulus must be considered (Gaut & Sugaya, 2015).

Given the clear advantages of Cartilage Tissue Engineering, but yet the continued inability to fully restore cartilage functionality in the long term, the present study seeks to further advance this technique toward an effective and lasting repair.

2.6.1 Cell Sources

A source of cells is one of the key components of a Tissue Engineering strategy. There is no current consensus on the optimal source of cell for cartilage tissue engineering, with division between the use of stem cells, fibroblasts, or chondrocytes – each with their relative merits and disadvantages.

Stem cells are particularly attractive due to their differentiation potential and the fact they may be harvested from various tissues. Though stem cells overcome the problem of limited supply of cell as they can be easily harvested from the patient's body itself (from bone marrow (Boeuf & Richter, 2010) and adipose tissue (Gir et al., 2012)), bone marrow stem cells have lower mechanical properties and matrix synthesis when compared to chondrocyte seeded scaffolds (Thorpe et al., 2010) and adipose stem cells demonstrate a

lesser potential than bone marrow stem cells despite being capable of being differentiated into chondrocytes (Kock et al., 2012). Furthermore, embryonic stem cells tend to differentiate hypertrophically and moreover, there exists many ethical and legal issues to overcome before considering embryonic stem cell use (Jukes et al., 2008). Mesenchymal stem cells are another potential source, however they have demonstrated high cartilage hypertrophy markers such as Collagen type X (*COL X*) & Matrix (*MMP-13*) (Mueller & Tuan, 2008).

Chondrocytes are well suited to cartilage tissue engineering because they are the native cells of cartilage tissue (Nicoll et al., 2001). However, they have limited availability and generally need to be harvested from a monolayer to get an high number of cells, meaning they eventually lose their cell phenotype (Cournil-Henrionnet et al., 2008).

Another potential source of cells for cartilage tissue engineering are the articular cartilage progenitor cells that are useful in producing the amount required for cell culture but do not have the capability to produce cartilage matrix (Zhou et al., 2014). It is reported that they may also cause donor site morbidity (Mathur et al., 2012).

A new approach should be using chondrocytes in an in-vitro culture systems that mimics the native environment to overcome the limitation of limited cell numbers and allows maintenance of cell phenotype.

2.6.2 Cell Signalling Strategies

A key aspect of Tissue Engineering is the integration of a cell signalling strategy alongside the cellular and scaffold components. This may include aspects such as biochemical cues, facilitation or stimulation of cell-cell interactions, biomechanical signalling, or manipulation of the environmental factors involved.

Human body tissues have various associated stimuli that help regulate normal function of the tissue. Whether it is electrical, mechanical, or chemical, body tissues undergo different kinds of stimulus; heart tissues undergo electrical stimulation (Cannizzaro et al.,

2007; Godier-Furnémont et al., 2015), bone tissues are subjected to tension and compression (Nyman et al., 2009; Romanos et al., 2015), and similarly, cartilage tissue undergoes compression, hydrostatic pressure, and shear strain (Ryan et al., 2009; Schätti et al., 2015). Cartilage tissue also experiences a unique stimulus, which is tension in oxygen (Portron et al., 2015). This is mainly due to the avascular nature of cartilage tissue (Hansen et al., 2001). When considering cartilage tissue, in particular, successful tissue engineering will be incomplete without a mechanical stimulus and low oxygen tension.

2.6.2.1 Mechanical stimulus

In the last decade, researchers have increasingly realised the importance of external mechanical stimuli to enhance the quality of produced cartilage (Temenoff & Mikos, 2000). However, much conflicting information has been reported regarding how chondrocytes behave in response to mechanical stimulation (Lee et al., 2005).

Physiologically, articular cartilage primarily undergoes compression at joint level (Lee et al., 2005). In an average human pressure of up to 1MPa during standing, 0.4MPa while walking, and up to 20MPa while standing up from a chair have been reported (Gooch & Tennant, 1997; Lee et al., 2005; Urban, 1994). A range of factors are affected by the compressive loading of articular cartilage. These include biochemical and physical gradients of nutrients, ion concentrations, electrical charge, and pH (Gray et al., 1988; Guilak et al., 1995). Different studies have shown that a mechanical stimulus positively influences cartilage development (Heath & Magari, 1996). The way ECM is composed and organised provides the cartilage with its biomechanical properties. The presence of type II collagen helps strengthen the cartilage while proteoglycans build up compressive resistance in the cartilage (McMahon et al., 2008). Grodzinsky A.J. and co-workers reported that mechanical stimuli on chondrocytes is essential in order to maintain the integrity of cartilage (Grodzinsky et al., 2000).

In its native environment cartilage is usually compressed to about 10% (Sanchez-Adams et al., 2014). Various studies showcase the importance of dynamic compression. Researchers have studied the effects of compressing the cartilage from about 5% to 50% with frequencies ranging from 0.001 Hz to 1Hz using various polymers and gel constructs (Albro et al., 2013; Appelman et al., 2011; Chen et al., 2015; Chowdhury et al., 2006; Chowdhury et al., 2003; Davisson, Twana et al., 2002; Démariseau et al., 2003; Di Federico et al., 2014; Hunter et al., 2002; Jeon et al., 2012; Kisiday et al., 2004; Li et al., 2013; Morel et al., 2005; Piscoya et al., 2005). The majority of the researchers have favoured dynamic compression and have demonstrated a higher GAG content with better cell proliferation and increased cartilage matrix specific gene expression of Type II collagen (*COL2A1*) and Aggrecan (*ACAN*) (Appelman et al., 2011; Chen et al., 2015; Davisson, Twana et al., 2002; Jeon et al., 2012; Kisiday et al., 2004). However, contradicting results are present for the amount of compression. Some studies support dynamic compression in the range of 0.001% to 31% (Appelman et al., 2011; Chen et al., 2015; Davisson, Twana et al., 2002; Démariseau et al., 2003; Jeon et al., 2012) while others have reported detrimental effect of dynamic compression ranging from 15% and up to 50% (Davisson, Twana et al., 2002; Di Federico et al., 2014; Hunter et al., 2002; Li et al., 2013; Piscoya et al., 2005). From the current literature it is evident that a dynamic compression beyond physiologic levels of 10% has proved to be detrimental for cartilage. One thing is noteworthy here: most of the studies executed to study the behaviour of cartilage tissue or cartilage cells are performed on agarose, hydrogels, alginate and type I collagen gels. All the aforementioned constructs/ gels can only be used in laboratory settings and lack the physical capabilities to be implanted clinically. Limited groups have reported dynamic compression on polymer/ polymer composite scaffolds which they deem to be physically compatible. Another important factor that seems neglected in the current study is the physiologic oxygen level. The majority of the studies of dynamic

compression in the domain of cartilage tissue engineering were carried out under normal oxygen settings without comparing the effect of atmospheric and physiologic oxygen concentration on dynamic compression.

2.6.2.2 Oxygen Tension/Hypoxia

Research suggests that the nature of articular cartilage is avascular; hence it receives its required nutrients and oxygen by synovial fluid following a passive diffusion mechanism (Malda et al., 2003). In relation to rest of the body tissues, articular cartilage experiences oxygen concentrations in the range of 1% to 10% as compared to 21% for other tissues (Co et al., 2014). Chondrocytes are reported to thrive in oxygen concentration range of 5% to 10% (Grimshaw & Mason, 2000), while losing their activity in anoxic conditions because 1% of Oxygen concentration is reported to exist in an abnormal or due to any pathological condition (Grimshaw & Mason, 2000; Zhou et al., 2004). Hypoxia Inducible Factors are responsible for chondrocytes adapting to low oxygen tension (Fedele et al., 2002). Various researchers have reported that hypoxia in chondrocytes has resulted in increased synthesis of ECM proteins in in-vitro conditions (Domm et al., 2002; Madeira et al., 2015; Yodmuang, Marolt, et al., 2015). Inhibition of collagen type X had also been demonstrated by inducing hypoxic conditions. The Collagen type X is major marker of hypertrophy in chondrocytes during the chondrogenesis of adipose-derived mesenchymal stem cells (Betre et al., 2006; Portron et al., 2015) and of epiphyseal chondrocytes (Chen, X. C. et al., 2006). A transcription factor, Hypoxia inducible factor 1 (HIF-1) is mainly responsible for regulation of hypoxic response in the cartilage tissue (Schipani et al., 2001). HIF-1 α is said to be responsible for angiogenesis and glycolysis while at the same time causing cells to proliferate (Denko et al., 2003; Goda et al., 2003). Hypoxia further plays a role in formation of collagen fibrils with the help of transcription factor HIF-1 α (Takahashi et al., 2000). Current research has reported an individual role of hypoxia for better engineered cartilage, however, not enough details are present in the current

literature as to how hypoxia will behave in combination with other bio-factors for cartilage tissue engineering.

However, many studies have highlighted the importance of hypoxia as a success for tissue engineering of cartilage (Meretoja et al., 2013; Munir et al., 2014; Schipani et al., 2001). Researchers have shown that hypoxia induces ECM synthesis in in-vitro chondrocyte culture (Domm et al., 2002) and also helps chondrocytes to proliferate (Choi et al., 2014). Another important research by Schipani E. et al. demonstrated that lack of hypoxia causes chondrocytes to terminally differentiate (Schipani et al., 2001). A study by Hansen U. et al. reported a combination of hypoxia and hydrostatic pressure to enhance collagen type II production while delaying expression of Collagen type I for in-vitro cartilage tissue engineering (Hansen et al., 2001). Further research has also displayed the potential of low oxygen tension to enhance Aggrecan and Collagen type II gene expression while decreasing Matrix Metalloproteinase – 13 (a pro catabolic gene) expression (Parker et al., 2013). Most of the studies were executed on chondrocytes on Tri Calcium Phosphate (TCP) plates (Hansen et al., 2001), under agarose gel (Chowdhury et al., 2006; Parker et al., 2013) or Alginate (Jeon et al., 2012). Others have used PEG (Appelman et al., 2011), PGA (Davisson, Twana et al., 2002), or articular cartilage explants (Piscoya et al., 2005). However, the above mentioned studies did not use scaffolds able to be used clinically as they either lack the requisite mechanical properties or do not mimic native cartilage structure in-vivo.

2.6.3 Tissue Engineering Scaffolds

Different natural and synthetic materials have been tested as scaffolds. Scaffolds have been developed by natural polymers (Van de Putte & Urist, 1965; Vandeputte & Urist, 1965), synthetic polymers (Elisseff et al., 1999; Meinig et al., 1997), composites (Peter et al., 1998; Zhang & Ma, 1999) and ceramics (Friedman et al., 1998; Hollinger & Battistone, 1986). Synthetic scaffolds have copious benefits such as a greater availability,

decreased risk of disease transfer, fabrication as per requirement, and the ability to be shaped into various shapes and sizes (Jeuken et al., 2016).

Just saying that a material should be biocompatible does not solve all the complications.

A tissue engineered scaffold should be readily available to the surgeon; it should promote cell ingrowth as well as it must degrade in correct ratio with formation of new tissue (Holmes, 1979; Levine et al., 1997). Also it should be able to fit into irregular places and must be soft enough to mould and hard enough to withstand the mechanical loads in daily routine activities (Lichte et al., 2011), meaning that the scaffold should possess mechanical strengths of site where it needs to be implanted. The architectural properties of the scaffold; which includes pore size and porosity, should be in relation to the actual tissue (Peter et al., 1998). The scaffold should also promote cell adhesion and proliferation (Lichte et al., 2011). Additionally the design of a scaffold should be biomimetic, implicating it must imitate all the characteristics of the tissue where it is going to be implanted; whether they are physical chemical or biological properties.

For the aforementioned reasons the polymeric scaffolds are a promising new approach towards tissue engineering for repairing cartilage defects. However, use of polymeric materials alone or with composites as cartilage tissue engineering scaffolds remains largely unexplored.

Various materials have showed their ability to be used as engineered tissues; this includes metals, ceramics, polymers and their combinations (Burg et al., 2000; Hidalgo-Bastida et al., 2007; Hollinger & Battistone, 1986; Liu & Ma, 2004). Among these only using materials and ceramics independently results in lack of degradability and processability. On the contrary, if polymers are used with metals and ceramics they allow tailored properties and proper biodegradability. Various scaffolds based on polymers and polymer composites are being developed that demonstrate a promising future (Burg et al., 2000; Liu & Ma, 2004; Peter et al., 1998).

Particularly for cartilage tissue engineering, various polymers and polymer composites have been used. Polymers such as Poly (ϵ -caprolactone) (Li, W.-J. et al., 2005), poly (D, L – Lactic acid-co-glycolic acid) [PLGA] and PLGA with Hyaluronic based polymers (Yoo et al., 2005), polyurethane based polymers (Grad et al., 2003), poly (ethylene glycol)-terephthalate and poly (butylene terephthalate) based polymers (Woodfield et al., 2004), poly (D, L – Lactic acid) [PLA] based polymers (Camarero-Espinosa et al., 2016), collagen/PLA and Chitosan/PLA polymers (Haaparanta et al., 2014), poly(γ -propargyl-l-glutamate) (PPLG) polymers (Ren et al., 2015), Poly (glycerol sebacate) [PGS] (Kemppainen & Hollister, 2010), and Polyoctanediol citrate polymers (Jeong et al., 2011).

Among several polymers and polymer composites, Poly 1, 8 Octanediol Citrate (POC) stands as a potential candidate due to its mechanical and chemical properties that suffice for cartilage tissue engineering applications. POC has proved to enhance cell attachment and helps in proliferation of cells, furthermore POC has been shown to enhance matrix production when seeded with chondrocytes (Kang et al., 2006). Studies have also reported POC polymer to be more effective than other polymers (PGS & polycaprolactone (PCL)) in enhancing chondrogenesis (Jeong & Hollister, 2010). Moreover, its physical properties can be tailored to those of native articular cartilage (Kang et al., 2006; Moutos et al., 2007).

2.7 Poly Octanediol Citrate (POC)

2.7.1 POC, its structure, synthesis, and form

Poly 1, 8 Octanediol Citrate (POC) elastomer is a synthetic polymer that is synthesised from cost efficient and non-toxic monomers; 1, 8 Octane diol and citric acid (CA). POC polymer was first fabricated in 2004 (Yang et al., 2004). Since then it has gained popularity in the field of tissue engineering. Among its advantages; non-toxic monomer,

catalyst free polymerisation and good cell adherence are most notable (Yang et al., 2004). Other properties include; simple synthesis, controllable mechanical and degradation properties and easy processing. In case of POC, CA which is a polyfunctional monomer reacts with a difunctional 1, 8 Octanediol monomer to form a crosslinked polyester network. CA is a non-toxic polyfunctional monomer because it is a by-product of kerbs cycle in body. Furthermore, it is readily available, inexpensive and it is Food and Drug Administration (FDA) approved to be used in humans (Shi et al., 2007). Moreover, CA can participate in hydrogen bonding in a polyester network (Yang et al., 2004; Zhang et al., 2004). The presence of –COOH groups due to CA helps in covalent attachment of ECM proteins and growth factors (Goddard & Hotchkiss, 2007). Presence of –COOH is a feature that is important in polymers for biomaterial applications (Li, B. et al., 2005; Sun et al., 2004). The second constituent of POC is a difunctional monomer; 1, 8 octanediol which is the largest water soluble aliphatic diol that is soluble in water without any reported toxicity (Webb et al., 2004). This means 1, 8 Octanediol does not leave any insoluble complexes when dissolved, a property beneficial for degradation.

2.7.2 POC as a biomaterial

Since its inception, POC has been used for cardiac (Hidalgo-Bastida et al., 2007), vessels (Jiang et al., 2015), bone (Guo et al., 2015), bladder (Sharma et al., 2010), cartilage, calvarial (Sun et al., 2014) and other biomedical applications (Hege & Schiller, 2015; Zhao et al., 2014). POC is attractive as its mechanical and degradation properties can be tailored (Ji et al., 2014; Yang et al., 2004). In a study by Hidalgo-Bastida L. A. et al., it was reported that POC demonstrated a good support for cardiac muscle engineering by exceeding the required mechanical properties in terms of elongation at break which complies with that at physiological level. Furthermore, it has been reported that POC scaffolds displays preference for HL-1 cells (Hidalgo-Bastida et al., 2007). POC is also used for large bone defects by Guo Y. and co-workers. They reported bone tissue

ingrowth and efficacy of POC for osteoinductive and osteoconductive behaviour. This potential of POC was due to citrate, as it allows better bone formation (Guo et al., 2015). Other studies have also reported the advantage of citrate based materials to enhance cell proliferation, excellent biocompatibility and osseointegration (Gyawali et al., 2013; Qiu et al., 2006; Tran, R. T. et al., 2014). Another desired feature of POC is its hydrophilicity. Higher hydrophilicity in POC is attributed to better water absorption capabilities that may result in better cell attachment (Zeimaran et al., 2015). More recently pure-POC was used in association with other monomers (POC-co-glycidyoxypropyl-trimethoxysilane and POC-co-aminopropyl-triethoxysilane) to study the effect of silica incorporation. The resulting elastomer was tested for thermal stability, mechanical properties, in-vitro cellular compatibility, degradation and cell proliferation and metabolic activity to be used in various biomedical applications. It was found that mechanical properties, thermal stability and degradation can be controlled easily by tuning monomer concentration. However, this was achieved at the loss of hydrophilicity (Du et al., 2015).

2.7.3 POC in cartilage tissue engineering

The potential of POC in the domain of cartilage tissue engineering was evaluated first by Kang Y. et al (Kang et al., 2006). They reported an excellent recovery of 98.7% of pure-POC scaffolds. Furthermore, they compared pure-POC scaffolds with Alginate, Agarose, Poly (glycolic acid) (PGA) and Poly-L- Lactic acid (PLLA) scaffolds. Agarose was reported to be fragile while Alginate constructs deformed without good recovery time as in case of POC scaffolds. Moreover, PGA and PLLA scaffolds never returned to their original state after compression. In the same study GAG and Type II collagen content was reported to increase along with increase in cell number (Kang et al., 2006). In a different study, Jeong C.G. et al. and co-workers compared pure-POC scaffold with poly (glycerol sebacate) (PGS) and well-known and FDA approved polycaprolactone (PCL) for cartilage tissue engineering purpose (Jeong & Hollister, 2010). They kept pore size,

porosity, pore shape and surface area the same for all the scaffold materials. The results were in favour of POC as higher Deoxyribonucleic acid (DNA) content, increased cell proliferation, enhanced cartilaginous matrix production, and cartilage specific gene expression was observed when compared to PCL or PGS scaffolds. Moreover, POC demonstrated decreased MMP-13 expression when compared to PGS scaffolds (Jeong & Hollister, 2010). It is noteworthy because MMP-13 takes part in cartilage matrix destruction and aggrecan degradation (Burrage et al., 2006; Wang et al., 2013). A more recent study reported a preference for clickable POC-hydroxyapatite (HA) polymer over other renowned polymers like β -tricalcium phosphate (β -TCP), PLLA, PGA and their copolymers due to their brittleness, poor degradation, low biocompatibility, and diminished mechanical properties (Stewart et al., 2004; Yang, W. et al., 2014). Furthermore, they reported excellent cartilage formation for spinal fusion; a surgical intervention to join two or more vertebrae in order to reduce movement between them. Histological evidence demonstrated that POC supported cartilage formation within the material pores (Tang et al., 2015).

Though POC is gaining fame in various areas of tissue engineering applications (Guo et al., 2014; Guo et al., 2015; Hege & Schiller, 2015; Tran et al., 2015; Zeimaran et al., 2015), nevertheless its use in the domain of cartilage tissue engineering has a great potential to be further explored. Being a synthetic biomaterial POC holds great promise as the most interesting part of this polymer is that its mechanical and chemical properties can be tailored as per need to adapt for a wide range of applications.

2.8 Infection and Anti-bacterial scaffolds

Thousands of surgeries are performed daily round the world, and more and more people are benefitting from these procedures but, at the same time they are being placed at risk of microorganisms that may create a problem later via formation of biofilms at the implant site, tissue implant, or at the site of sutures.

A biofilm is a layer made up of microorganisms that tends to develop at the site of an implant or surgery or tissue that has been operated upon. It is a community of bacteria living in layers. These layers can be formed on biotic, abiotic and even on human tissues (Hoffman et al., 2005). The gravity of this problem can be so high at times that there is a need for removal of implants (Pawlowski et al., 2005). As the number of biomaterial implants increases, there is a requirement of more inert and more biocompatible biomaterials. This is due to the fact that whenever an implanted biomaterial gets infected, the infection is not just limited to the biomaterial itself; rather it affects the adjacent tissue or bone. Ultimately the outcome may be devastating as there may be a need for reoperation, amputation, and at times death (Gristina et al., 1989).

Biofilms can cause the bulk of microbial infections in the body. Extensive literature is available that communicates clearly the areas affected by biofilm formation; this includes urinary tract infections (Hoffman et al., 2005), middle-ear infections (Pawlowski et al., 2005), oral implant infections (Heuer et al., 2007), infections after surgery (Singhal et al., 2010) and on polymeric implants as well (Pavithra & Doble, 2008).

Many scientists around the world are working on how to cope with the formation of biofilm. Many techniques have been devised to treat the problem of biofilm formation. The scientists have tried numerous techniques for the prevention of biofilms; but using antibiotics (Burns et al., 1993; Costerton et al., 1999; Hoiby, 1993) and coatings incorporated with different antibacterial materials (Bakhshi et al., 2012; Paladini et al., 2012; Regina et al., 2012) remains most promising against the bacterial biofilms.

Using antibiotics may be helpful in short term efficacy to prevent bacterial infections and it may be used for catheters, sutures and surgical instruments. However, for long term applications like cardiac assist devices, bone implants and tissue implants, a material is needed with no degradation at all or a long degradation time. For tissue engineering

applications different scaffolds are now being developed that have showed successful results for cell compatibility but there is a void space in relation to antibacterial scaffolds. Things began to change in the 90's and much work was undertaken on incorporation of different anti-bacterial materials to be used in dental (Guigand et al., 1997; Imazato et al., 1995; Morrier et al., 1998; Torabinejad et al., 1995) and wound dressing applications (Blaker et al., 2004; Kudi et al., 1999; Stashak et al., 2004) and their antibacterial activity was measured.

It is not known when the first research for antibacterial scaffolds started but the idea of incorporating antibacterial materials flourished in late 90's and in past decade when antibacterial materials were being suggested to be used as coatings for implantable medical devices (Fu et al., 2005) and dental materials (Guigand et al., 1997; Imazato et al., 1995; Morrier et al., 1998; Torabinejad et al., 1995).

Not much is known about the antibacterial scaffolds as it is a relatively new field that is being explored. However, the antibacterial properties of various materials have been studied in different situations. Many materials exhibit antibacterial properties; but for tissue engineering applications there is a need for a material that not only possesses antibacterial properties but also enhances material integrity. The antibacterial effect of metal oxides is much explored and has a promising future, similarly it is also responsible for the mechanical integrity of a material (Fielding et al., 2012; Salinas et al., 2011; Vitale-Brovarone et al., 2008).

More recent studies have reported a selective killing effect of ZnONP by killing all the cancer cells while bearing no harm to healthy human cells (Akhtar et al., 2012; Taccola et al., 2011).

An investigation into the effect of ZnONP on fetal development in rats resulted in no significant toxicity in rats due to excess ZnONP (Hong et al., 2014). Furthermore, recent reports in favour of ZnONP have arisen that demonstrate enhanced angiogenesis due to

the presence of ZnONP (Augustine, Dominic, et al., 2014). The beneficial effects of ZnO for tissue engineering applications are also reported for bone tissue engineering (Feng et al., 2014), vessel tissue engineering (Augustine, Dominic, et al., 2014), dentistry (Toledano et al., 2012) and hip implants (Chang et al., 2014). Zinc is a trace element that is essential for normal growth (Haase & Rink, 2014b). It also plays a significant role in the proliferation of cells, their differentiation and their survival (Haase & Rink, 2014a). Furthermore, Zn deficiency in the diet is reported to result in rheumatoid arthritis (Mierzecki et al., 2011), cartilage defects (Westmoreland & Hoekstra, 1969) and growth retardation (Prasad et al., 1961). More specifically Zn deficiency is reported to inhibit chondrocyte proliferation and cause apoptosis (MacDonald, 2000). In a study by Seo H-J. and co-workers, it was reported that Zn stimulates cell proliferation and synthesis of collagen in osteoblastic cells (Seo et al., 2010). In a comparative study by Helliwell et al., Zn levels were monitored in femoral heads of individuals having fractures of femoral neck and degenerated joints. The study concluded that fractured femoral head (154 µg/g) and degenerated joints (167 µg/g) had lower levels of Zn content than in control group (205 µg/g) (Helliwell et al., 1996). In a separate study it was reported that resting and proliferative regions of growth plate contains high levels of Zn²⁺ ions while they are significantly lower in hypertrophic cartilage zones. They also related chondrocyte apoptosis with diminished Zn levels (Sauer et al., 2003). Addition of Zn also supports chondrocyte proliferation as reported by Koyano Y. and their group (Koyano et al., 1996). Recent studies have advised the use of nano Zn in biomedical applications (Varaprasad et al., 2016). However, to date there are no studies that relate the role of Zinc Oxide nanoparticles (ZnONP) at macro level with chondrocyte proliferation, morphology and its ECM synthesis.

2.9 Antibacterial Activity of ZnO

Zinc Oxide mostly used in industry, including rubber, medicine, cream, lotions, pigments, and food items (Kołodziejczak-Radzimska & Jesionowski, 2014). It is available in the form of oxide in 2 major forms; hexagonal, and cubic (known as wurtzite (Figure 2.2) and zinblende respectively). The former is the most stable and readily available.

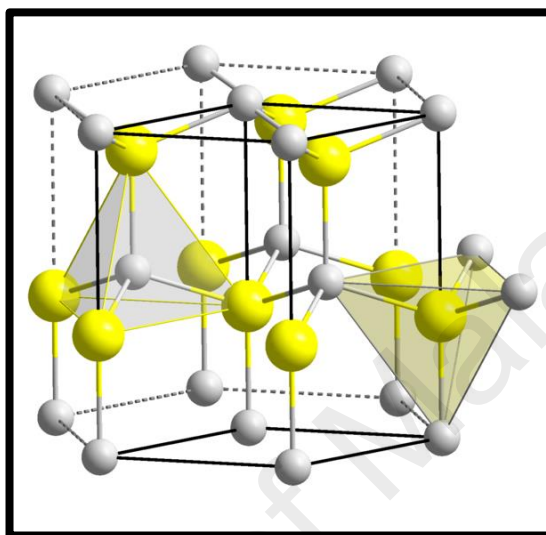


Figure 2.2: Wurtzite structure of ZnO crystal.

Testing of antibacterial properties of oxides dates back to as early as 1978. A team of researchers (Cox Jr et al., 1978) explored antibacterial properties of zinc oxide for dental treatment. They tested zinc oxide against 3 bacterial strains but they failed to deliver. Inhibition of several species was confirmed in 1982 by endodontic gutta-percha cones (Moorer & Genet, 1982). These cones released Zn^{2+} ions slowly and it was concluded that zinc oxide should be used in medicine and dentistry for its antibacterial effect and biocompatible nature, but this research lacked biocompatible testing. Later in 1990, the root canal filling material known as gutta-percha was challenged for its toxicity due to the presence of zinc oxide (Pascon & Spangberg, 1990). It was proved in the same study that zinc oxide displays toxicity, and this was attributed to the leeching of zinc ions into the fluid. In another study, both in vivo and in vitro studies were carried out and zinc oxide was used in root filling cements (Nielsen et al., 1993). The results were successful against streptococcus sanguis, staphylococcus aureus and Prevotella intermedia. Research

was carried out to cater for zinc oxide as an antifungal material (Odell & Pertl, 1995). In this research, the hypothesis that zinc is a growth factor for *Aspergillus* species was tested. Five different strains of *aspergillus* were tested by zone of inhibition method. The results indicated that the incorporation of zinc as dental fillings can inhibit the growth of *Aspergillus*. Other bacterial inhibitory effects in favour of zinc oxide has been tested, few similar successful results for inhibitory effects of zinc oxide were produced by (Gordon et al., 2011; Liedtke & Vahjen, 2012; Skoog et al., 2012) against *Escherichia coli*, by (Gordon et al., 2011; Skoog et al., 2012) against *staphylococcus aureus*, by (Liedtke & Vahjen, 2012) against *Enterococcus faecalis*, and by (Liedtke & Vahjen, 2012; Skoog et al., 2012) against *bacillus subtilis*.

2.10 Motivation for current study

Previously discussed limitations for cartilage tissue engineering strategies suffice us to research degradable, biocompatible and physically strong scaffolds that mimic native articular cartilage properties. Cartilage cells grown in a monolayer culture gradually lose their phenotype by converting to a fibroblastic morphology (Figure 2.3), hence they need to be grown in a three dimensional (3D) culture system that mimics its native environment.

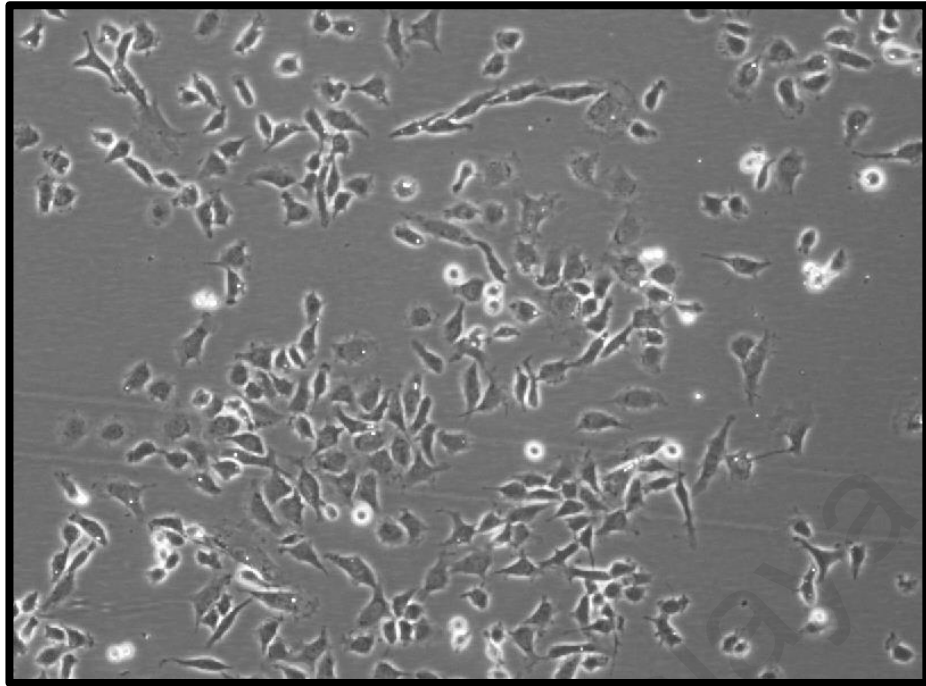


Figure 2.3: Chondrocytes cultured in a T-75 flask losing their morphology and turning flat only after 24 hours of culture.

Furthermore, the problems that arise due to biofilm formation and bacterial infection reinforce the rationale to develop an anti-bacterial scaffold for cartilage tissue engineering without compromising biocompatibility. Zinc Oxide (ZnO) is a potential candidate that has shown anti-bacterial effects on bacteria while demonstrating no confrontational effect on cells. ZnO has also been demonstrated to play a vital role in bone and cartilage generation in early stages, while lower Zn levels are reported to be associated with rheumatoid arthritis.

The majority of the research executed in the domain of cartilage tissue engineering neglects the native environmental factors of mechanical stimulation and low oxygen tension.

The cells in cartilage reside in an environment that is profoundly influenced by mechanical forces. In its native environment cartilage undergoes around 10% compression during routine activities. Biomechanical stimulation plays a major role in upregulation of cartilage matrix specific genes. However conflicting results are present for the type of genes that upregulate during dynamic mechanical compression of cartilage.

Cartilage comprises only one cell type (Chondrocyte) that too is avascular. Another bio factor that researchers neglect is low oxygen tension for cartilage tissue engineering. Low oxygen has been demonstrated to prevent hypertrophy in chondrocytes.

The current thesis describes the detailed fabrication process of a porous scaffold that possesses native articular cartilage properties. Furthermore, in the present thesis the optimised percentage of ZnO nanoparticles (ZnONP) is reported as having an antibacterial effect while demonstrating no adverse effect on chondrocytes. Later in the thesis, the synergistic effect of hypoxia in combination with dynamic mechanical compression is studied. The combination of hypoxia and dynamic mechanical compression gives an insight into the fundamental behaviour of chondrocytes under native 3D environment.

University of Malaya

CHAPTER 3: MATERIALS AND METHODS

3.1 Introduction

This chapter provides all the procured materials used and the methods applied in this research. This chapter describes all the procedures and protocols necessary to repeat the experiment. Section 3.2 describes the preparation of POC pre-polymer, while Section 3.3 describes preparation process of POC scaffolds with varying percentages of ZnONP.

Furthermore, section 3.4 provides the protocol for preparation of Chondrocyte specific medium and isolation of Bovine Articular Chondrocyte (BAC) cells from cow legs. Section 3.5 elaborates cell viability assay to assess the number of viable cells after isolation from cow legs.

The protocol to perform biochemical assays for DNA quantification and production of S-GAGs are presented in sections 3.6 and 3.7 respectively.

Finally this chapter describes the protocol to assess the regulation of cartilage specific genes (*COL2A1* and *ACAN*), hypoxia inducible gene (*HIF1A*), and genes for catabolic destruction of cartilage (*MMP-13*), in section 3.8.

3.2 Preparation of POC pre-polymer

To fabricate scaffolds from POC, it needs to be derived from a viscous pre-polymer solution by heating Citric Acid (CA) and 1, 8 Octanediol (OD) in calculated ratios. A pre-polymer solution of POC was synthesized by a polycondensation reaction. A polycondensation reaction is one in which water between alcohol and acid is eliminated, forming a polyester. In the current study monomers 1, 8 Octane diol (OD) (Sigma #O3303) and Citric acid (CA) (Sigma #C0759) were reacted in the ratio of 1:1 molecular weight.

Equal ratios, according to the molecular weights of the OD and CA monomers, were placed in a 250 ml two-neck round bottom flask (Fisher #12418996) and heated in a

silicon oil (Sigma #85409) bath gradually to 165-170 °C with constant stirring induced by a magnetic stirrer for 10 – 15 minutes. Once the contents in the round bottom flask melted completely and the mixture became transparent, the temperature was lowered to 140-145 °C for a further 45 minutes with continuous stirring. One neck of the round bottom flask was fitted with a nitrogen (N₂) inlet while other was covered with perforated foil. Throughout the reaction a constant purge of N₂ gas was allowed inside the flask to remove water build-up due to condensation. An overview of the reaction process is provided in Figure 3.1-A. while its synthesis scheme is shown in figure 3.2-B

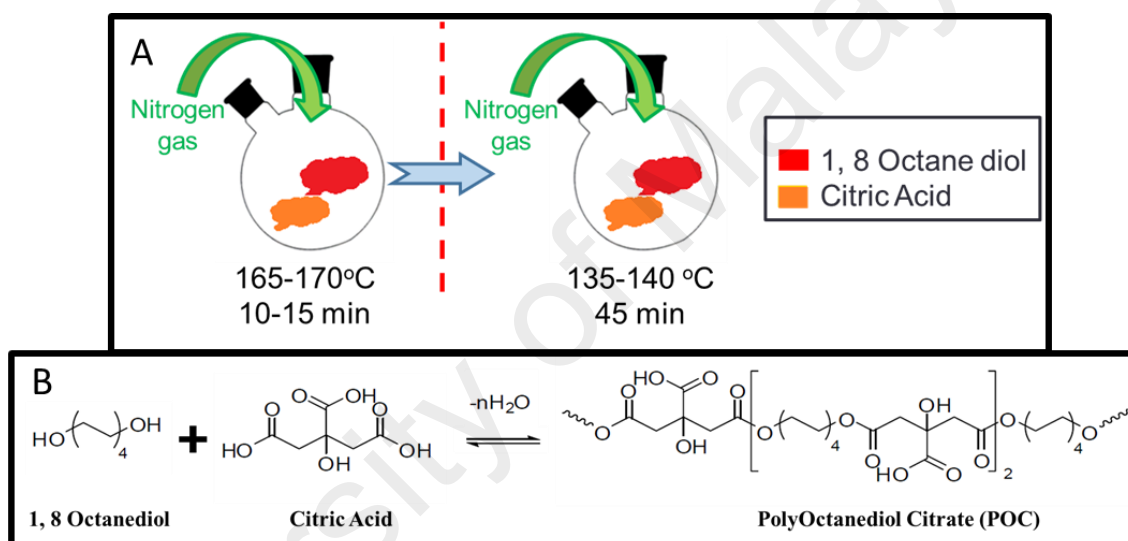


Figure 3.1: (A) The reaction scheme of POC pre-polymer fabrication via the polycondensation reaction in a two necked round bottom flask with a nitrogen purge to remove excess water content. (B) Synthesis scheme of monomers reacting to form POC polymer.

At the end of 45 minutes the pre-polymer solution was then taken out in a sterile glass petri dish (Duran) with the help of a sterile spatula and stored between 4 – 8 °C until further use.

3.3 Fabrication of POC and ZnO-POC composites

Pure-POC scaffold and 3 different ZnO-POC composite scaffolds with varying w/w percentages of ZnO NPs (1%, 3% and 5%) were prepared. ZnONP were obtained from Sigma-Aldrich (Sigma #544906). The particle size for ZnONP was less than 100 nm. Their specifications and raman FTIR are attached in appendix I. All scaffolds were prepared by dissolving POC pre-polymer in 1, 4 Dioxane (50% w/v) (Sigma #360481); for fabricating ZnO-POC scaffolds, an additional step was involved by adding pre-calculated amounts of ZnO (Sigma #544906) (1%, 3% and 5% w/w with respect to weight of the pure pre-polymer) to Pure-POC pre polymer solution. The POC-ZnO-dioxane mixtures were sonicated (Sono Swiss SW12H, Sonoswiss AG, Ramsen, Switzerland.) for 10 minutes for homogenous distribution of ZnONP (Pure-POC-dioxane mixture was also sonicated to follow uniform procedure). This was followed by adding sieved Sodium Chloride (NaCl) (Sigma #S7653) crystals of size 200 – 300µm the ZnO-POC mixture (NaCl/ZnO-POC = 9:1). The composite ZnO-POC-NaCl-dioxane slurry was poured in custom designed Teflon™ moulds and placed for solvent evaporation and curing at 80°C for 1 week in an oven (Mettmert GmbH, Schwabach, Germany). During the curing process, the slurry in Teflon moulds was mixed via spatula every 2 hours for 24 hours to enhance elimination of trapped Dioxane. Steps involved in pre-polymer fabrication are illustrated in Figure 3.2.

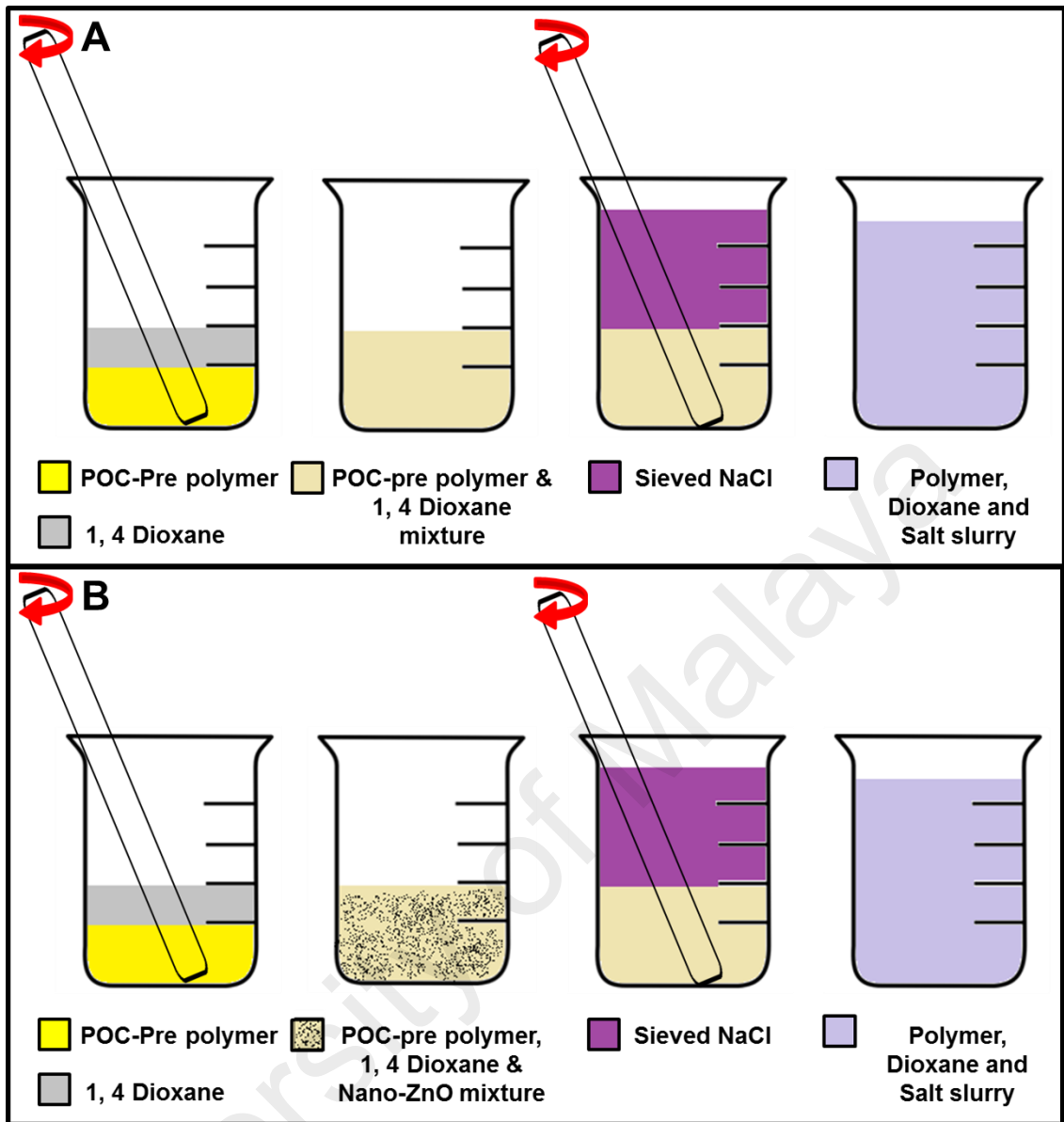


Figure 3.2: Steps involved in fabrication of (A) Pure-POC and (B) POC-ZnONP scaffolds, films and coatings prior to curing.

Following the curing period, the solidified blocks of each of four samples (Pure-POC, 1%, 3% & 5% ZnO-POC) were removed from TeflonTM moulds and placed in a custom designed rack as shown in Figure 3.3, to separate Pure-POC scaffold from ZnO-POC scaffolds and to leach out the salt with sequential progressions in distilled water for 5 days at room temperature.

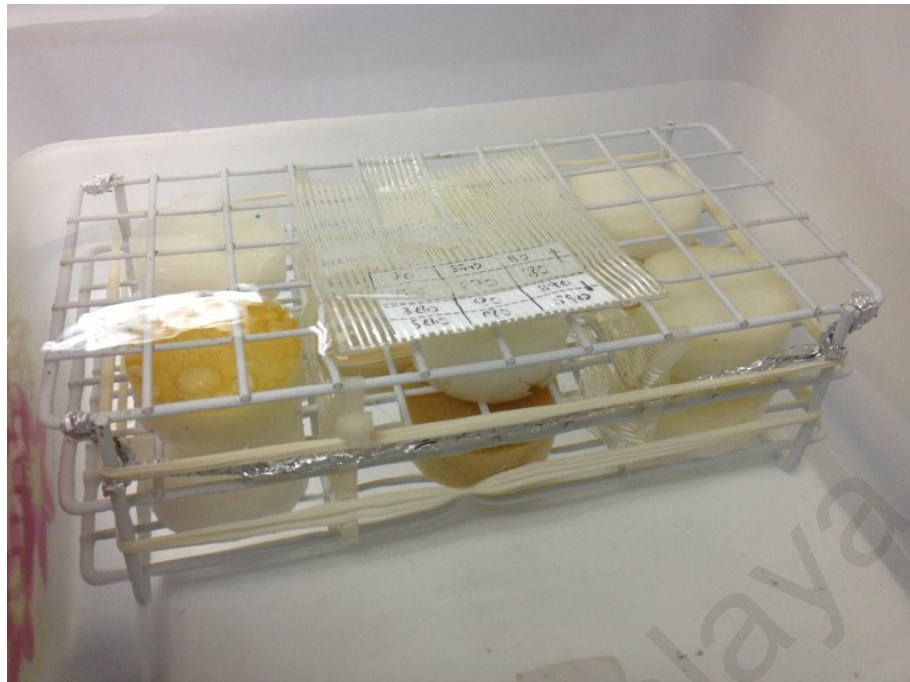


Figure 3.3: A custom-designed rack placed under water to categorise Pure-POC scaffolds from ZnO-POC scaffolds and to leach out the salt from scaffolds.

Scaffolds were frozen in -80°C (Thermo Scientific, Waltham, MA, USA) for 1 hour and sliced (~ 6 mm thickness) using a stainless steel blade. The slices were further cut using a cork borer to produce cylinder-shape samples 6 mm in diameter. All samples were freeze-dried (FreeZone 2.5, Labconco, Kansas, USA) for 24 hours and were kept in a desiccator until further use. Pure-POC Scaffold was used as control in all measurements.

3.4 Chondrocyte Isolation

Chondrocytes were isolated from bovine metacarpal-phalangeal joints of cattle less than 2 years old. Cow legs were obtained within 4 hours of slaughter. The legs were thoroughly washed with hot running water and washing detergent. After the wash, legs were soaked for 45 minutes in 70% ethanol. Joints were opened using scalpel handle number 4 and full thickness cartilage explants from articular cartilage were sliced using scalpel handle number 3. A brief illustration of the procedure is provided in Figure 3.4.

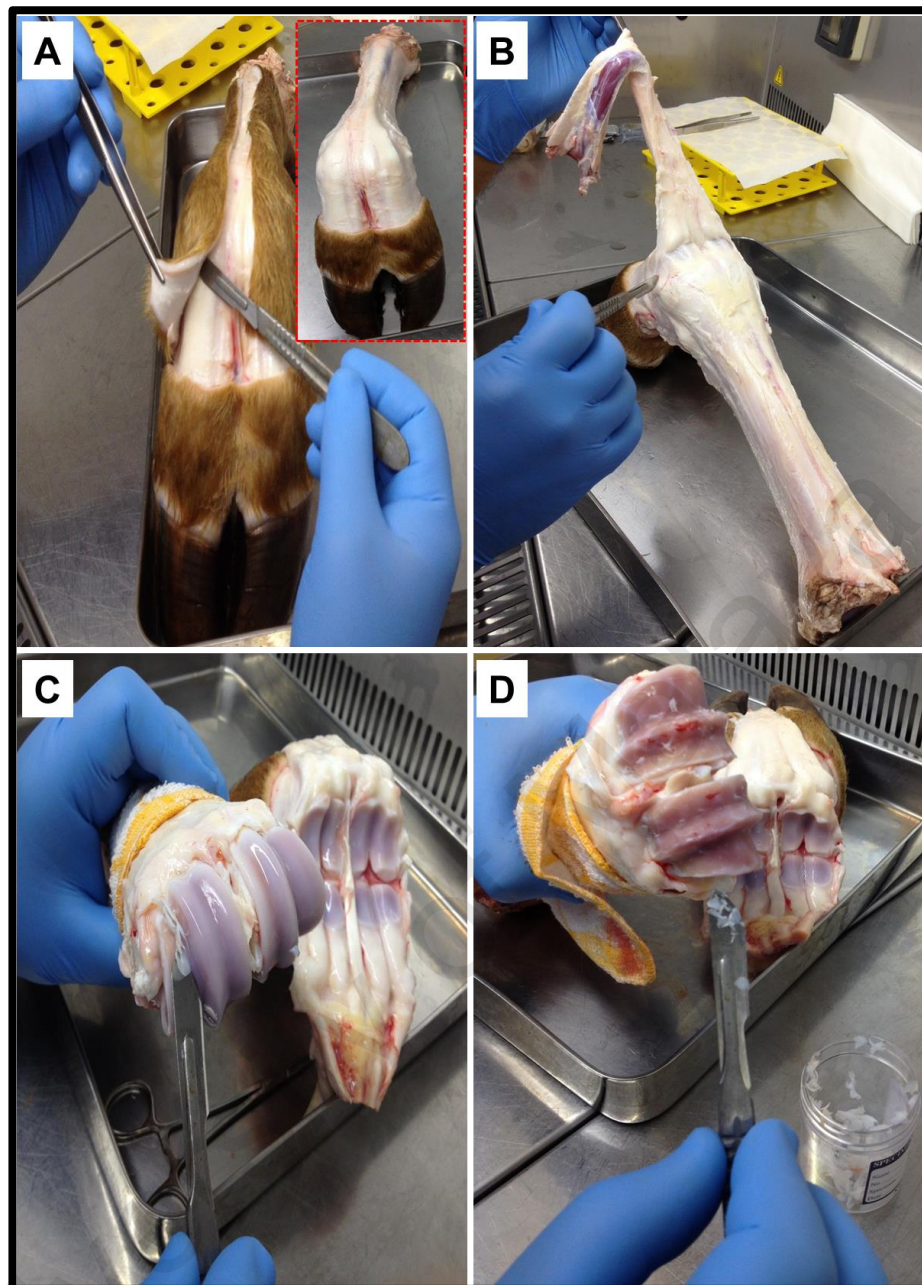


Figure 3.4: Procedure of isolation of primary chondrocytes from cow legs. (A) Removal of hide from cow leg insert shows completely removed hide, (B) Opening of joint by removing ligament, (C) Cutting of cartilage and (D) Complete shaved cartilage joint and explants placed in sterile container.

Sliced cartilage explants were immediately immersed in chondrocyte culture medium. The protocol to make chondrocyte culture medium is provided in the subsequent section.

3.4.1 Chondrocyte Culture Medium

Chondrocyte culture medium was prepared using the ingredients mentioned in table 3.1.

Table 3.1: Ingredients to prepare chondrocyte culture medium

Name	Quantity	Product
Dulbecco's Modified Eagle's Medium (DMEM)	500.00 ml	(Corning #10-013-CMR)
Foetal bovine serum (FBS)	100.00 ml	(Gibco, #10270, Life Technologies)
20 mM 4-(2-hydroxyethyl)-1-piperazineethanesulfonic acid (HEPES)	10.00 ml	(Biowest, #L0180)
2 μ M L-glutamine	5.00 ml	(Sigma, #G3126)
Antibiotic-Antimycotic	10.00 ml	(Cellgro, #30-004-CI, Mediatech, USA)
0.85 μ M L-ascorbic acid	0.075 g	(System, ChemAR, #AS093-00)

All ingredients were poured in a sterile glass bottle under laminar hood and was mixed using a whirling action until the ascorbic acid was dissolved completely. A bottle top filter was used to filter all the contents in a new sterile bottle. The medium was aliquoted in batches of 50 ml in sterile conical tubes (Corning, USA) and frozen at -20°C until further use.

3.4.2 Cartilage ECM digestion

In order to obtain BACs from cartilage of cow legs, the Extra Cellular Matric (ECM) of cartilage needs to be digested to provide fresh BACs. The digestion process is two-tier. The first step is to use protease and secondly to use collagenase for digestion of cartilage ECM. Preparation of Protease and Collagenase solutions are presented in the next sections.

3.4.2.1 Protease preparation

Protease was prepared by weighing 1g of protease (Sigma, #P8811) via an analytical weighing balance (Shimadzu, AY220) and dissolving it in 175.00 ml of DMEM+20% FBS. This solution was then filtered using a 0.20 µm syringe filter.

3.4.2.2 Collagenous preparation

Collagenase was prepared by weighing 0.021 g of collagenase type XI (Sigma, #C6885) via an analytical weighing balance (Shimadzu, AY220) and dissolving it in 300.00 ml of DMEM+20% FBS. This solution was then filtered using a 0.20 µm syringe filter.

After the entire joint was shaved, the medium was aspirated using a Pasteur pipette, and 10.00 ml of protease solution 700 unit/ml (Sigma #P8811) was added to digest the ECM of BAC explants for 1 hour with gentle rotation in a hybridisation oven (Problot, Labnet, NJ, USA). After 1 hour of protease digestion the medium was removed with a sterile Pasteur pipette and 30.00 ml of fresh medium supplemented with 100 unit/ml of collagenase type XI (Sigma #C6885) was added for a further digestion of 16 hours with gentle rotation in hybridisation oven (Problot, Labnet, NJ, USA).

After 16 hours of collagenase digestion, the cell suspension was filtered with a 70 µm nylon cell filter (BD Falcon, NJ, USA). The cell suspension was centrifuged at 1000 RPM and the supernatant was carefully removed. The process was repeated twice to remove any impurities of Protease or Collagenase.

3.4.3 Cell Viability

Cell viability was calculated using trypan blue exclusion assay. Trypan blue solution was prepared by dissolving 0.2 g of Trypan Blue (Sigma #T6146) in 99.8 ml of ultra-pure water which was filtered through 0.45 µm hydrophobic membrane syringe filter (Thermo Scientific, #9057, Thermo Scientific, Waltham, MA, USA). A working solution of trypan

blue was made by mixing 2ml of trypan blue stock solution to a solution of 9.58 ml Ultra-pure water and 0.43 g NaCl.

20 μ l of filtered cell concentrate and same amount of trypan blue working solution was taken in a micro centrifuge tube. A 20 μ l mixture of cell and trypan blue was placed in Heamacytometer covered with a cover slip and read under a microscope. Viable (unstained) cells and non-viable (stained blue) cells were counted using a cell counter in each chamber. The total number of viable cells was divided by the total number of cells (Viable + Non-Viable) and the resulting percentage was calculated for viable cells. Only passage zero cells were used, with $\geq 95\%$ viability.

3.5 Cell proliferation assay

Cell proliferation was determined via Resazurin reduction assay (Ataollahi et al., 2014). Briefly, 140 mg of Resazurin powder (Sigma #R7017) was dissolved in 1000 ml of phosphate buffered saline (PBS) (Sigma #P4417) to make the stock solution. It was then diluted with PBS to 10% volume working solution. 1 ml of resazurin working solution was added into each well at different time points. Prior to reading the plate via microplate reader (FLUOstar OPTIMA, BMG labtech, GmbH, Ortenberg, Germany), at every time point each plate was incubated for 4 hours at 37°C and 5% CO₂ (Thermo Scientific, Waltham, MA, USA). After the incubation, the plate was wrapped in aluminum foil and was shaken at 30 RPM on a bench top shaker for 1 minute. From each well, 100 μ l of resazurin solution was placed in wells of a 96-well plate, and resazurin solution from unseeded scaffold was taken as blank. Absorbance was read by a microplate reader for wavelengths of 570 nm and 595nm.

3.6 DNA Biochemical Assay

The Hoechst binding dye method was used to quantify DNA within the scaffolds at each time point. For this method, the cells needs to be lysed followed by their quantification.

Subsection 3.6.1 details the process of cell lysis and 3.6.2 provides the steps involved in quantifying the DNA.

3.6.1 Lysis of BACs

To quantify the number of cells present in a particular scaffold, the cells first need to be separated from the scaffold and lysed to obtain DNA. In order to obtain cell lysate, papain is used as primary agent that digest protein substrates while leaving behind the DNA intact and unharmed. To dissociate the cells from the scaffold, the scaffold laden with cells was placed in a 1.5 ml micro-centrifuge tube and papain digest buffer topped with papain was added to it. A manual tissue homogeniser was used to tear the scaffold apart to expose BACs to papain. Ingredients presented in Table 3.2 were used to prepare papain digest buffer.

Table 3.2: Ingredients to prepare papain digest buffer

Name	Quantity	Product
L-Cystein HCl monohydrate	0.788g	(Sigma #C7880)
Ethylenediaminetetraacetic acid (EDTA)	0.403g	(Sigma #E6758)
PBS	500ml	(Sigma #P4417)

All ingredients were dissolved at a pH of 6.0; the pH was adjusted using 1M Sodium Hydroxide (NaOH). Furthermore 3 μ l of Papain (Sigma #P3125) per construct was added. Cells were lysed overnight at 65°C because papain has the highest activity in the range of 60 – 70°C. After overnight activity, the cell-scaffold lysate was stored at -20°C until further analysis. At -20°C the DNA can be kept safe for several months.

3.6.2 DNA quantification

For DNA quantification, a Hoechst binding assay was used (Pingguan-Murphy & Nawi, 2012). Hoechst is a dye that specifically binds to DNA to produce fluorescence at a wavelength of 460 nm. Stock solution of Hoechst was prepared by dissolving 50.0 mg of Hoechst (Sigma

#861405) in 25.0 ml of ultra-pure water in an amber bottle wrapped with aluminum foil to prevent degeneration of Hoechst.

3.6.2.1 DNA Standard

To calculate the quantity of DNA, a standard needs to be set for the microplate reader in order to assess the quantity in the sample presented. A DNA standard was prepared by dissolving 5 mg of Deoxyribonucleic acid sodium salt from calf thymus (Sigma #D1501) in 5 ml of EDTA/PBS solution. The EDTA/PBS solution acts as a buffer for DNA from calf thymus. EDTA/PBS solution was prepared by weighing EDTA (0.02922g) using an analytical balance (Shimadzu, AY220) and dissolving it in 100 ml PBS (Sigma #P4417) (pH 7.8), followed by autoclaving.

The solution of DNA from calf thymus and EDTA/PBS was left overnight in a 0-4°C fridge. The DNA formed a gel which was then sheared by pipetting using a glass pipette vigorously several times. A syringe filter of 0.45 µm (minisart SRP15, Sartorius, Germany) was used to filter out the DNA. The DNA concentration was checked via Nanodrop ND 2000 (Thermo Scientific, Waltham, MA, USA). Aliquots of DNA standard were stored at -20°C in sterile glass bijoux tubes to prevent absorbance of DNA in plastic. After Papain digestion, the DNA standard was diluted to 20 µg/ml with 2xSSC/Papain digest buffer. A 20x stock Saline Sodium Citrate (SSC) buffer was prepared by dissolving 87.65 g of Sodium Chloride (NaCl) (Sigma # S7653) and 44.1 g of CA (Sigma # C0759) in 500 ml of distilled water. The pH was adjusted to 7.0 using 1M NaOH/1M HCl.

A serial double dilution was prepared at 20, 10, 5, 2.5, 1.25, 0.625 and 0.3124 µg/ml. For 0 µg/ml of DNA, 2xSSC/Papain digest buffer was used.

Cell-scaffold lysate (100µl each) in triplicates were pipetted into wells of black flat-bottomed 96-well plates (Falcon, Corning #3916) and 100 µl of Hoechst working reagent (20µl Hoechst stock added to 20ml of 2xSSC/Papain digest buffer) was added to each well. All these processes were carefully carried out in a dark room. Aluminium foil was

used to wrap the plate before transferring it to the microplate reader. The plate was read for fluorescence at wavelengths of excitation (ex) 355 nm and emission (em) 460 nm using FLUOstar Optima, BMG Labtech, Ofdenberg, Germany.

3.7 Sulphated Glycosaminoglycan (S-GAG) quantification assays

Glycosaminoglycans (GAGs) are polysaccharides that are present in abundance in a healthy cartilage. Sulphated-GAGs (S-GAGs) are the types that can be measured via a 1, 9-dimethylmethylene blue assay.

Total S – GAG was measured from Cell-scaffold lysate at each time point. The same cell-scaffold lysate is used for S-GAG quantification as the ones used for DNA quantification because papain digestion does not affect the S-GAGs. Released S – GAG was measured by collecting the culture medium at every medium change from the wells. Total S – GAG and released S – GAG were analyzed by Dimethyl Methylene Blue (DMMB) assay (Lee & Bader, 1997; Pinguan-Murphy & Nawi, 2012). DMMB was prepared by using the ingredients presented in Table 3.3.

Table 3.3: Ingredients used in preparation of DMMB solution for DMMB assay

Name	Quantity	Product
1, 9-dimethylmethylene blue	0.016g	(Sigma, #341088)
Ethanol	5.0 ml	(Merck)
Sodium Formate	2.0 g	(Sigma, #247596)
Formic Acid	2.0 ml	(Sigma, #F0507)

DMMB was dissolved in ethanol, followed by the addition of 950.00 ml of distilled water and sodium formate. The final pH was adjusted by adding formic acid drop by drop. The solution was then transferred to an amber bottle wrapped in aluminium foil.

The S-GAG standard stock solution was prepared by dissolving 1mg of Chondroitin Sulfate-A sodium salt from Bovine trachea (Sigma, #C9819) in 1ml of distilled water. A

working solution for S-GAG assay was prepared by diluting to 100 µg/ml in distilled water. A series of standard dilutions were made and distilled water was used as 0 µg/ml. Briefly, 40 µl of cell-scaffold lysate for total S – GAG, 40 µl culture medium for released S – GAG and serially diluted standards of Chondroitin sulfate salt in triplicates were mixed with 250 µl of DMMB reagent in a transparent 96-well plate and absorbance at a wavelength of 595nm was read via microplate reader. All the procedures were performed in a dark room.

3.8 Quantitative Polymerase Chain Reaction (q-PCR)

To observe the behaviour of BACs at gene level Cartilage matrix specific genes; Collagen type II (*COL2A1*) and Aggrecan (*ACAN*) were observed. *COL2A1* is responsible for producing type II collagen in the cartilage, while *ACAN* is responsible for producing Aggrecan proteoglycan in the cartilage. The matrix degradation gene (*MMP-13*) and hypoxia inducible factor gene (*HIF1A*) were also observed. *MMP-13* provides an insight in to the catabolic activity that the cartilage is undergoing, while *HIF1A* demonstrates the effect of oxygen concentration on the BACs. Glyceraldehyde-3-phosphate dehydrogenase gene (*GAPDH*) expression was determined and used as a house keeping gene. Gene expressions were determined by the *TaqMan* gene expression assay using StepOnePlus™ Real-Time PCR system (Applied Biosystems, Foster City, USA).

3.8.1 RNA Isolation

At each time point, culture medium was removed and scaffolds were washed with PBS (Sigma #P4417) and placed in TRIzol reagent (#AM9738, Lifetechnologies™, Carlsbad, CA, USA). Total ribonucleic acid (RNA) was extracted according to manufacturer's guidelines using TRI reagent (Hummon et al., 2007). Briefly, samples were homogenized using a tissue homogenizer, followed by phase separation by adding 0.2ml of chloroform (Fisher Scientific, UK, #BP1145-1) per 1ml of TRIzol reagent. Samples were then centrifuged at 12000

RCF for 15 minutes (CYT12, Centurion Scientific, West Sussex, UK) and upper aqueous layer was carefully transferred to a new tube. RNA was precipitated by adding 0.5ml of 100% isopropanol (Sigma, #I9516) and centrifuging at 12000 RCF for 10 minutes at 4°C. Supernatant was removed leaving precipitated RNA. Visible RNA pellet was washed by 1.0 ml of 75% ethanol (prepared from absolute ethanol from Merck and with Ultra-Pure distilled RNase/DNase free water from Invitrogen) and left to air dry. 20 µl of RNase free water (Invitrogen, #10977) was added to dissolve the pellet and its purity was read via NanoDrop (ND2000, Thermo Scientific, Waltham, MA, USA) at absorbance ratio of 260/280 nm. Only RNA samples with absorbance ratio greater or equal to 2 were further used for analysis.

3.8.2 cDNA synthesis

Conversion of RNA to complementary Deoxyribonucleic acid (cDNA) was performed using a high capacity RNA-to-cDNA (Applied Biosystems, #4387406, Foster City, USA) kit. Briefly, for every 2 µg of total RNA (2000 ng/ µl) 20 µl reaction mixture was used to reverse transcribe RNA into cDNA by incubating the reaction plate for 60 minutes at 37°C followed by heating it to 95°C for 5 minutes, followed by holding the reaction plate at 4°C for half an hour using MyGene series Peltier thermal cycler (MG96G).

3.8.3 Gene Expression

Quantitative gene expression of all the genes listed in Table 3.4 was identified using 1 µl of cDNA sample in triplicates for each gene. 1 µl of cDNA sample was transferred to a 96-well plate (MicroAmp® InduraPlate™, Applied Biosystems®), topped up with 10 µl TaqMan master mix, 8 µl of RNase/DNase free Ultra-Pure water, and 1 µl of target/housekeeping gene (TaqMan assay). The plate was sealed with a transparent adhesive film and QPCR was performed using StepOnePlus™ Real-Time PCR system (LifeTechnologies).

Gene expression was normalized with Glyceraldehyde-3-phosphate dehydrogenase (*GAPDH*) gene expression using Delta-Delta Ct method using the equations 3.1, 3.2 and 3.3.

$$RQ = 2^{-(\Delta Ct_{Target} - \Delta Ct_{Reference})} \text{----- Equation 3.1}$$

Where;

RQ = Relative Quantification

$$\Delta Ct_{Target} = \Delta Ct_{TargetGene} - \Delta Ct_{HousekeepingGene} \text{----- Equation 3.2}$$

$$\Delta Ct_{Reference} = \Delta Ct_{ReferenceTargetGene} - \Delta Ct_{ReferenceHousekeepingGene} \text{----- Equation 3.3}$$

All genes were purchased from Life Technologies as shown in Table 3.4 with their respective ID and amplicon length. Data were expressed as fold change with respect to Pure-POC in normoxia as a control (POC in normoxia on day 1).

Table 3.4: Gene identities and their respective amplicon length from LifeTechnologies.

Gene	ID	Amplicon length
<i>GAPDH</i>	Bt03210913_g1	66
<i>COL2A1</i>	Bt03251861_m1	54
<i>ACAN</i>	Bt03212186_m1	55
<i>MMP-13</i>	Bt03214045_g1	79
<i>HIF-1A</i>	Bt03259343_m1	77

3.9 Scanning Electron Microscopy (SEM) for cell adhesion

For SEM (Quanta FEG 250, FEI, Oregon, USA) imaging, cell seeded scaffolds at each time point were fixed in 2.5% glutaraldehyde at 4°C overnight. Ensuing steps were followed to fix the cell-laded scaffolds.

1. All the cell-laden scaffolds were washed with PBS (Sigma #P4417) 2 times for 10 min each.
2. 2.5% Glutaraldehyde (SEM grade, Sigma, G7651) was added to each scaffold [2.5% Glutaraldehyde must be in PBS], enough to cover the sample.

3. All the samples were kept overnight at 4°C. (*2.5% Glutaraldehyde penetrates only 1mm per hour*).
4. Graded Alcohol was used to dehydrate the sample.
5. Starting from 25% followed by 35%, 50%, 70% and 90%. Each 10-15 minutes.
6. Finally 100% ethanol was placed in the well that contain cell-laden scaffolds twice for 20 minutes each.
7. Finally the samples were dried in freeze dryer (FreeZone 2.5, Labconco, Kansas, USA) for 2 hours.

n.b: samples can be kept in 2.5% glutaraldehyde at 4°C for up to one month.

3.10 Live/Dead Assay

The qualitative cell viability was determined using a LIVE/DEAD[®] viability kit (Molecular Probes[®] LifeTechnologies[™], Carlsbad, CA, USA). Briefly, a working solution was made by adding 1µl Calcein and 2.5 µl Ethidium homodimer-1 in 1ml of PBS (Sigma #P4417). Each scaffold was placed in 200 µl of working solution for 30 minutes before imaging. Imaging was performed with green fluorescence at ex/em ~495nm/~515nm for live cells and red fluorescence at ex/em ~495 nm/~635 nm for dead cells using confocal laser scanning microscopy (CLSM) (Leica TCS SP5 II, Leica Microsystems CMS GmbH, Mannheim, Germany).

3.11 Statistical Analysis

Data are represented as average \pm standard deviation at each time point. Statistical analysis was performed using IBM SPSS v21, with a two-way analysis of variance (ANOVA) to determine significance between groups, and a post-hoc Tukey's test was applied to test significance between oxygen tension and within the days. In all conditions, a p value of less than 0.05 ($P < 0.05$) was considered to be significant. The number of biological replicates in all the studies ranges from 5 to 12.

Chapter 4: CHARACTERISATION OF POLYOCTANEDIOL CITRATE-ZINC OXIDE NANO-COMPOSITE SCAFFOLD

4.1 Introduction

Tissue engineering strategies utilize polymeric scaffolds that serve as a temporary extracellular matrix (ECM) for seeding cells (Díaz et al., 2014; Goh et al., 2013; Kamoun et al.; Tran, P. et al., 2014). The adopted strategy is that a scaffold should biologically degrade over time, leaving a fully developed and functional tissue. Production of tissues may be accomplished *in vitro*, where cell-seeded scaffolds are placed in bioreactors, or *in vivo*, where the cell/scaffold “composite” is surgically placed inside the human body. The latter is of particular interest in the development of multifunctional advanced materials for scaffold fabrication. Every surgical implantation of biomaterials (or medical devices) requires tissue incision and therefore serious consideration must be given to control of infection. Apart from the necessary support for tissue growth, scaffolds should also possess antibacterial properties in order to battle serious problems related to scaffold implantation.

Drug delivery devices are generally considered to be an effective route for administration of bio-active substances to the site of implantation. Postoperative infections are a major threat and a challenging issue that may have deleterious effects on a patient’s life (Husted & Toftgaard Jensen, 2002; Trampuz & Zimmerli, 2006). Various intrusions that are presently carried out, and which are focused on minimizing the risk of infections, include prophylactic antibiotics as well as the treatments prior to surgical intervention. These treatments include: ultra-violet exposure (Berg-Perier et al., 1992; Taylor et al., 1993), povidone-iodine lavage (von Keudell et al., 2013), antibiotic irrigation (Taylor et al., 1993) and laminar airflow (Salvati et al., 1982). Infection risk is closely linked to initial bacterial attachment and subsequent proliferation on the implant surface. The bacteria adhere, forming a layer, more commonly known as “biofilm”. These biofilms are resistant

to antibiotics and the host immune system, and therefore treatment requires more measures (Costerton et al., 1999). For that reason it is essential to prevent initial bacterial attachment on the implant surface.

One of the materials that has proven to be effective against bacteria in general is zinc oxide (ZnO) (Sirelkhatim et al., 2015). This substance is currently considered a Generally Recognized as Safe (GRAS) material, approved by the FDA (Espitia et al., 2013). Furthermore, ZnO can be fabricated into nanoparticles (NPs) (Khalil et al.; Wallace et al., 2013; Zak et al., 2011), that can be embedded inside a biodegradable polymer matrix and subsequently released in a highly controlled manner. Polyoctanediol citrate (POC) elastomer is one of the prominent new materials for scaffold fabrication (Djordjevic, Choudhury, et al., 2010; Djordjevic, Szili, et al., 2010; Serrano et al., 2010). POC and other types of citric acid (CA)-based elastomers have shown excellent performance in various biomaterial applications, including scaffolds for soft tissue engineering, biodegradable bone fixation devices and drug delivery devices (Qiu et al., 2006; Serrano et al., 2011; Zhang et al., 2009).

In the current chapter, a newly-developed ZnO-POC scaffold produced by a well-established solvent-casting / particulate-leaching technique is reported. Tissue engineering applications require three-dimensional structures with high level of porosity and pore sizes in the range of 100-200 μ m. In many cases such porous structures alter the material properties that were originally recorded for sample films (Djordjevic et al., 2009; Kompany et al., 2014). Apart from antibacterial properties of the ZnO-POC composite scaffolds, the scaffolds must be investigated for their potential support of cellular growth, proliferation and toxicity. Similar to other polymer/solid composite scaffolds, the presence of ZnO NPs physically, strengthens the scaffold thus providing necessary toughness for engineering of hard tissues. In particular, the target was to explore the possibility of using ZnO-POC nano-composite scaffolds for engineering of cartilage

tissue. ZnO-POC nano-composite scaffolds with variation of ZnO concentration and a series of experiments was conducted in order to: (i) investigate the influence of ZnO concentration on material characteristics; (ii) establish bactericidal properties by measuring the proliferation rate of *Escherichia coli* and *Staphylococcus aureus*; and (iii) examine the bioactivity, biocompatibility and potential of ZnO-POC scaffolds for cartilage tissue engineering by *in vitro* experiments with primary bovine chondrocyte cells

4.2 Materials and Methods

4.2.1 Surface and elemental properties

Pure-POC scaffolds and 3 different ZnO-POC composite scaffolds with varying w/w percentages of ZnO NPs (1%, 3% and 5%) were prepared, the details of the fabrication methods can be found in Section 3.3. The final dimension of the scaffold is 6mm (Ø) x 6mm height. The scaffold morphology and element composition analysis were assessed using Quanta FEG 250 Field Emission Scanning Electron microscope (FESEM) equipped with Energy Dispersive X-ray (EDX) analysis.

4.2.2 Zinc oxide nanoparticles distribution within POC

Optical microscopy (OLYMPUS, BX51TRF, Japan) was used to view zinc oxide nanoparticles distribution within POC. Before the experiment, POC and 1%, 3% and 5% ZnO-POC (50% w/v in dioxane) solutions were prepared and spin-coated on microscope coverslips, using Laurell (WS-650MZ-23NPP) spin coater. Briefly, the microscope coverslip was placed inside the spin coater followed by turning on the vacuum suction to prevent the microscope coverslip from moving. The spin coater was rotating at 3000 RPM for 10 seconds. During rotation, 200 µl of polymer solution was dropped at the centre of the coverslip and the process was repeated thrice to make sure the coverslip is uniformly

covered with polymer. Subsequently, the coated coverslips were placed flat in the oven at 80°C for another week for curing and solvent evaporation. The coated coverslip was placed on the microscope and the distribution on ZnO was captured by camera.

4.2.3 Surface wettability test

Good wettability of a surface will ensure good cell bonding with polymer (Arima & Iwata, 2007). Water-in-air contact angle (WACA) experiments were performed on both ZnO-POC and POC samples. POC and 1%, 3% and 5% ZnO-POC (50% w/v in dioxane) solutions were coated on the microscope coverslip. The sample preparation method is similar to the one described earlier in Section 4.2.2. The WACA experiments were carried out at room temperature by a sessile drop method using an OCA 20 optical contact angle measuring instrument (DataPhysics Instruments GmbH, Filderstadt, Germany) After the droplet (2µl) was dispensed on the prepared sample, the image was captured within 5 seconds and analysed. Each measurement was repeated 5 times (5 new samples were prepared for each condition). The water angles were measured at 3 different spots on each sample and the results were averaged (n=5).

4.2.4 Mechanical property and porosity

The compression tests were performed on POC and 1%, 3% and 5% ZnO-POC scaffolds using Instron mechanical tester (Instron Microtester 5848, Instron Corp., Norwood, MA, USA) equipped with a 2kN load cell. Scaffolds were cut into cylindrical shapes (6 mm-diameter / 6 mm-height) and subjected to 50 % compression at a rate of 1 mm/min. For percentage recovery, the height of each cylindrical scaffold was measured 2 min after the compression test was completed (n= 5). The porosity of the scaffolds was measured based on the Archimedes principle (Zhu et al., 2008).

4.2.5 Swelling test

For Swelling test, 10ml of each POC and 1%, 3% and 5% ZnO-POC (50% w/v in dioxane) solutions were poured into custom designed (5cm diameter X 2 mm thickness) TeflonTM moulds. The polymer filled moulds were placed flat in the oven at 80°C for curing and solvent evaporation for 1 week. After that, the samples were removed from the moulds and cut into disk shape (6mm diameter X 1 mm thickness) using a cork borer. Each sample was placed separately in a conical tube containing 10 ml of distilled water which was taken out at different time points (For first hour every 10 min then every hour for 6 hours). The weight was measured after lightly cleaning the surface with lint-free paper. Percentage swelling was calculated using equation 4.1.

$$\text{Swelling}(\%) = \frac{W_s - W_o}{W_o} * 100 \text{ ----- Equation 4.1}$$

Where; W_s is the weight of the swollen polymer disk at each time point and W_o is samples' dry weight.

4.2.6 Fourier transform infrared spectroscopy (FTIR) analysis

Fourier transform infrared spectra were obtained for the POC and 1%, 3% and 5% ZnO-POC scaffolds using spectrophotometer-Thermo Scientific Nicolet iS10 (Thermo Scientific, Waltham, MA, USA) operating in attenuated total reflectance mode (ATR-FTIR) at room temperature, within a wavelength range of 450 – 4000 cm^{-1} .

4.2.7 Thermal analysis

For assessing thermal properties, thermo gravimetric analysis (TGA) was performed on POC and 1%, 3% and 5% ZnO-POC scaffolds within a temperature range of 30-900 °C at a rate of 10 °C/min using PerkinElmer, TGA 4000 (PerkinElmer, Waltham, MA, USA). The onset of degradation temperature was measured after 10 % of degradation.

4.2.8 Degradation analysis

For degradation analysis, POC and 1%, 3% and 5% ZnO-POC scaffolds were immersed in a conical tube containing 10 ml of Phosphate Buffered Saline (PBS) The samples were incubated at 37°C and at each time point the samples were taken out and freeze dried overnight, and the mass loss was measured by equation 4.2. Each condition was repeated 5 times.

$$\text{Massloss}(\%) = \frac{W_o - W_{t1}}{W_o} * 100 \text{ ----- Equation 4.2}$$

Where, W_o is the initial dry weight of the scaffold, W_{t1} is the weight of the scaffold at each time point after freeze-drying.

4.2.9 ZnO NPs release kinetics in physiological conditions

To observe the release of ZnO NPs, POC and 1%, 3% and 5% ZnO-POC scaffolds were placed in 10 ml of PBS in conical tubes and kept at 37°C throughout the whole experiment. The scaffolds prepared for this experiment have a thickness of 2mm, elsewhere in the thesis, when scaffold is mentioned the thickness should be 6mm. Two milliliter of solution from each conical tube was withdrawn at each time point (day 1, 7, 14 & 28) and was kept at 4 – 8°C until further analysis. The concentration of Zn²⁺ (ppm) was detected by atomic emission spectroscopy (AAS) using Agilent 4100 (Agilent Technologies, Inc., Santa Clara, CA, USA) microwave plasma-atomic emission spectrophotometer (MP-AES). The standard for Zn²⁺ was purchased from Sigma-Aldrich Malaysia (Sigma, #18827).

4.2.10 Anti-bacterial properties

The antibacterial properties of POC and its composites were tested. POC and 1%, 3% and 5% ZnO-POC scaffolds were placed in direct contact with the bacteria, a technique known as the liquid culture method (Raffi et al., 2008). Briefly, rectangular strips (30 mm x 10 mm x 5 mm) of POC and 1%, 3% and 5% ZnO-POC scaffolds were placed in 15 ml conical tubes with 10 ml of Luria-Bertani (LB) broth inoculated with 50 μ l of 10^{4-5} CFU/ml *E. Coli* (ATCC 15597). Samples were placed in a shaking incubator at 37⁰C with a speed of 50 RPM. Pure-POC scaffold and LB broth (without any scaffold) were inoculated with similar bacterial densities and were used as positive and negative controls respectively. The optical density was measured at 595 nm every 2 hours (for 8 hours) with a micro plate reader (BMG LABTECH, Offenburg, Germany).

4.2.11 In vitro tests with chondrocyte cell culture

POC and 1%, 3% and 5% ZnO-POC scaffolds were tested for their cytotoxicity towards bovine chondrocytes. Bovine legs of post-slaughtered cows were obtained up to carpal joint only. Bovine chondrocytes were isolated from metacarpalphalangeal joints as described in section 3.4. Cells were used when only greater than 95% viability was obtained (refer to section 3.4.3). Toxicity was measured by resazurin reduction cell viability test as described earlier in section 3.5. Scaffolds were autoclaved before cell seeding and then were allowed to neutralise in chondrocyte medium overnight. Scaffolds were then placed in 24 well plates and dried under laminar flow for an hour. A volume of 20 μ l cell suspension with a concentration of 3×10^7 cells/ml was spotted on top of the scaffold. Cells were allowed to attach for 2 hours, after which 2ml of medium/well was added. Reduction in resazurin was determined after 24 and 72 hours as described previously in section 3.5 (Larson et al., 1997). Briefly, medium was removed from the wells containing cell seeded scaffolds and then washed with PBS. 1ml of resazurin was

added to each well and then kept in the incubator for 4 hours at 37°C and 5% CO₂. After the incubation time the plate was wrapped in aluminium foil and was shaken at 30 RPM on a bench top shaker for 1 minute. From each cell-scaffold well, 100 µl of resazurin solution was placed in 96-well plate and resazurin solution from unseeded scaffold was taken as blank. Absorbance was read by a microplate reader. Scaffolds with cells were taken out after 24 hours and 72 hours and the morphology of cells was observed by FESEM by using a standard protocol of cell fixation (refer to section 3.9 for complete protocol).

4.3 Results

The analysis of this section has been previously published in Digest journal of nanomaterials and biostructures volume 10, issue 2, reproduced by permission of the publisher.

4.3.1 Surface morphology

FESEM images (Figure 4.1 (A-D)) of Pure-POC (control) and 1%, 3% and 5% ZnO-POC scaffolds demonstrate that the pores were formed into semi-rectangular shapes after leaching out the salt crystals. In comparison to Pure-POC (control) (Figure 4.1A), addition of ZnO NPs did not have any significant impact on the pore size or pore structure that could be observed through FESEM images. Inserts in Figure 4.1 (A-D) are representative images of surfaces recorded within the pores of produced scaffolds. Furthermore, EDX analysis confirmed the presence of Zn on the outermost surface layer and the detected amount of Zn on ZnO-POC surfaces was 0.49%, 1.64%, and 2.02 % for 1% ZnO-POC, 3% ZnO-POC and 5% ZnO-POC respectively. It is important to note that the increase in surface concentration of Zn corresponds to the pre-determined concentrations of ZnO NPs in composite scaffolds.

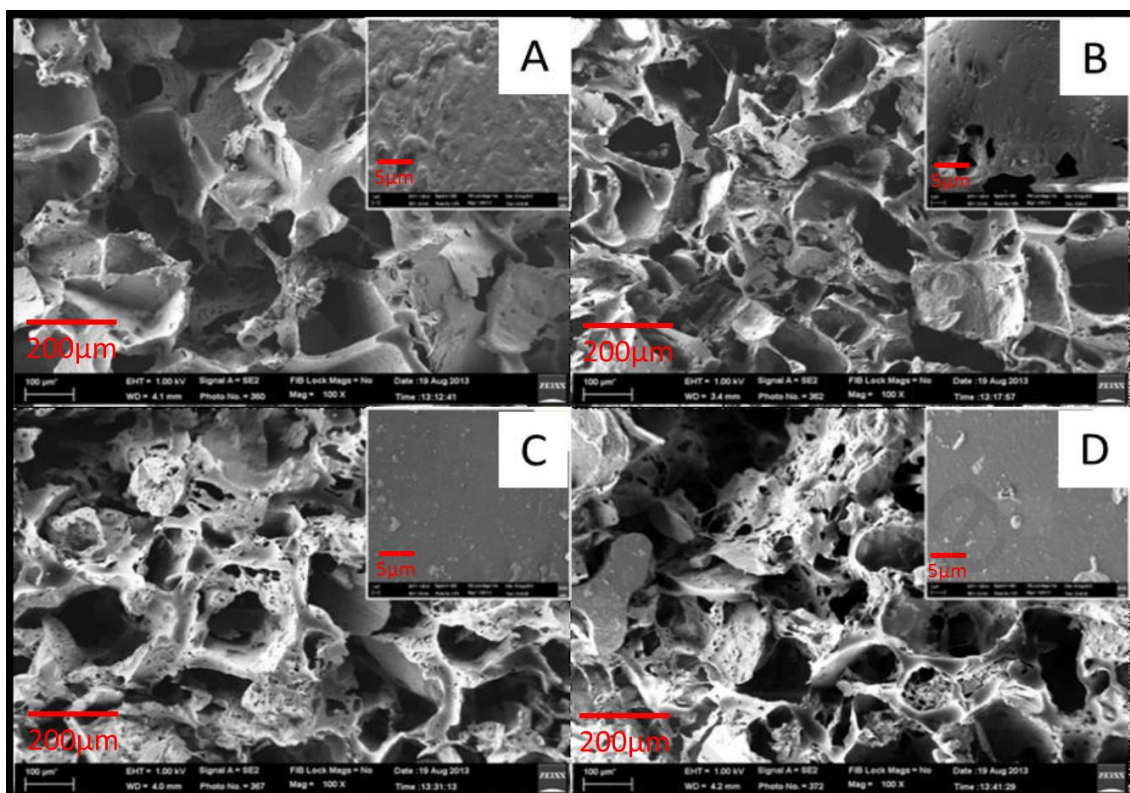


Figure 4.1: FESEM images of POC (control) and 1%, 3% and 5% ZnO-POC composite scaffolds; (A) POC, (B) 1% ZnO-POC, (C) 3% ZnO-POC and (D) 5% ZnO-POC; inserts show representative magnified surfaces of pore walls within scaffolds.

4.3.2 Influence of ZnO-NPs on relative hydrophilicity

Pure-POC (control) and 1%, 3% and 5% ZnO-POC polymer coatings on glass slide were processed by spin-coating technique for wettability measurements and the surface morphologies of the samples (observed by optical microscopy), which are shown in Figure 4.2 (A-D). The presence of ZnO NPs can be observed both on the surface of the films (Figure 4.2-B) and within the bulk of the material (Figure 4.2-C).

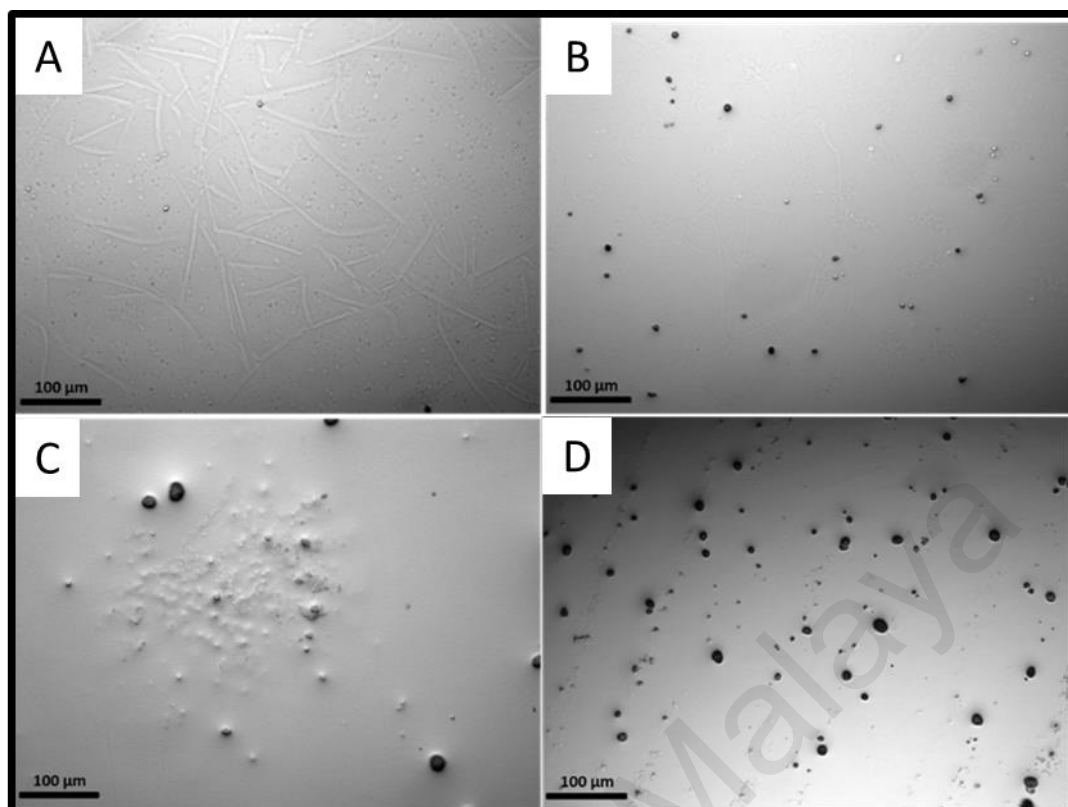


Figure 4.2: Optical microscopy images of Pure-POC and ZnO-POC surfaces developed by spin-coating technique at a magnification of 100X; (A) POC, (B) 1% ZnO-POC, (C) 3% ZnO-POC and (D) 5% ZnO-POC.

Water-in-air contact angle values on polymer coated glass slides were measured to determine the effect of surface ZnO concentration on hydrophilicity and the results are shown in Figure 4.3. Evidently, an increase in ZnO content results in more hydrophobic surfaces. There is no significant difference between contact angles measured for 3% and 5% ZnO-POC, although all ZnO-POC composite coatings displayed a consistently higher contact angle values in comparison to hydrophilic POC.

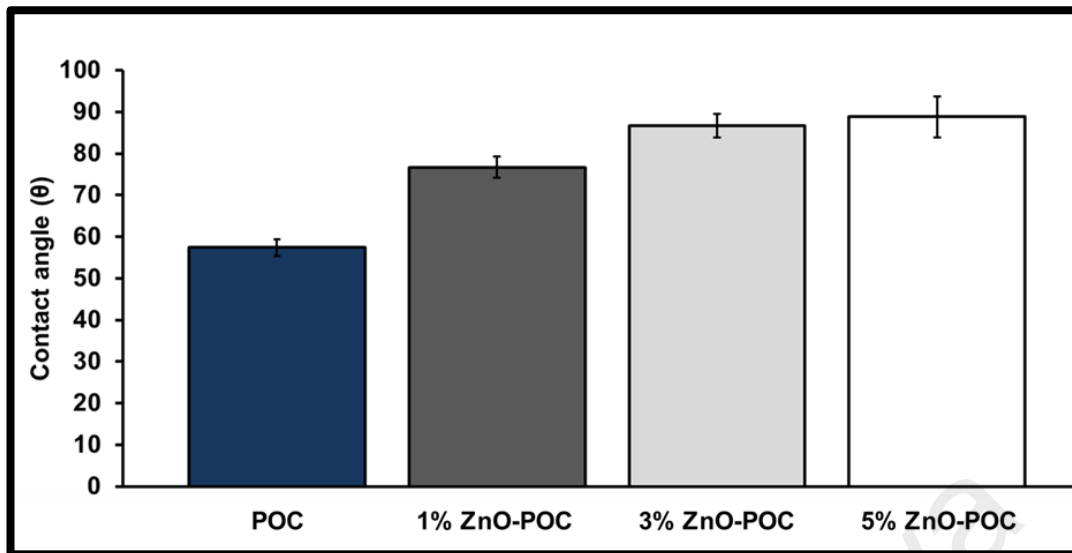


Figure 4.3: Water-in-air contact angle results measured for thin films of Pure-POC and 1%, 3% and 5% ZnO-POC produced by spin-coating technique.

4.3.3 Physical properties of scaffolds

Table 4.1 represents the porosities of Pure-POC (control) and 1%, 3% and 5% ZnO-POC scaffolds. The porosities for all the scaffolds are ranging from 82 to 86%.

Table 4.1 Compression properties and porosities of ZnO-POC scaffolds

Scaffold	Compressive Modulus (MPa)	Recovery (%)	Porosity (%)
Pure-POC	0.243 ± 0.09	94.55 ± 2.52	82.91 ± 3.49
1% ZnO-POC	0.31 ± 0.10	91.94 ± 4.5	85.92 ± 2.41
3% ZnO-POC	0.537 ± 0.33	76.81 ± 4.82	86.01 ± 1.92
5% ZnO-POC	0.442 ± 0.23	60.66 ± 4.49	82.57 ± 7.33

The compression moduli increase with increasing concentration of ZnO, as expected for a contribution of the filler within the composite scaffold (Table 4.1).

4.3.4 Swelling and cross-linking density

Swelling percentages for Pure-POC (control) and 1%, 3% and 5% ZnO-POC films in distilled water were found. The results from swelling experiments are shown in Figure 4.4. The initial swelling rate in water was the same for all the tested films. After 1 h, a lower swelling rate was observed for POC and 1% ZnO-POC while other two composite films (3% and 5% ZnO-POC) showed a constant equilibrium percentage swelling (EPS). An obvious decrease in EPS after 6 hours is a result of increasing cross-linking density with ZnO concentration (Figure 4.4).

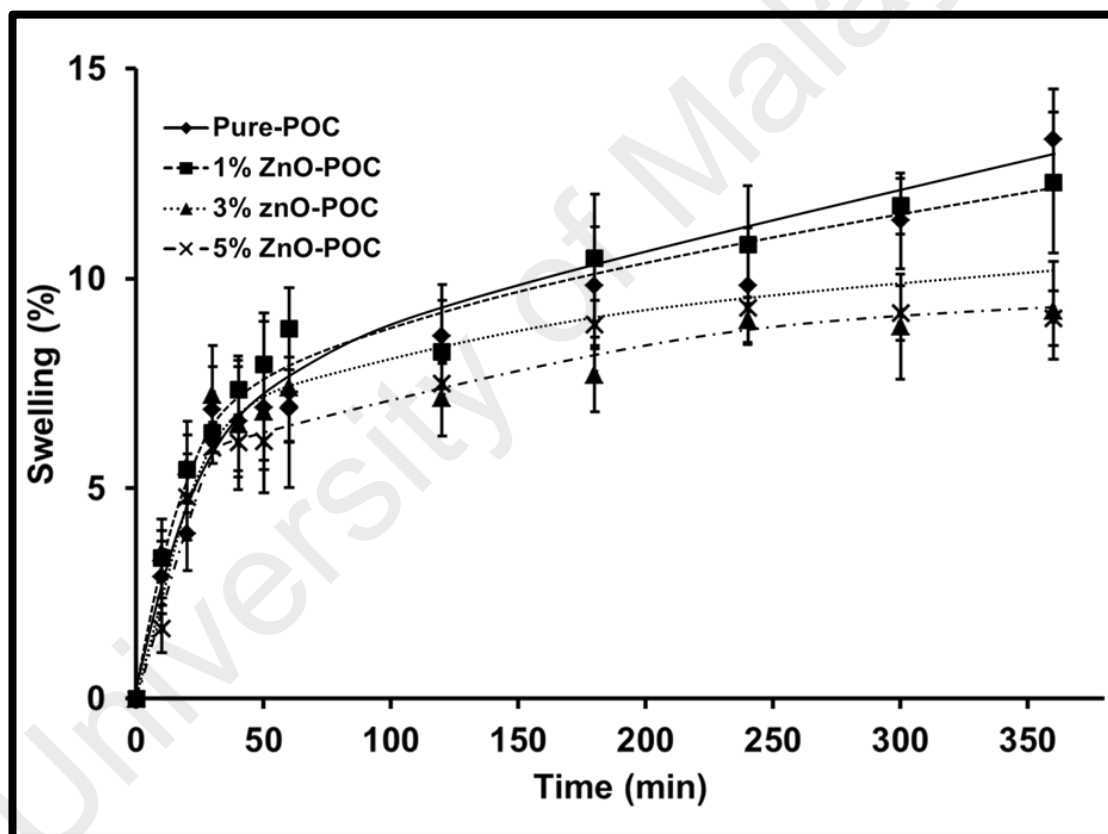


Figure 4.4: Percentage swelling in water for Pure-POC (control) and 1%, 3% and 5% ZnO-POC composite films.

4.3.5 Chemical composition

The ATR-FTIR spectra of Pure-POC and 5% ZnO-POC are shown in Figure 4.5. The FTIR spectrum of POC that shows peaks at 1178 CM^{-1} which expresses both functional

groups i.e. alcohols and carboxylic acids of OD and CA respectively. A peak at 1723 CM^{-1} shows the C=O stretch that confirms the presence of carboxylic acids, while a peak at 3468 CM^{-1} confirms the alcohols of 1,8 Octanediol (OD). It is to be noted that peaks at 1178 CM^{-1} , 1723 CM^{-1} and at 3468 CM^{-1} are similarly present in the POC-1%, 3% and 5% ZnO scaffolds. Peaks at 1630 cm^{-1} and 610 cm^{-1} indicate the presence of ZnO NPs within the POC matrix at the depth of several microns, detectable with ATR-FTIR. A broad peak at $\sim 1720\text{ cm}^{-1}$ (present in all samples) indicates successful polyesterification between CA and OD monomers (Qiu et al., 2006). Other ZnO-POC scaffolds (1% and 3%) did not show any significant difference when compared to 5% ZnO-POC (Shirazi et al., 2014; Yang et al., 2006)

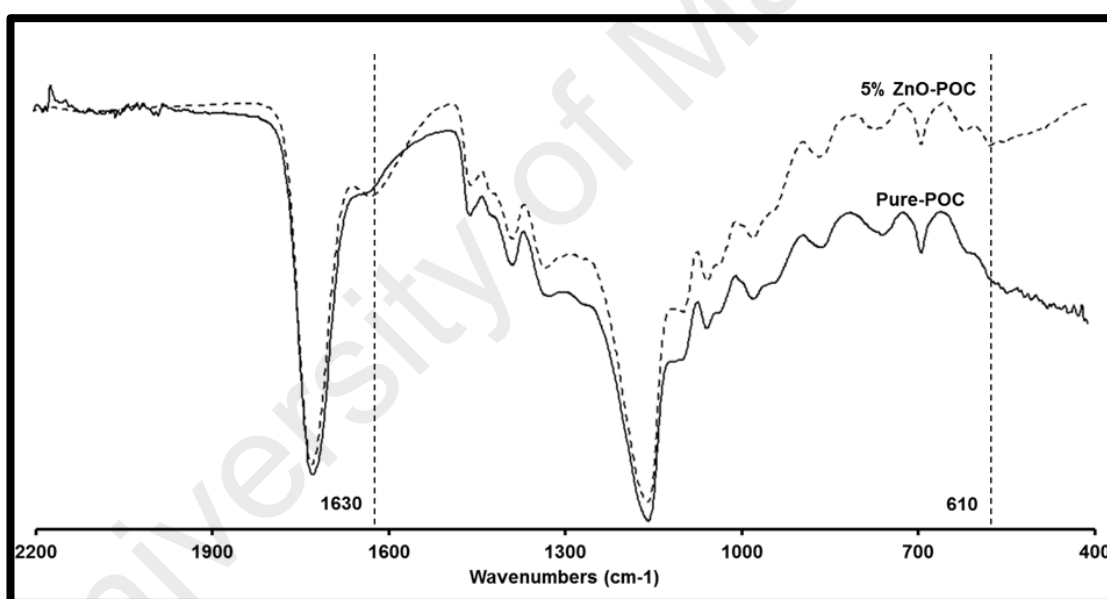


Figure 4.5: Representative ATR-FTIR spectra of POC and 5% ZnO-POC scaffolds.

4.3.6 Thermal stability

To investigate thermal stability of the developed scaffolds, Thermograms of Pure-POC (control) and 1%, 3% and 5% ZnO-POC scaffolds were recorded in TGA experiment. Figure 4.6 indicates a high stability and a high degree of polymerization without detection of low molecular weight residues. TGA results show a two-step thermal degradation

process, recorded for all the examined samples. The onset of degradation was detected in the range of 200-220 °C, where POC has the lowest and 5% ZnO-POC the highest onset of degradation temperature, corresponding to the pre-determined concentrations of ZnO (Moradi et al.).

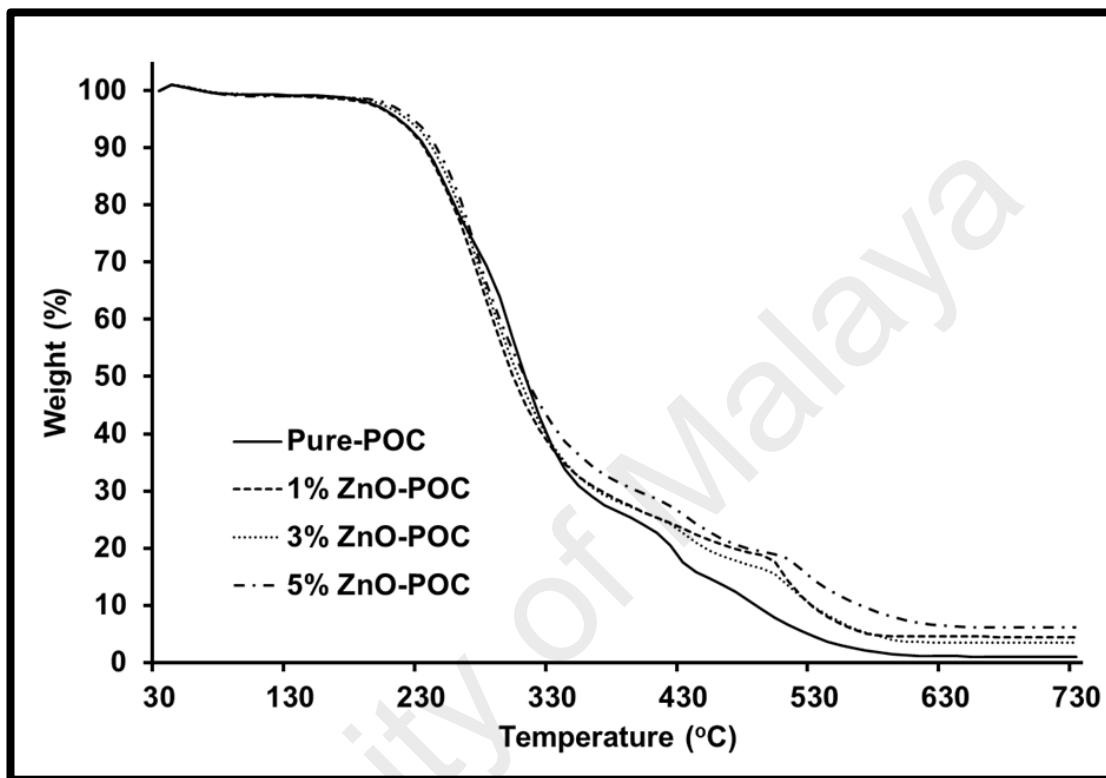


Figure 4.6: Thermal degradation curves of Pure-POC and (1%, 3% & 5%) ZnO-POC scaffolds measured by TGA.

4.3.7 Degradation

The degradation rates of Pure-POC and 1%, 3% & 5% ZnO-POC scaffolds are shown in Figure 4.7. It is observed that there is a gradual weight loss. However, for the first couple of weeks no significant change can be seen in the weight loss. After week 2 a weight loss of about 2% was seen in all the scaffolds. This fell to 24%, 22%, 15% and 13% for Pure-POC, 1%, 3% & 5% ZnO-POC respectively in the tenth week. At week 10 there was no significant difference between Pure-POC & 1% ZnO-POC and 3% & 5% ZnO-POC, however, a highly significant difference was seen when Pure-POC was compared with

3% & 5% ZnO-POC. At the end of week 20 there was no significant difference between Pure-POC and 1% ZnO-POC, whereas on the other hand a significant difference was seen on comparing Pure-POC with 3% & 5% ZnO-POC. There was no significant difference between 3% and 5% ZnO-POC and between Pure-POC and 1% ZnO-POC at all phases.

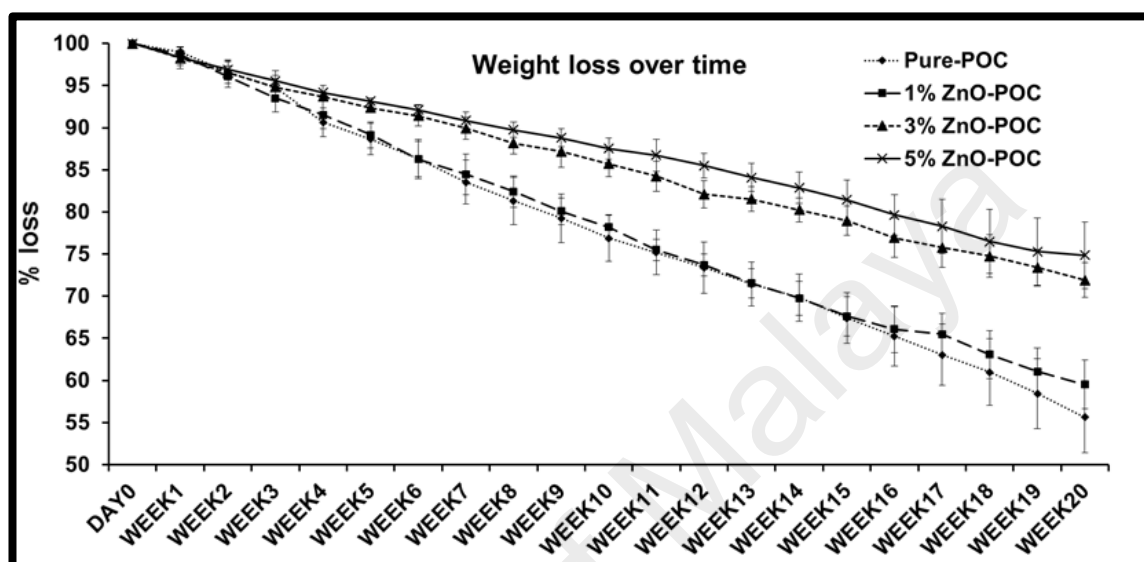


Figure 4.7: Weight loss of Pure-POC, 1%, 3% and 5% ZnO-POC scaffolds over the period of 20 weeks in Phosphate Buffered Saline (PBS).

4.3.8 ZnO release kinetics

The release studies were performed in order to evaluate the relative concentration of Zn^{+2} ions liberated from 1%, 3% and 5% ZnO-POC scaffolds. Ion concentration was reasonably considered as directly proportional to the release of ZnO NPs into an aqueous medium. This simulation of physiological conditions (*in vitro*: 37 °C; PBS) is important in order to assess the scaffolds for future experiments with cell seeding and subsequent implantation *in vivo*. The release kinetics curves after 24 h are presented in Figure 4.8. Only after 7 days relatively small difference in the amount of ZnO released from ZnO-POC scaffolds was observed. The relative concentration of Zn^{2+} after days 14 and 28, measured for 5% ZnO-POC was much higher in comparison to other two scaffolds (1% and 3% ZnO-POC) (Figure 4.8). The high concentration of ZnO inside the POC matrix

(5%) caused a “burst release” between days 14 and 28, where the Zn^{2+} concentration doubled between two time points. As expected the lowest concentration of Zn^{2+} was detected for 1% ZnO-POC after 28 days. Unlike 5% ZnO-POC, both 1% and 3% ZnO-POC scaffolds maintained “zero order release kinetics” in the period of three weeks (between day 1 and day 28 in Figure 4.8) (Hahn et al., 2011). There are two possible mechanisms of ZnO NPs release from the POC matrix: (1) particle erosion after polymer swelling; and (2) polymer degradation and subsequent particle release.

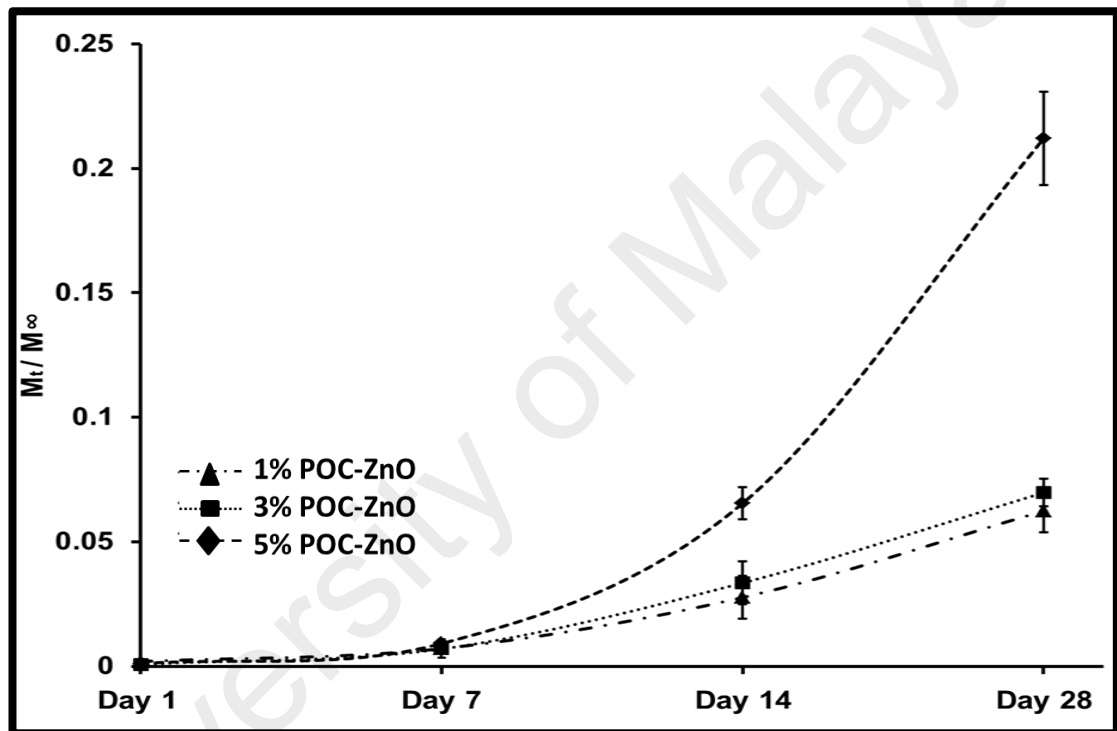


Figure 4.8: In-vitro Release kinetics profile of ZnO (Zn^{2+}) from ZnO-POC scaffolds in PBS at 37°C; M_t = mass of ZnO released at time intervals; M_∞ = total mass of ZnO within the scaffold (all M_t/M_∞ ratios are the mean values for five samples measured with AAS).

The actual concentration of ZnO released in the medium over the period of 28 days revealed that highest release of Zn ions was 4.61 ppm from scaffold containing 5% ZnONP while 1% and 3% ZnONP-POC demonstrated a significantly lower amount of Zn ions released with values of 2.7 and 2.68 respectively (Figure 4.9).

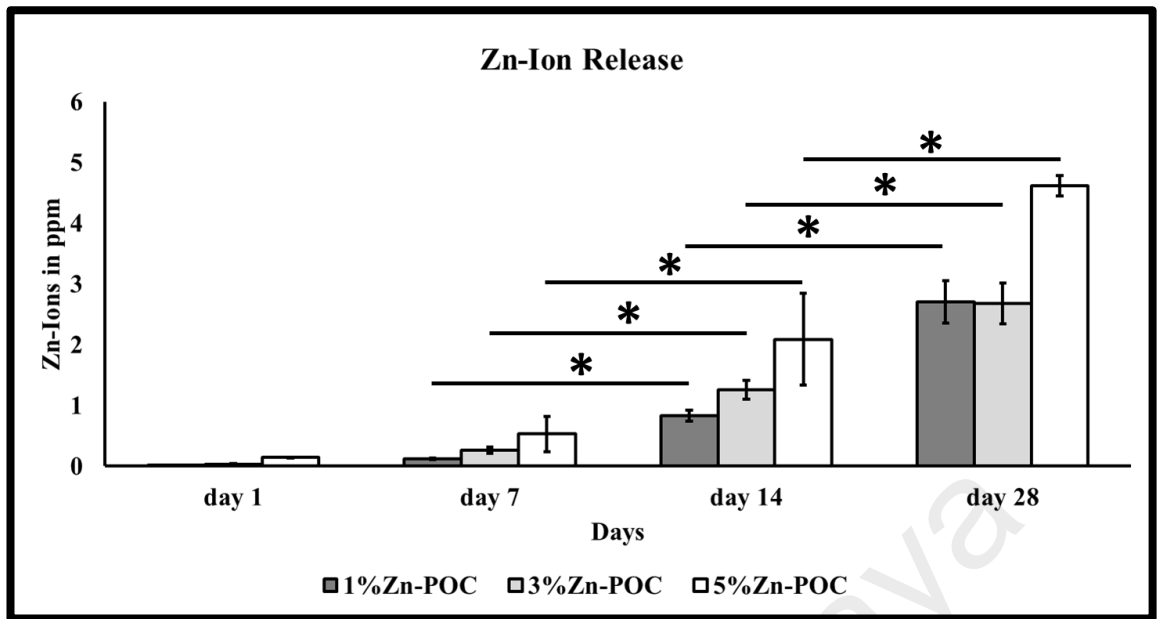


Figure 4.9: Zn-ions released over the period of 28 days calculated in ppm via AAS. Where * shows a significant difference between the number of days, $p < 0.05$.

4.3.9 Anti-bacterial properties of ZnO-POC scaffolds

Bacterial growth of *E. Coli* and *S. Aureus* in the presence of both Pure-POC (control) and 1%, 3% and 5% ZnO-POC scaffolds over the period of 8 h is shown in Figure 4.10. There is a possibility that small amounts of ZnO had been released into the surrounding medium due to the polymer swelling and thus caused the depletion of bacteria. On the other hand, the highest concentration of Zn was present on the surface of 5% ZnO-POC (Figure 4.2 and EDX results, section 4.3.2).

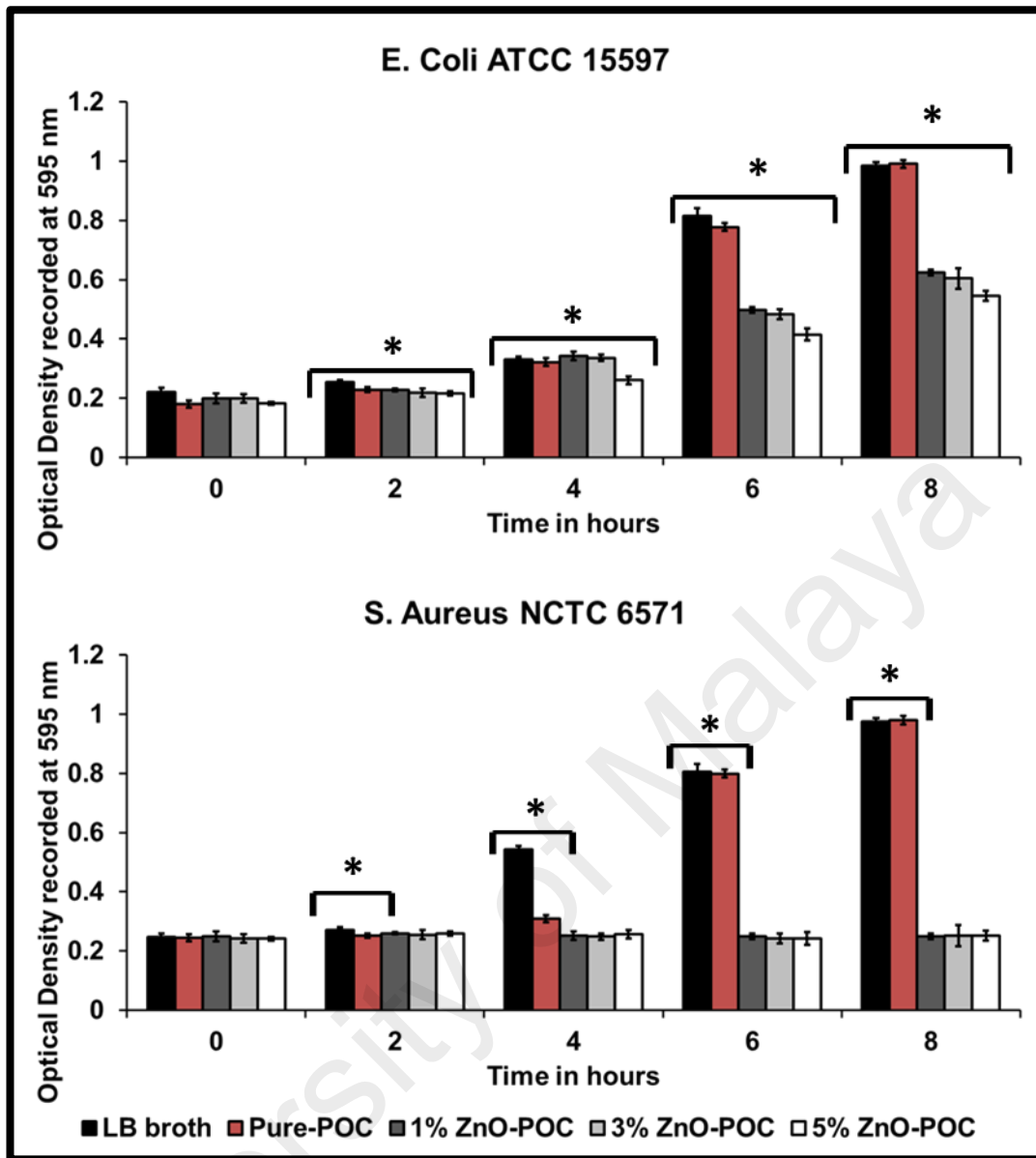


Figure 4.10: Growth rates of E. coli and S. Aureus in LB broth inoculated with 50 μ l of 10^4-5 CFU/ml for Pure-POC (positive control), LB Broth (negative control) and 1%, 3% and 5% ZnO-POC scaffolds (optical density at 595 nm was measured in microplate reader and is proportional to bacterial growth). Where * shows significant difference among scaffold types at various time intervals, $p < 0.05$.

4.3.10 Cytotoxic effects of ZnO NPs on primary chondrocytes

Resazurin reduction results in (Figure 4.11-A) revealed that Pure-POC and 1% ZnO-POC did not have any adverse effect on cell viability, however 3% and 5% ZnO-POC demonstrated highly cytotoxic behaviour towards primary bovine chondrocytes even after 24 hours. Another important aspect of biomaterials in general is the cellular morphology of adhering cells. Images from FESEM (Figure 4.11-B and 4.10-C) reveal a healthy morphology of seeded chondrocytes within the scaffolds.

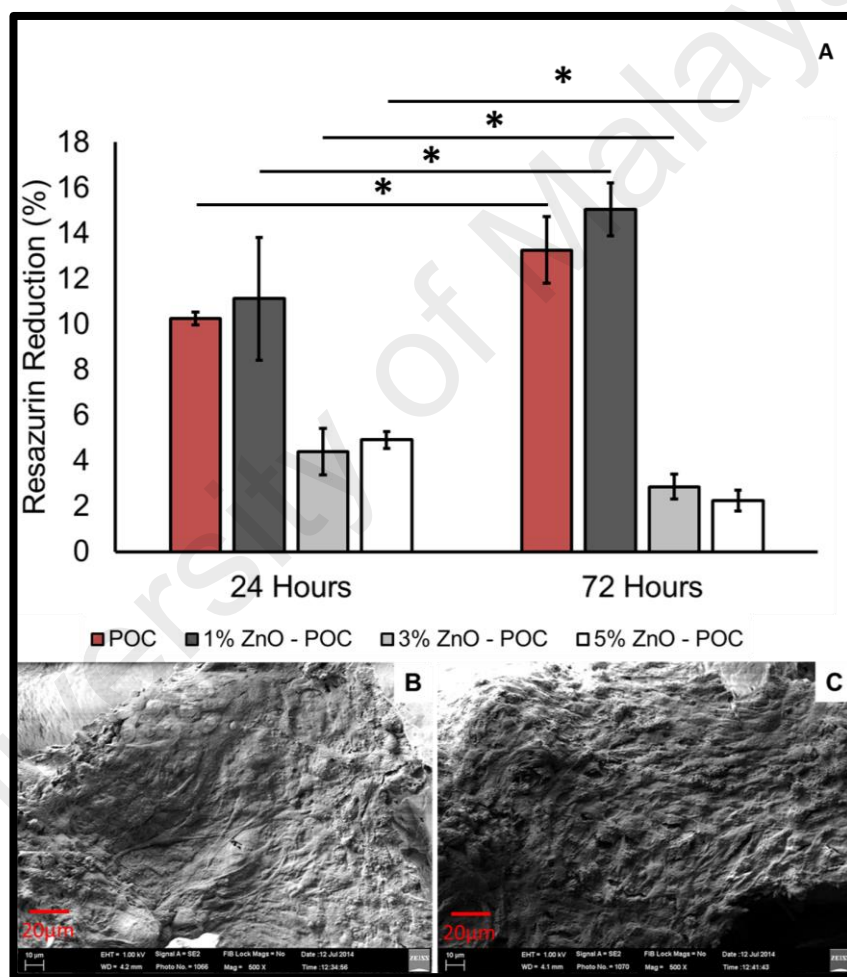


Figure 4.11: (A) Resazurin reduction (%) for Pure-POC (control) and 1%, 3% and 5% ZnO-POC scaffolds after 24 and after 72 hours. Where * shows a significant difference within the scaffold type at different times, $p < 0.05$. FESEM images of scaffolds after 72 hours in chondrocyte culture: (B) Pure-POC; and (C) 1% ZnO-POC (bar = 20 μm).

4.4 Discussion

POC is an established elastomer that have long been characterised and its synthesis scheme has been established (Yang et al., 2006). HNMR and MALDI-TOF have already been performed to establish the confirmation of polymerisation (Ivan et al., 2009). However, as in this research ZnONP are incorporated in POC hence related characterisation of the polymeric scaffold is done. This section determines the potential of POC scaffolds incorporated with ZnONPs for cartilage tissue engineering. Moreover, this section discusses the evidence that indicates higher ZnONPs concentrations are cytotoxic.

4.4.1 Surface morphology

FESM images in Figure 4.1 (A-D), revealed that the pore sizes were in the range of 100-200 μm , (which is smaller than the dimensions of the sieved salt in the range of 200-300 μm), consistent with previously reported results (Moradi et al.). Most importantly, FESEM images reveal a random distribution of pores with interconnecting channels, which is a desirable feature for optimal cell distribution after the seeding (Hou et al., 2003; Karageorgiou & Kaplan, 2005). Furthermore, presence of ZnO NPs on the scaffold surface inside the pores were observed in the scaffold containing ZnO NPs (Figure. 4.1-(A-D)). The presence of ZnO NPs would most likely have an influence on both bactericidal properties and cell toxicity.

4.4.2 Influence of ZnO-NPs on relative hydrophilicity

In comparison to nano-composite coatings, Pure-POC showed polymer delamination from the glass surface. Such irregular morphology could not be detected on composite coatings (Figure 4.2 (A-D)). ZnO NP aggregates of 10-20 μm were observed that could not be avoided in the current method (Gawish et al., 2012). However, in the case of 1%

ZnO-POC, ZnONP are visibly lower, when compared to the other coatings. This result somehow opens a new possibility to develop nano-composite coatings with a high level of control over surface composition and homogenous spreading of NPs.

Contact angle results in Figure 4.3 show an increasing trend in contact angles due to higher ZnO NP content. Higher contact angles are due to increase in cohesive forces associated with bulk water, more than that of the water with the surface (Vafaei et al., 2006). Higher contact angles can also be attributed to increased surface roughness which results in trapped air between liquid and solid to cause greater repellence (Athauda et al., 2013). Such surface interactions with water are causing the more hydrophobic behaviour of the ZnO-POC composite material in comparison to POC control.

4.4.3 Physical properties of ZnO-POC scaffolds: porosity and elasticity

Differences in calculated and measured porosity imply that after salt leaching the actual porosities may drop 4-8% from expected value due to the recovery of the elastomeric material (Thadavirul et al., 2014) (Table 4.1). Moreover, it was found that the scaffolds can withstand stresses of up to 70 MPa at around 50% strain, which is far greater value than what a human tissues experience during normal activity (Brand, 2005; Moradi et al.; Thambyah et al., 2005). It is also reported that the average compressive modulus of human articular cartilage is ranges from 0.2 to less than 0.5 MPa (Boschetti et al., 2004). The results in Table 4.1 are close to what is required for clinical implementation. Judging from compression test alone, ZnO-POC scaffolds possess great potential to be exploited for load bearing tissues such as cartilage.

Overall, the analysed samples showed elastic nature which is an important feature in biomaterials. If a degree of compressive elasticity can be judged from the recovery after stress, ZnO-POC scaffolds showed substantial variation for recovery within the range of 94-60 %. As the concentration of ZnO increases, the scaffolds tend to recover at a slower pace. This is most likely a result of agglomeration of ZnO NPs. Increased stiffness is

attributed to solid ZnO NPs and facilitated interaction between both phases of the scaffold. On the other hand, the addition of ZnO NPs increased the ductility, as previously described for other polymer nano-composites (Luo et al., 2009; Meng et al., 2011). Apart from the expected influence on mechanical properties by the presence of “filler” in polymer composite materials, ZnO is expected to show antibacterial, wound healing, and cell proliferating capabilities, which are the major attributes in current research (Colon et al., 2006; Moezzi et al., 2012). However, all tissues responded to the physical properties of the biomaterial so the fundamental physical tests are necessary in order to establish sensitive and highly complex interactions at cell-biomaterial interfaces.

4.4.4 Swelling and cross-linking density

According to the rubber elasticity theory, Young’s modulus is directly proportional to cross-linking density of elastomers. Therefore, the lowest swelling rate is expected to show the highest value for Young’s modulus (Table 4.1). Another important feature that could influence swelling behaviour is a relative hydrophilicity/hydrophobicity of developed composite materials. A significant increase in water contact angle (observed after addition of ZnO; Figure 4.3) also influences the swelling behaviour (Figure 4.4). The hydrophobic component of the composite material (ZnO NPs) does not allow water to penetrate into the material and therefore causes decreased swelling (Djordjevic et al., 2009). This is an important result which would most likely influence the initial release of ZnO NPs from POC matrix and would subsequently influence different interactions with biological systems.

4.4.5 Chemical composition

FTIR results show successful polyesterification between CA and OD monomers. In a separate, previous work the films were examined that were produced with higher

concentrations of ZnO (2.5%, 5% and 10%) (Kompany et al., 2014). In case of the films (thickness: 1 mm) the intensities of the peaks at 1630 cm^{-1} and 610 cm^{-1} were much more pronounced even for 2.5% and 5% ZnO-POC. The peak at 3468 CM^{-1} refers to the hydroxyl groups which hints at increased mechanical strength (Wang et al., 2002). The peaks at 1723 CM^{-1} and at 3468 CM^{-1} indicates successful polymerisation along with the formation of polyester groups (Moradi et al.; Yang et al., 2006). Moreover, at around 1630 CM^{-1} gradual decrease in transmittance can be seen as there is an increase in nano-ZnO content, which might give rise to the fact that, the oxides of ZnO have partially cross-linked during the curing process. Results presented in Figure 4.5 are of scaffolds and it is most likely the consequence of porosity of scaffolds (in comparison to composite films) when measured in ATR mode, because scaffolds are porous and they may allow light to pass through them. More accurate results can be obtained by analysis of polymer composite films with a flat surface.

4.4.6 Thermal stability

An important structural feature is that thermal stability increases with increasing concentration of ZnO in the ZnO-POC scaffolds (Figure 4.6). Such a feature is likely to influence other material properties such as swelling in water and release kinetics of ZnO from a polymer matrix. Similar results were reported by Laachachi and co-workers. They reported that increase in wt% of nanoparticles caused lowered heat release rate (Laachachi et al., 2005). Moreover, the increase in concentration of nanoparticles cause slowing of ablation of the surface (Laachachi et al., 2005) and ultimately reducing degradation rate. In another study, Tang E. and co-workers reported that presence of ZnONP in polymer matrix can cause an alteration in wettability (Tang et al., 2006) due to change in hydrophobicity as can be seen in this research as well (Figure 4.3). The experiments were repeated for different sections of the scaffolds and the solid residue after complete degradation corresponded to ZnO concentrations within the scaffolds. This

result proves the efficiency of the method and the even distribution of ZnO NPs over the entire volume of the scaffolds.

4.4.7 Degradation

Degradation studies imply that the increase in content of nano-ZnO particles stemmed in sinking the degradation rate. At the end of week 20 the Pure-POC, 1%, 3% & 5% ZnO-POC degraded 45%, 41% 29% and 26% respectively (Figure 4.7). These results are in accordance with another study (Meng et al., 2011), where they showed that with the increase in carbon nano-tube content the weight loss of the POC-nano composite was lesser as compared to Pure-POC. An ideal tissue culture construct must be able to maintain its mechanical integrity until the natural tissue grows and adapt to the environment and produce a sufficient extracellular matrix prior to complete degradation or absorption by the body (Wu & Ding, 2004).

4.4.8 ZnO release kinetics

The release kinetics of ZnO (Figure 4.8) indicate that the most likely release mechanism is through the degradation process. Since there was a minimal concentration of Zn^{2+} detected after 1 day it is less likely that the swelling would have any influence on the release of ZnO (Figure 4.8 and Figure 4.9). The degradation rate of POC can vary depending on the processing conditions, in particular, curing temperature, pressure and time have a strong influence on a cross-linking density and subsequent *in vitro* degradation properties of the final product (Yang et al., 2006). POC reported in this paper substantially degrades in physiological conditions within the period of one month (70 % of degradation) (Djordjevic et al., 2009). For that reason it is expected for the amount of released particles is proportional to the content of solids inside the scaffold. Since there is evidence of a strong anti-bacterial property of ZnO, it is important to establish the correlation between ZnO release kinetics and influence on surrounding bacteria.

4.4.9 Anti-bacterial properties of ZnO-POC composite scaffolds

All scaffolds demonstrated antibacterial properties which contained ZnO-NPs. The results can be related to anti-bacterial activity, given that bacteria perish more rapidly in the presence of increasing surface concentration of ZnO (Figure 4.10). As mentioned before, ZnO is known to possess anti-bacterial properties. T. Jin et al. have tested ZnO NPs against various bacteria and it was suggested that ZnO particles should contact or penetrate the bacterial cell wall to demonstrate antibacterial behaviour (Jin et al., 2009). For that reason ZnO NPs must come in contact with the bacteria in order to express their anti-bacterial behaviour. ZnO containing scaffolds showed ZnO NPs on the outermost surface layer (Figure 4.1 and Figure 4.2) which is a desirable feature that would help fight infections and formation of biofilm. Other polymer matrices have also been mixed with ZnO in order to produce the anti-bacterial scaffolds. Zhang et al. have used ZnO NPs that were mixed with polyethylene glycol (PEG) and polyvinylpyrrolidone (PVP) as dispersants.

They reported that the antibacterial activity against *E. Coli* increases with the increase in concentration of NPs (independent of particle size) (Zhang et al., 2007). Till submission of current thesis, no attempt has been made to produce biodegradable tissue engineering scaffolds from CA-based polyester elastomer and ZnO NPs that would have strong anti-bacterial properties.

Biological systems are complex and ZnO-NPs (or Zn^{2+} ions) can directly influence some processes. For example, Zn is attributed to cause a reduction in inflammation among cells by lowering oxidative stresses (Prasad et al., 2007). It has also been reported that Zn-deficient cells are more susceptible to DNA damage and development of cancer (Ho et al., 2003; Prasad, 2008). In tissue engineering applications, different “bio-activity” factors must be considered, such as: (i) influence of released particles on the growth and

proliferation of tissue-specific cells, (ii) particle influence on phenotype, (iii) blood compatibility and inflammatory response, and (iv) ECM formation.

POC is known to have excellent biomaterial properties (Serrano et al., 2010; Yang et al., 2004). The elastic nature and non-toxic components (used in the preparation process) are the key features of POC and other CA-based elastomers. The addition of ZnO retains the elastic nature (Table 4.1) and does not change the chemical composition of the synthesised polymer (Figure 4.4). There are reasonable concerns about the influence of ZnO on cellular growth since ZnO effectively inhibits the growth of bacterial cells (Figure 4.10) (Yang, S. et al., 2014). 1, 3 and 5% of ZnONP were selected based on the literature available, as higher concentrations can cause severe toxicity to healthy cells (Liu et al., 2009; Reddy et al., 2007). Moreover, the antibacterial activity of ZnONP is concentration dependent (Jin et al., 2009) and if the concentration is too low the scaffolds might no longer act as antibacterial scaffolds. All concentrations of ZnO-NPs have shown better performance than Pure-POC in terms of bacterial inhibition (Figure 4.10). A key feature of ZnO-POC composite scaffold is that these scaffolds can be produced in the same fashion as POC but with significant advantages over POC. The presence of ZnO enables anti-bacterial potential that would “shield” the implanted scaffold in both initial stages of implantation and over periods of bio-degradation time *in vivo*.

4.4.10 Cytotoxic effects of ZnO NPs on primary chondrocytes

Cytotoxicity of NPs has long been discussed. Higher ZnO content exhibited cytotoxic effects towards chondrocytes. Cytotoxic outcomes were also reported by Feng Pei et al. where 3.5 wt% of ZnO in β -tricalcium phosphate scaffolds demonstrated cytotoxicity for MG-63 cells (Feng et al., 2014). In the same study, 2.5 wt% of ZnO was reported to enhance osteoblast cell proliferation and increase cell viability. The scaffold matrix must be carefully considered in such system. Degradation rate, swelling and hydrophilicity of

the polymer scaffold (or ceramic) must have a strong influence on particle release and therefore the influence on both bacterial and tissue-specific cells.

Cytotoxicity results for reduction of resazurin is presented in Figure 4.11-(A). Cells on control scaffolds (POC) tend to be more fibroblastic which is a characteristic of monolayer cultures (Figure 4.11-B) (Brodkin et al., 2004). In particular, nano-composite 1% ZnO-POC scaffold (Figure 4.11-C) is more uniformly covered by cells with spherical morphology characteristic of chondrocyte cells (Dwivedi et al., 2014). Another reason why cells on ZnO-POC scaffold showed more characteristic morphology is that NPs could provide anchorage to the cells and a rough surface that prevents the chondrocytes changing their morphology to fibroblasts (Gutwein & Webster, 2002; Na et al., 2007). Findings reported in this section reveal that 1% ZnO-POC is a prospective candidate for cartilage tissue engineering, while higher concentration of ZnO will compromise cellular health. Better cell morphology preservation and no cytotoxicity of ZnO-NPs in low concentrations can be attributed to the role of ZnO in reactive oxygen species (ROS), anti-inflammatory and wound healing capabilities (Kumar et al., 2011; Lang et al., 2007; Prasad, 2008). It is widely documented that ZnO is a producer of ROS, which may damage cell health at high concentration, but at low concentrations is beneficial for cell proliferation (Augustine, Malik, et al., 2014).

CHAPTER 5: EFFECT OF HYPOXIA ON BOVINE ARTICULAR CHONDROCYTES

5.1 Introduction

The physiological environment of articular cartilage is typically avascular and aneural (Park & Lee, 2014). Moreover, it is well established that the microenvironment of cartilage is hypoxic, with oxygen tension ranging from <10% at the surface and <1% in the deepest layer (Grimshaw & Mason, 2000).

However, although cartilage naturally resides in this specific low oxygen tension microenvironment, articular chondrocytes are customarily cultured at normal atmospheric oxygen tension (19–21 %) (Balasundaram et al., 2014; Chen et al., 2013). Many studies have reported that hypoxia is nevertheless a key factor in the growth and survival of chondrocytes (Ab-Rahim et al.; Genes et al., 2004; Meyer et al., 2010), a factor which enhances the production of cartilage-like ECM, and which maintains cell phenotype (Murphy & Polak, 2004; Murphy & Sambanis, 2001). How chondrocytes make use of oxygen is not clear, however, researchers have recognized that 5% oxygen tension up-regulates matrix synthesis (Hansen et al., 2001; Murphy & Polak, 2004; Murphy & Sambanis, 2001; Saini & Wick, 2004). Due to the avascular nature of cartilage, its complex biological characteristics and low cell concentration, articular cartilage have a limited capacity for self-repair (Yodmuang et al., 2013). Tissue engineering (TE) offers an alternative option for is cartilage treatment (Chen, F. H. et al., 2006; Hollister, 2005). Many studies have focused on tissue-engineering methods to create cartilaginous tissue *in vitro*, to enable cartilage transplantation (Peretti et al., 2000; Yodmuang, McNamara, et al., 2015).

Zinc (Zn) is an essential trace element for human and animal growth (Haase & Rink, 2014b) and has a critical role in cell proliferation, differentiation, and survival (Haase & Rink, 2014a). A Zn-deficient diet has been shown to result in inhibiting chondrocyte

proliferation and increased apoptosis (MacDonald, 2000). Zn deficiency has also been related to rheumatoid arthritis (RA) (Mierzecki et al., 2011) defects in epiphyseal cartilage (Westmoreland & Hoekstra, 1969) and growth retardation (Prasad et al., 1961). Besides that, Zn is also known to possess anti-bacterial, anti-inflammatory, and anti-oxidant properties (Azizi et al., 2014; Geilich, 2013; Kompany et al., 2014; Memarzadeh et al., 2014; Prasad, 2014; Rink & Haase, 2007; Sunzel et al., 1997), hence the inclusion of Zn in an *in-vitro* scaffold is attractive because the infection is a common problem for cell culture. Previously, it was found that a 1wt% of Zinc Oxide nanoparticles (ZnONP) yields a higher cell viability than does a higher dose, and yet still maintains its anti-bacterial properties. It was reported that at higher doses of Zinc Oxide (ZnO) are considered toxic {Reddy, 2007 #373}.

The full effect of ZnO nanoparticles, particularly in combination with a physiological oxygen level (5% O₂), remains poorly characterized and understood. In order to address this, it was hypothesized that the combination of hypoxia and ZnONP would further enhance cell proliferation and cartilage matrix production. In order to test this hypothesis, chondrocytes were seeded in porous POC scaffolds, which have been previously shown to be able to support chondrocyte attachment, proliferation, and differentiation *in-vitro* (Kang et al., 2006). Furthermore, the production of transcription factor hypoxia-inducible factor 1A (*HIF-1A*) in response to hypoxic condition was also evaluated, with and without ZnONP. *HIF-1A* is a transcription factor that regulates genes related to cellular survival under hypoxia, and so it is desirable that it not be disrupted by ZnONP.

5.2 Materials and Methods

Pure POC and 1% ZnO-POC scaffolds were immersed in 70% alcohol for half an hour followed by autoclaving at 121⁰C for 15 minutes at 15 psi. Once removed from the autoclave, the scaffolds were immersed in medium to neutralise overnight prior to cell seeding. Isolated bovine articular chondrocytes (BAC) (refer to section 3.4 for details of

BAC isolation) were seeded on the scaffolds. The final cell concentration was 0.6×10^6 cells per scaffold. The cells were allowed to attach for 4 hours and then the wells were replenished with chondrocyte culture medium (refer to section 3.4.1 for formulation).

5.2.1 Experimental Design

Pure-POC and 1% ZnO-POC scaffolds were kept in 2 conditions; one in hypoxia (5% O₂) and the second one in normoxia (21% O₂) for 1, 3, 7, or 14 days. The experimental design is summarised in figure 5.1.

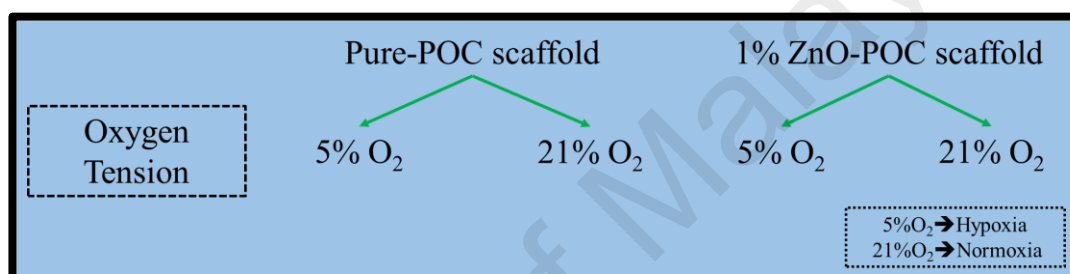


Figure 5.1: Summary of experimental design.

5.2.2 Cell Proliferation Assays

Cell viability was determined via Resazurin reduction assay (refer to section 3.5 for detailed protocol). Moreover, the Hoechst binding dye method was used to quantify DNA within the scaffolds at each time point (refer to section 3.6 for detailed protocol). The qualitative cell viability was determined using a LIVE/DEAD[®] viability kit (Molecular Probes[®] LifeTechnologies[™], Carlsbad, CA, USA) (refer to section 3.10 for detailed protocol). Scanning electron microscope (SEM) was used to view cell-materials interactions (refer to section 3.9 for experimental protocol).

5.2.3 Sulphated glycosaminoglycan (S-GAG) quantification assays

Glycosaminoglycans (GAGs) are polysaccharides that are present in abundance in healthy cartilage. Sulphated-GAGs (S-GAGs) are the types that can be measured via a 1,

9-dimethylmethylene blue assay. Total S – GAG was measured from Cell-scaffold lysate at each time point. Released S – GAG was measured by collecting the culture medium at every medium change from the wells (refer to section 3.7 for detailed protocol).

5.2.4 Quantitative Polymerase Chain Reaction (q-PCR)

To observe the behaviour of BACs at gene level Cartilage matrix specific genes; Collagen type II (*COL2A1*) and Aggrecan (*ACAN*) were observed. Moreover the matrix degradation gene (*MMP-13*) and hypoxia inducible factor gene (*HIF1A*) were also observed. Q-PCR gene expressions were determined by the *TaqMan* gene expression assay using StepOnePlus™ Real-Time PCR system (refer to section 3.8 for detailed protocol).

5.2.5 Statistical Analysis

Data are represented as average \pm standard deviation for Day 1, 3, 7 and 14. Statistical analysis was performed using IBM SPSS v21, with a two-way analysis of variance (ANOVA) to determine significance between groups (Pure-POC vs 1% ZnO-POC), and a post-hoc Tukey's test was applied to test significance between oxygen tension and within the days. In all conditions, a p value of less than 0.05 ($P < 0.05$) was considered to be significant. The number of biological replicates in all the studies ranges from 5 to 12.

5.3 Results

This section describes the proliferation behavior, ECM formation and regulation of ECM specific genes for chondrocytes seeded on Pure-POC and 1% ZnO-POC scaffolds over the period of 14 days under normoxia (21% O₂) and hypoxia (5% O₂).

5.3.1 Cell proliferation

As shown in Figure 5.2, cell proliferation results indicated an increase over the period of the study in all groups. Hypoxic groups had a higher proliferative response independent of the presence of 1% ZnONP, other than on day 14 when there was no statistically significant difference between normoxia and hypoxia for the group without 1% ZnONP. There was no statistically significant influence of the presence of 1% ZnONP on proliferation at any time point (Figure 5.2).

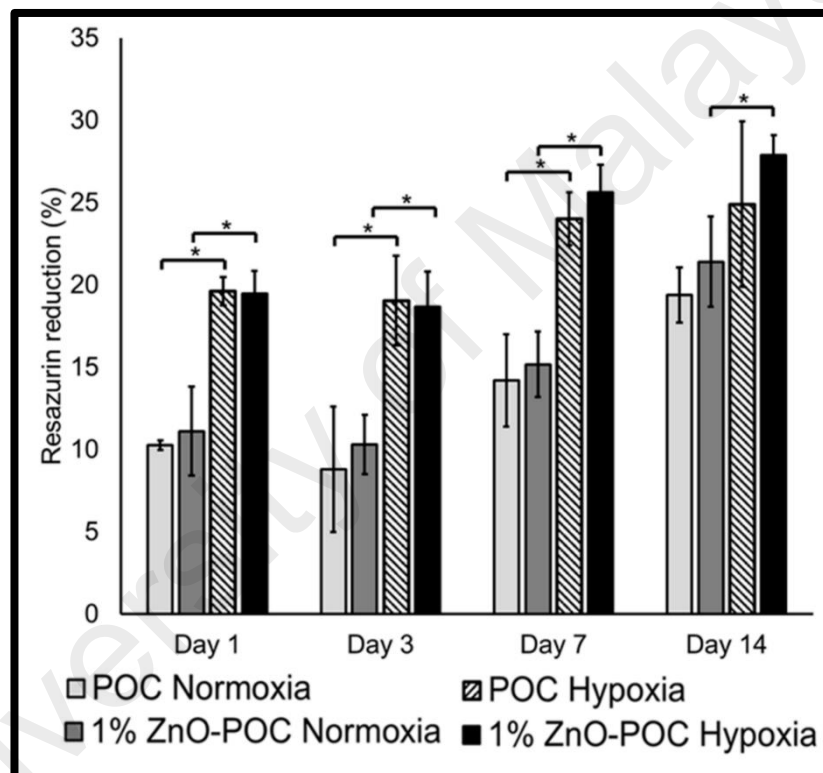


Figure 5.2: Cell vitality determined via resazurin reduction assay, of chondrocytes, seeded on Pure-POC and 1% ZnO-POC in normoxic (21%O₂) & hypoxic (5%O₂) conditions. Where * shows a significant difference between O₂ tension. 5 ≤ N ≤ 6, p < 0.05.

Comparative confocal images of chondrocytes cultured for 14 days on Pure-POC and 1% ZnO-POC either in normoxia or hypoxia are displayed in Figure 5.3 (A-L).

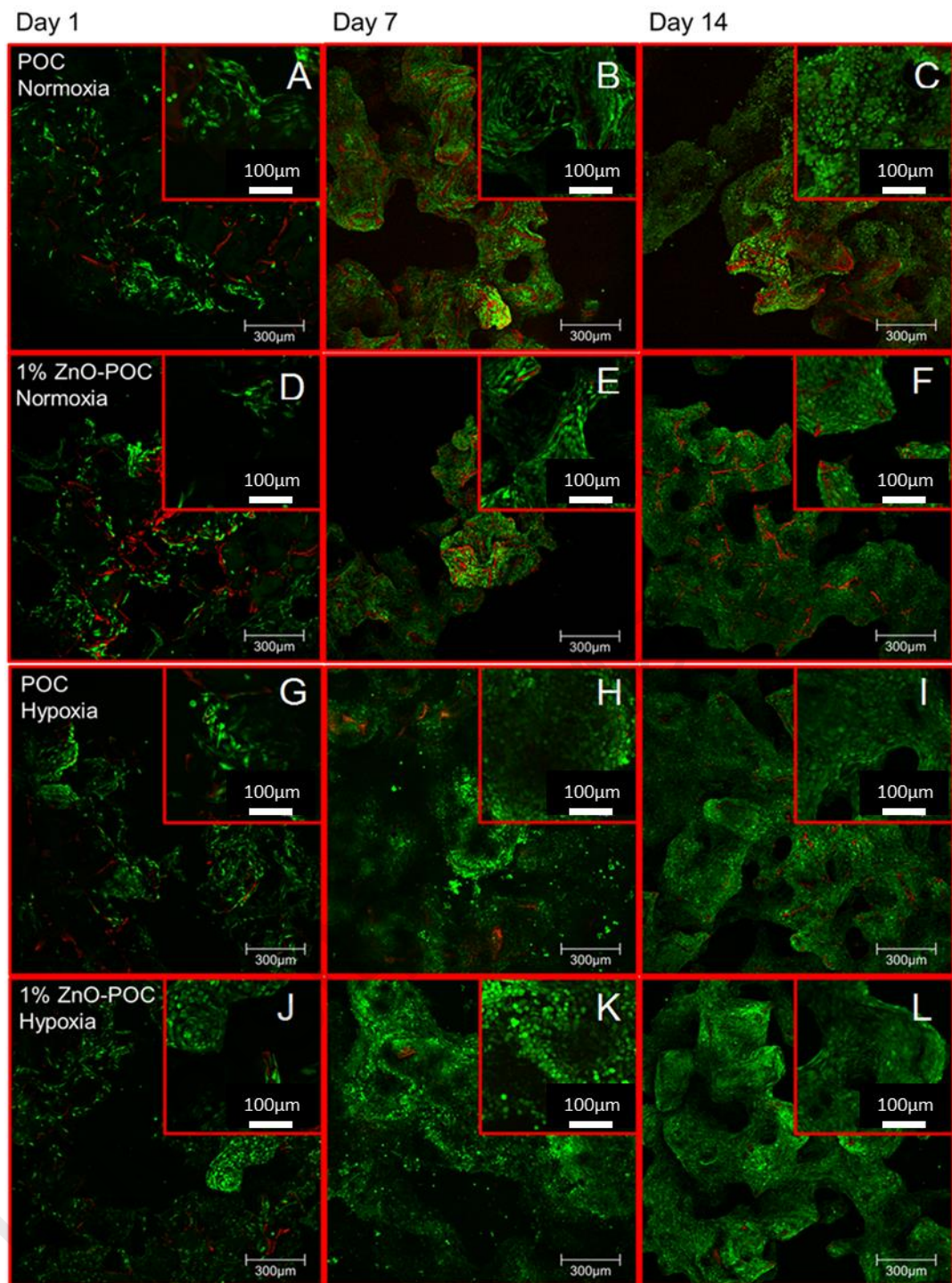


Figure 5.3 (A – L): Live/Dead assay of Chondrocytes seeded on the scaffold at day 1, 7 and 14 under normoxic and hypoxic conditions. Outer images are at 10X magnification with a scale bar of 300 µm and their respective inserts are at 40X magnification with a scale bar of 100 µm.

DNA quantification results (Figure 5.4) indicate a positive correlation with time in all groups, and the amount of DNA had increased from day 1 for each group. The hypoxic

groups yielded a statistically significant increase in DNA at all points as compared to the equivalent normoxic group. These results agree with the CLSM images (Figure 5.3 A-L.) A live/dead assay based on Ethidium Homodimer and Calcein-AM was used to differentiate between live cells and dead cells. There are clearly more live cells (more green stain) in the hypoxic group as compared to the normoxic group. The presence of 1% ZnONP produced no statistically significant effect in normoxia (comparative to CLSM images (Figure 5.3 (A-F))), but produced a statistically significant increase in DNA content in hypoxia until day 7 (no statistically significant difference was found at day 14) (Figure 5.4).

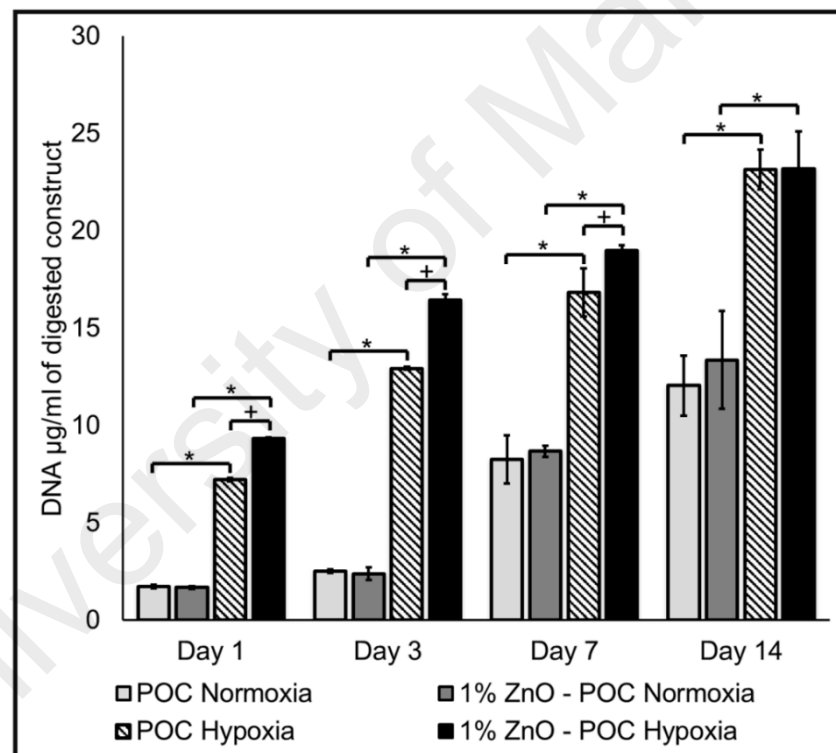


Figure 5.4: Cell quantification through DNA Hoechst fluorescence assay method, of chondrocytes, seeded on Pure-POC and 1% ZnO-POC in normoxic (21%O₂) & hypoxic (5%O₂) conditions. Where + shows significant differences between groups and * shows a significant difference between O₂ tension. 5 ≤ N ≤ 6, p < 0.05.

Similarly, by day 14, both Pure-POC (Figure 5.3-I) and 1% ZnO-POC (Figure 5.3-L) scaffolds in the hypoxic group show dense and packed live cells. The CLSM images also

confirm that both Pure-POC and 1% ZnO-POC scaffolds support chondrocytes as there are hardly any red staining that shows dead cells. FESEM images in Figure 5.5 (A-L) display an increase in cell population over time. It further shows that incorporation of ZnO in polymer maintains the cell phenotype over 14 days (Figure 5.5-F & 5.5-L) and improves ECM formation.

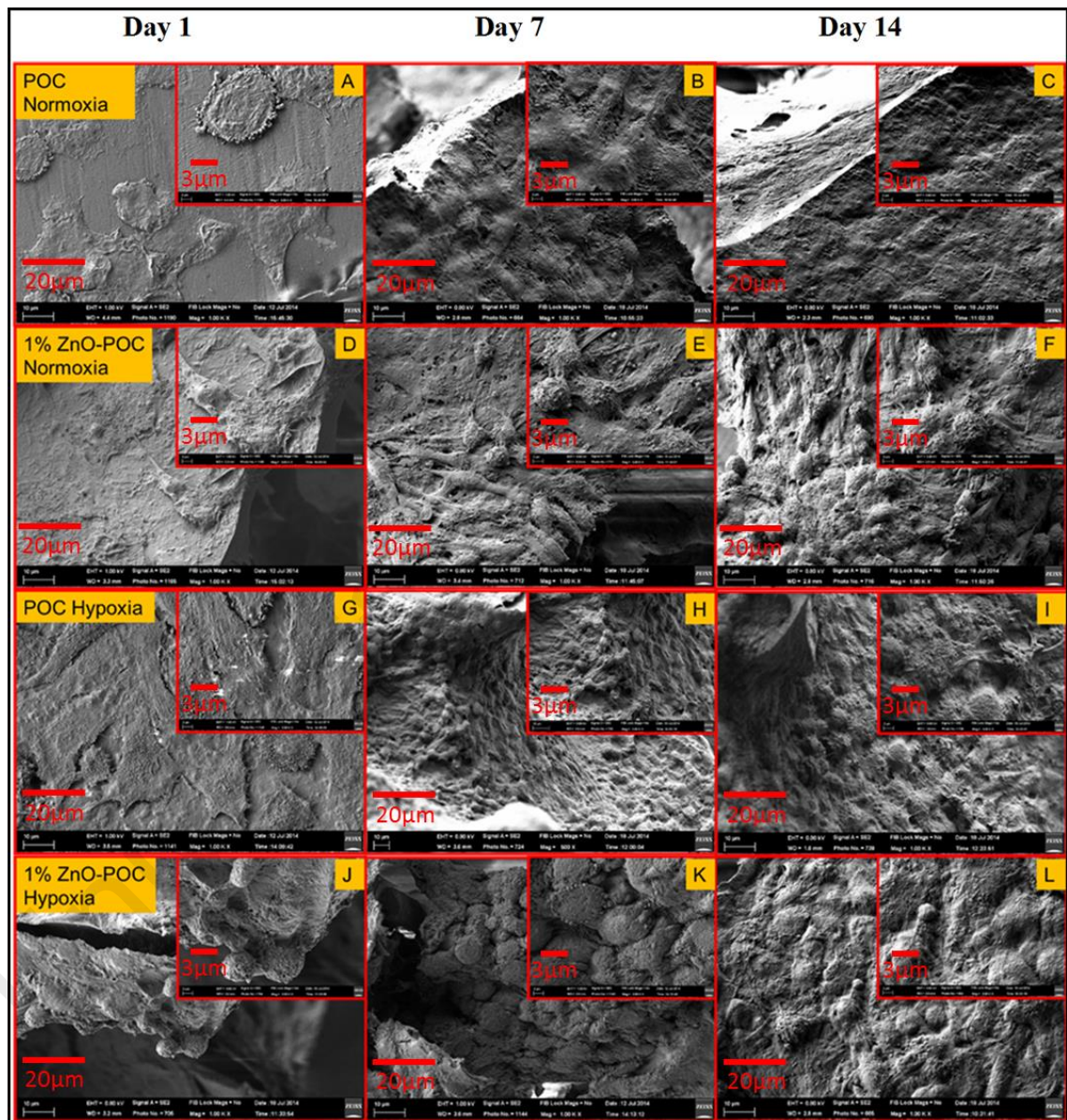


Figure 5.5 (A – L): SEM images showing the morphologies of Chondrocytes seeded on the scaffold at day 1, 7 and 14 under normoxic and hypoxic conditions. Outer images are at 1000X magnification with a scale bar of 20 μm and their respective inserts are at 3000X magnification with a scale bar of 3 μm.

5.3.2 Proteoglycan Synthesis

S-GAG incorporation in the scaffolds was in all cases positively correlated over time, with hypoxia producing a statistically significant increase over normoxia at every time point (Figure 5.6-A). Whilst 1% ZnONP did not affect S-GAG incorporation in the scaffold, it did produce a statistically significant increase in S-GAG release to the medium by day 14 in the hypoxic group (Figure 5.6 (A & B)). No significant increase was observed due to hypoxia in released S-GAG until day 3. However, on day 7 and day 14 a significant difference was observed due to hypoxia in released S-GAG (Figure 5.6-B).

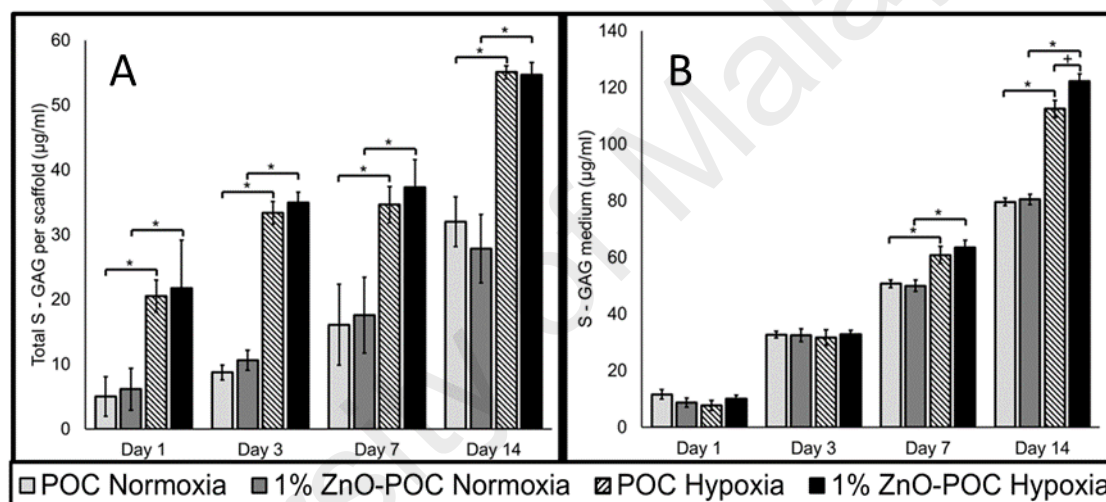


Figure 5.6: (A) Total S-GAG, measured in digested scaffolds and (B) S-GAG measured in medium via DMMB assay for chondrocytes seeded on Pure-POC and 1% ZnO-POC in normoxic (21%O₂) & hypoxic (5%O₂) conditions. Where + shows significant differences between groups and * shows a significant difference between O₂ tension. 5 ≤ N ≤ 6, p < 0.05.

5.3.3 Gene expression

The effect of hypoxia and normoxia, with and without ZnO on anabolic (type II collagen and aggrecan) and catabolic (*MMP-13*) gene expression, is presented in Figure 5.7 (A-C). *COL2A1* gene expression results indicate an increase over the period of the study in all groups (Figure 5.7-A). Only at day 3, there is a statistical difference between hypoxia and normoxia without Zn, otherwise, at every time point, the *COL2A1* gene expression was higher in hypoxia and 1% ZnONP conditions (all groups, $p < 0.05$; Figure 5.7-A). A highly significant difference was observed for *COL2A1* gene expression, however for *ACAN* gene expression the results indicate an increase over the period of the study in all groups (Figure 5.7-B). *ACAN* gene expression results demonstrated a similar trend as of *COL2A1* gene expression results except on day 14, when there was no difference between hypoxia and normoxia for Pure-POC. At every time point, scaffold containing 1% ZnONP had a higher reading of *ACAN* gene expression irrespective of hypoxic or normoxic condition ($p < 0.05$). A highly significant difference was observed for *COL2A1*, *ACAN* and *MMP-13* at every time point when Pure-POC scaffold in Normoxia was compared to scaffolds with ZnONP in hypoxia. The presence of 1% ZnONP in POC greatly suppressed the expression of a catabolic gene such as *MMP-13* from day 3 to day 14 ($p < 0.05$, compared to Pure-POC (figure 5.7-C)). *HIF-1A* is a well-known regulator of the hypoxic response. In all hypoxia cases, the up-regulation of *HIF-1A* gene expression (figure 5.7-D) from day 3 to day 14 is shown ($p < 0.05$, compared to the normoxic group). The up-regulation of *HIF-1A* in the hypoxic group is not affected by the presence of 1% ZnONP. No effect of ZnONP incorporation in POC polymer was seen for *HIF-1A* gene expression throughout the study.

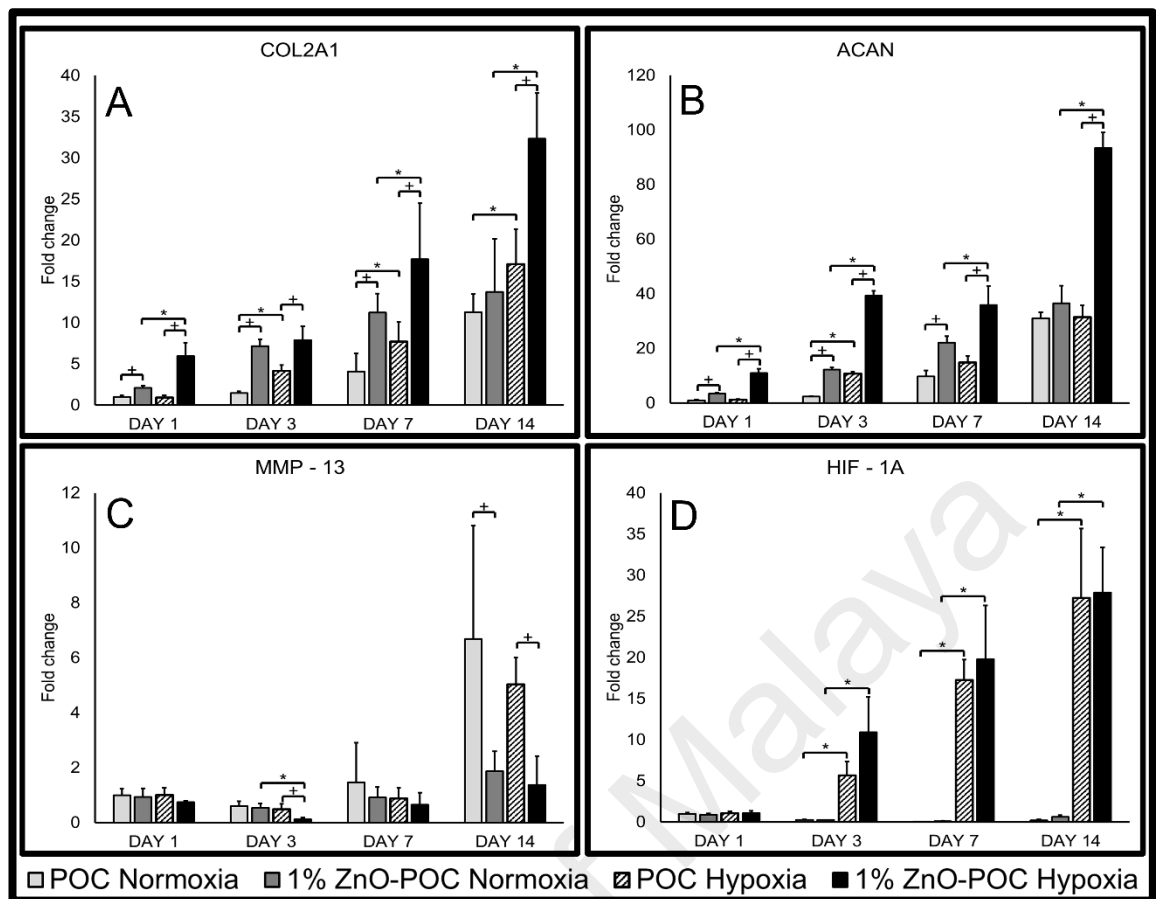


Figure 5.7 (A, B, C & D): mRNA expression of *COL2A1*, *ACAN*, *MMP-13* and *HIF-1A* respectively normalized to *GAPDH* with respect to Pure-POC on day 1. Where + shows significant differences between groups and * shows a significant difference between O₂ tension. 3 ≤ N ≤ 5, p < 0.05.

5.4 Discussion

In this study, the effect of native oxygen tension in cartilage (hypoxia, 5% O₂) was compared with normoxia (21% O₂) on 3D Poly 1, 8 Octane diol Citrate scaffolds fused with 1% ZnONP. Scaffolds were seeded with bovine chondrocytes and their cell behavior and protein synthesis was reported. Further, gene expression analysis of ECM specific genes (*COL2A1* and *ACAN*) and catabolic gene expression *MMP-13* was performed. If the combination of 1% ZnONP and hypoxia promotes cartilage synthesis through maintaining chondrocyte phenotype and morphology, then the following observations would be expected, compared to control, to just 1% ZnONP, or to hypoxia:

- a) Increased cell viability and proliferation
- b) Increased synthesis of cartilage protein such as sulfated GAG (S-GAG)
- c) Up-regulation of characteristic cartilage matrix genes (such as *COL2A1* and *ACAN*)
- d) Downregulation of catabolic genes (*MMP-13*)
- e) The role of *HIF-1A* in hypoxic environment

Discussion of each aforementioned observations is presented in turn, with reference to the results presented in section 5.3 of current thesis.

5.4.1 Cell proliferation

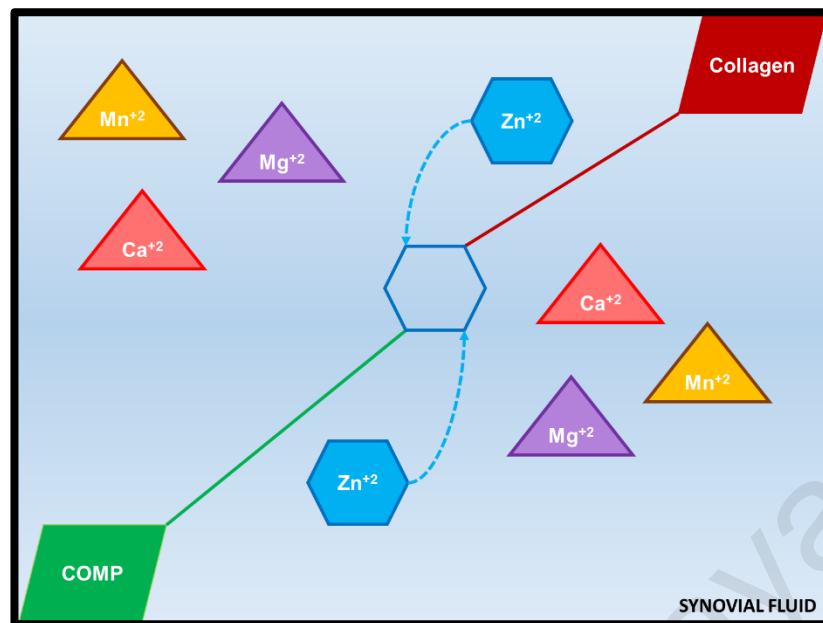
Several investigators have shown that hypoxia can influence cell proliferation *in-vitro* (Hubka et al., 2014; Schipani et al., 2001; Thoms et al., 2013) and results in Figure 5.2, agreeably demonstrated cell proliferation increasing considerably in a hypoxic environment. Previously, it was reported that hypoxia contributed to a better cell viability for chondrocytes cultured in the hypoxic environment (Tsuchida et al., 2014). An oxygen tension of 5% was selected because it is well documented that 5% O₂ tension mimics physiological O₂ tension (Domm et al., 2002). Whereas lower O₂ tensions may lead to reduced cell viability and chondrocyte health is compromised (Collins et al., 2013; Grimshaw & Mason, 2000). To further quantify cell proliferation, a nucleic acid binding dye, Hoechst DNA Assay was used, a more sensitive test for cell proliferation. Statistically the results demonstrated that there was a synergistic effect of hypoxia and ZnONP on cell proliferation for every time point, except day 14. Although at day 14 both hypoxic groups (with or without 1% ZnONP) showed the highest reading of DNA, they did not show a differential effect of ZnONP on cell proliferation (Figure 5.4). However, under a closer examination of the FESEM micrographs (Figure 5.5-K & 5.5-L), it is clear that all the surface area of scaffolds on the day 14 was covered by cells, suggesting the presence of contact inhibition (Abercrombie, 1979; Takai et al., 2008).

5.4.2 Proteoglycan Synthesis

Besides promoting cell proliferation and DNA production, cells cultured in a hypoxic environment showed a higher production of sulfated GAG production in both scaffolds (Figure 5.6-A). Present findings are consistent with previous studies by various researchers who studied the effect of oxygen levels on bovine chondrocytes matrix synthesis (Domm et al., 2002; Hansen et al., 2001). Furthermore, current findings are supported by a separate study by Malda J. et al (Malda et al., 2004), where human nasal chondrocytes were subjected to 21% O₂, 5% O₂, and 1% O₂. Their results demonstrated a higher S – GAG production after just 7 days under 5% O₂ concentration. It is also notable that GAG released into the medium was higher than the GAG within the scaffold (Figure 5.6-B). This finding can be explained by the fact that cells were covering all the polymer and the cells were in direct contact with the culture medium as the material was porous. Also, the size of the scaffold (6x6 mm) was substantially smaller than the volume of culture medium in each well (2ml). similar findings were reported by Bassleer C. et al (Bassleer et al., 1998).

5.4.3 Gene expression

In previous studies, POC (Kang et al., 2006) and oxygen tension (Saini & Wick, 2004) have been employed individually in order to support chondrocyte proliferation, attachment, and ECM production. However, this is the first time that hypoxia in combination with 1% ZnONP producing a stimulatory effect on *COL2A1* and *ACAN* synthesis has been reported (Figure 5.7-(A & B)). Rosenberg K. et al has previously shown that Zinc ions (Zn⁺²) have a preference for binding between cartilage oligomeric matrix proteins (COMP) and collagen type I and II. Moreover, they also are responsible for promoting binding of collagen to COMP (Figure 5.8) (Rosenberg et al., 1998).



N.B: The idea is modified from (Rosenberg et al., 1998).

Figure 5.8: Schematic of divalent ion involvement in binding COMP with collagens with a selective preference of Zn⁺² binding phenomenon within synovial fluid.

Zn⁺² ions have been demonstrated as playing a functional and biological role in organizing cartilage matrix by modulating link proteins in bovine articular cartilage (Rosenberg et al., 1991). A closer examination of the SEM micrographs demonstrates the difference between all the groups in terms of cell morphologies and matrix synthesis. The greatest contrasts were shown on scaffolds incorporating ZnONP and cultured in a hypoxic environment. Similarly, the SEM image in Figure 5.9 shows a denser fibril formation in 1% ZnO-POC scaffold under hypoxia at day 14. The cells in these groups have round and spherical morphologies and produced a dense matrix, which is agreeable to phenotypic stability (Benya & Shaffer, 1982). A possible mechanism is the release of Zn⁺² ions from the polymer. It has also been reported that Zn⁺² ions take an active functional and biological role in organizing cartilage matrix by modulating link proteins in bovine articular cartilage (Rosenberg et al., 1991).

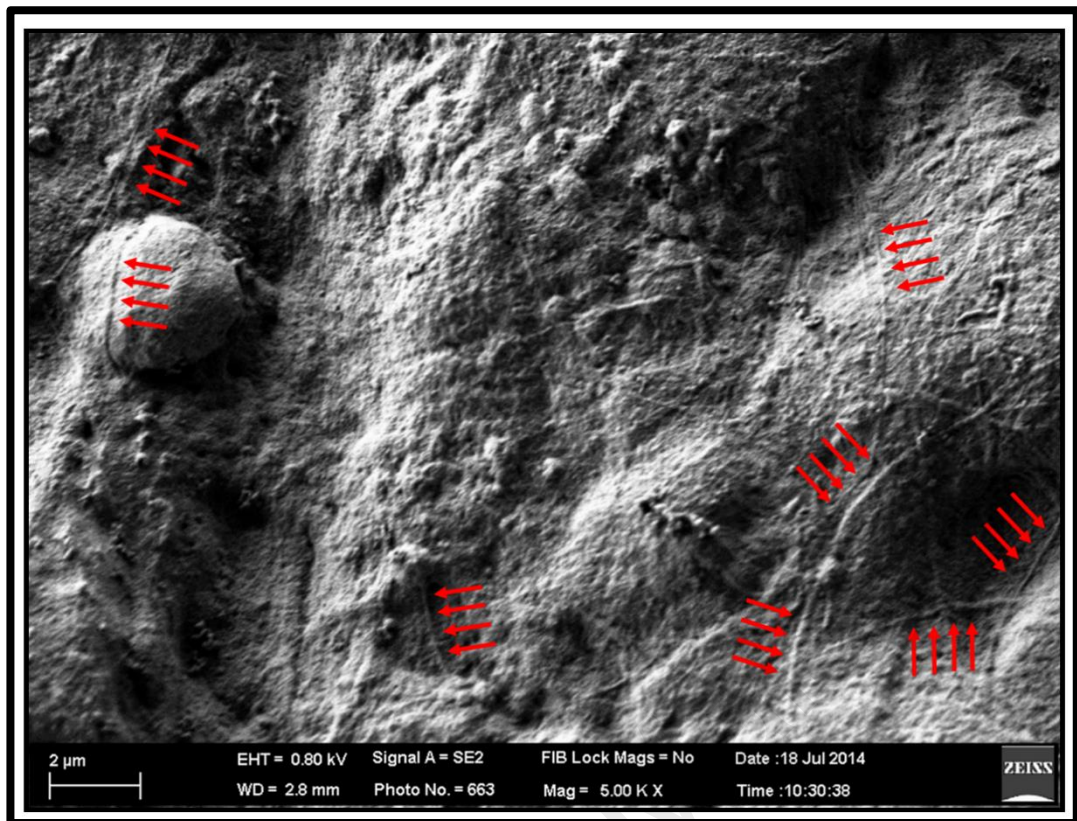


Figure 5.9: FESEM image at 5000X magnification of 1% ZnO-POC in hypoxia at day 14. Set of red arrows points to visible fibrils in ECM.

A highly significant difference was observed for *COL2A1*, *ACAN* and *MMP-13* at every time point when Pure-POC scaffold in normoxia was compared to scaffolds with ZnONP in hypoxia. The presence of 1% ZnONP in POC greatly suppressed the expression of catabolic gene *MMP-13* from day 3 to day 14 ($p < 0.05$, compared to Pure-POC (Figure 5.7-C), but conversely yielded no statistically significant effect under normoxia from day 3 onwards. *HIF-1A* is a well-known regulator of the hypoxic response. Present findings elaborated the role of hypoxia in the regulation of cartilage destruction gene, more commonly known as *MMP-13* (Fosang et al., 1996; Wang et al., 2013). The up-regulation of *MMP-13* was suppressed by the 1% ZnONP present in the scaffolds but hypoxia alone did not prevent the up-regulation of *MMP-13*. These results suggest ZnONP has a chondroprotective role. Previously, it was reported that serum Zn levels are found to be substantially decreased in rheumatoid arthritis (RA) (Mierzecki et al., 2011; Zoli et al.,

1998) and that the reduced level of serum Zn in RA is associated with immune inflammatory processes (Honkanen et al., 1989; Milanino et al., 1993).

In all hypoxia cases, up-regulation of *HIF-1A* gene expression (Figure 5.7-D) from day 3 to day 14 is shown ($p < 0.05$, compared to the normoxic group). The up-regulation of *HIF-1A* in the hypoxic group is not affected by the presence of 1% ZnONP. It was reported by Schipani et al that *HIF-1A* is a major regulator of the hypoxic response in chondrocytes (Schipani et al., 2001). Current results show that in hypoxic condition there was a higher level of cartilage matrix and gene up-regulation. While other studies have also implicated the role of *HIF-1A* in the regulation of cartilage-specific genes (Dahlin et al., 2013; Robins et al., 2005; Thoms et al., 2013).

University of Malaya

CHAPTER 6: EFFECT OF DYNAMIC MECHANICAL COMPRESSION ON BOVINE ARTICULAR CHONDROCYTES

6.1 Introduction

Trauma or disease of articular cartilage leads to articular cartilage lesions, which have a very limited ability to repair themselves, and gradually progress to osteoarthritic conditions. The incidence of the cartilage-related disease is increasing throughout the world (Humphreys et al., 2013; Lawrence et al., 2008; Theis et al., 2007). Various treatments are used for individuals with cartilage-based problems (Filardo et al., 2013; Marcacci et al., 2013), however, the drawbacks associated with these treatments are many, including inconsistency in treatment outcomes (Farr et al., 2011) and diminutive mechanical properties of replaced tissue resulting due to fibrocartilage formation (Gomoll & Minas, 2014). Therefore, new options are required to deal with the current situation. A key area for such new solutions is the application of Tissue Engineering to cartilage.

Cartilage comprises only one type of cell, the chondrocyte (Palukuru et al., 2014), and are currently used for autologous chondrocyte implantation (Chilelli et al.) as well as being the mainstay of many other therapies. However, the use of chondrocytes entails numerous constraints (Harris et al., 2011) that hamper their use. The foremost is difficulty in obtaining chondrocyte-bearing tissues for isolation of cells and *in vitro* expansion (Minas & Nehrer, 1997). Such a method can result in donor site morbidity (Harris et al., 2011; Hjelle et al., 2002; Pelttari et al., 2008), and a consequent increased long-term risk of the development of osteoarthritis (Hunziker, 2002; Messner & Gillquist, 1996). Further, due to the scarcity of chondrocytes even in healthy articular cartilage, there is typically a lack of sufficient numbers of chondrocytes available (Dahlin et al., 2013; Palukuru et al., 2014). Even where sufficient cells can be obtained for expansion, typical *in vitro* methods can easily produce dedifferentiation of chondrocytes (Schulze-Tanzil et al., 2004).

Given this resultant need to maximise expansion of what chondrocytes are available, and to maintain a useful phenotype, a number of factors have been identified which promote more effective chondrocyte culture.

First, the use of three-dimensional culture models has been introduced, in view of the identification of a two-dimensional culture with the tendency of chondrocytes to dedifferentiate toward a fibroblastic morphology (Yoon et al., 2002). Second, research into replicating a physiological mechanical environment within culture systems has shown the beneficial effect of dynamic mechanical loading on metabolic activity and the promotion of cartilage formation (Jeon et al., 2012; Li et al., 2013). Chondrocytes are highly mechanosensitive (Madej et al., 2014), and different studies have supported the role of mechanical stimulation on chondrocytes to enhance extracellular matrix (ECM) production and deposition (Ikenoue et al., 2003; Millward-Sadler et al., 2000). More recently, this research direction has included the addition of hypoxic conditions, mimicking the low oxygen tension found within diarthroidal joints (Li et al., 2013; Madej et al., 2014). In the native environment, chondrocytes are continuously under a gradient of oxygen tension that ranges from 10% O₂ in the superficial layers to around 1% O₂ in the deepest layers (Grimshaw & Mason, 2000). Chondrocytes adapt well to decreased O₂ concentrations and hypoxia has been proved to play a major role in chondrocyte proliferation and their function *in vivo* (Foldager et al., 2011; Schipani et al., 2001).

More recently, research has shown that combining three-dimensional culture with hypoxic conditions was enhanced through the incorporation of Zinc Oxide nanoparticles (ZnONP), with marked chondroprotective benefits, including the promotion of cartilage synthesis, upregulation of matrix gene expression, downregulation of catabolic genes, and the preservation of cell morphology (Mirza, Pan-Pan, et al., 2015). Zinc (Zn) is an essential element for humans and animals, particularly in cell proliferation, differentiation, and survival (Beyersmann & Haase, 2001; Haase & Rink, 2014b). In

addition, it is known to possess antibacterial properties (Mirza, Wan Ibrahim, et al., 2015). In light of this, it is important that the further interaction of ZnONP with mechanical loading be evaluated to establish whether such findings can be extended to such models for a further advancement in chondrocyte culture.

6.2 Materials and Methods

Pure POC and 1% ZnO-POC scaffolds were placed in sterile bijoux tubes and immersed in 70% alcohol for 30 minutes. Alcohol was then aspirated and scaffolds were left to air dry under a laminar flow, followed by autoclaving at 121°C for 15 minutes at 15 psi. Once removed from the autoclave, the scaffolds were immersed in chondrocyte medium to neutralise (neutralisation helps better cell attachment) overnight prior to cell seeding. Isolated bovine articular chondrocytes (BAC) (refer to section 3.4 for details of BAC isolation) were seeded on the scaffolds, with a concentration of 1×10^6 cells per scaffold (higher cell seeding density prevent dislodging of cells under dynamic mechanical compression). The cells were allowed to attach for 4 hours and then the wells were replenished with chondrocyte culture medium (refer to section 3.4.1 for formulation).

6.2.1 Experimental Design

Pure-POC and 1% ZnO-POC Scaffolds were kept in under 2 different oxygen concentrations; one in hypoxia (5% O₂) and second in normoxia (21% O₂). Furthermore, scaffolds under each oxygen concentration were subjected to either; (a) static culture or (b) dynamic mechanical compression, for 72 hours. The experimental design is summarised in figure 6.1.

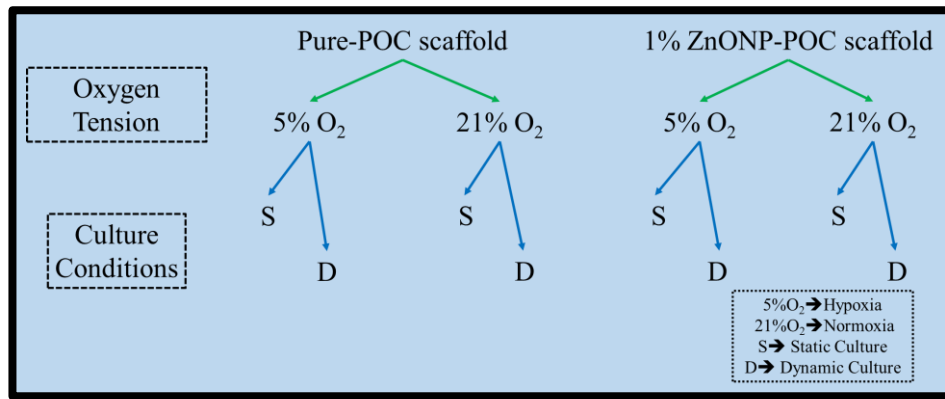


Figure 6.1: Illustration summarizing all experimental groups with respect to culture conditions and oxygen tensions.

6.2.2 Application of dynamic compression

An incubator-housed ex-vivo bioreactor (Bose, ElectroForce® 5500 USA) was used to apply dynamic compression to cell-seeded scaffolds at 5% or 21% oxygen tension (Figure 6.2-A). The scaffolds were transferred into individual wells of a 24-well plate fixture chamber (Figure 6.2-B) for compressive loading.

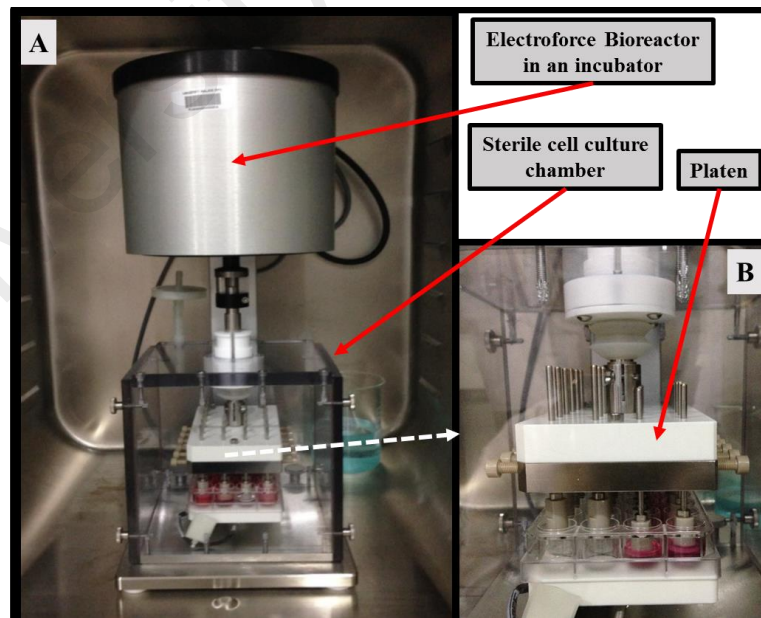


Figure 6.2: Bose ElectroForce® 5500 USA. (A) Bose Bioreactor setup with 24-well plate fixture in a 5% CO₂ incubator. (B) 24-well plate with compression platens in a box chamber.

The scaffolds were left in the bioreactor for a 24-hour free swelling period, followed by intermittent compression under unconfined conditions, with a profile of 10 minutes (min) compression followed by a 5-hour 50-min unstrained period for 48 hours (Figure 6.3).

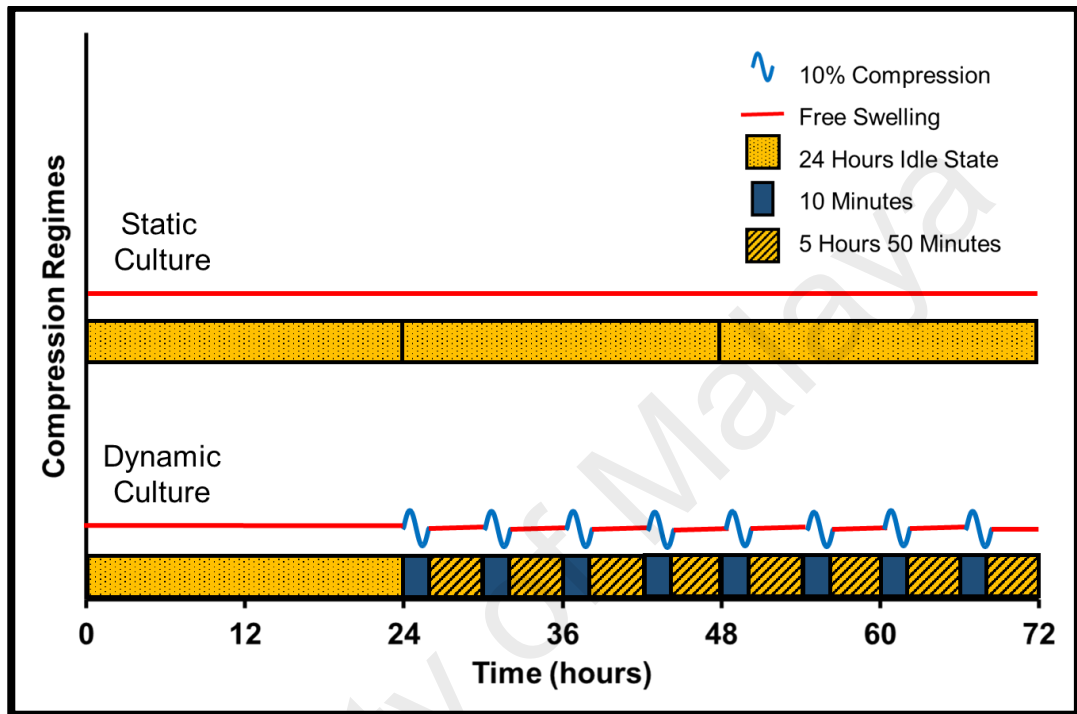


Figure 6.3: Schematic illustration of the intermittent dynamic compression profile of cell culture regimes.

The bioreactor was programmed for 10% compression at a frequency of 1Hz via WinTest 7 software. Control scaffolds were unstrained and were left inside the ex-vivo system.

6.2.3 Cell Proliferation Assay

The Hoechst binding dye method was used to quantify DNA within the scaffolds at each time point (refer to section 3.6 for detailed protocol).

6.2.4 Sulphated glycosaminoglycan (S-GAG) quantification assays

Glycosaminoglycans (GAGs) are polysaccharides that are present in abundance in a healthy cartilage. Sulphated-GAGs (S-GAGs) are the types that can be measured via a 1, 9-dimethylmethylene blue assay. Total S – GAG was measured from Cell-scaffold lysate at each time point. Released S – GAG was measured by collecting the culture medium at every medium change from the wells (refer to section 3.7 for detailed protocol).

6.2.5 Quantitative Polymerase Chain Reaction (q-PCR)

To observe the behaviour of BACs at gene level Cartilage matrix specific genes; Collagen type II (*COL2A1*) and Aggrecan (*ACAN*) were observed. Moreover, the matrix degradation gene (*MMP-13*) and hypoxia inducible factor gene (*HIF1A*) were also observed. Q-PCR gene expressions were determined by the *TaqMan* gene expression assay using StepOnePlus™ Real-Time PCR system (refer to section 3.8 for detailed protocol).

6.3 Results

This section elaborates proliferation behavior, ECM formation and regulation of ECM specific genes for chondrocytes seeded on Pure-POC and 1% POC-ZnO scaffolds over the period of 48 Hours under normoxia (21% O₂) and hypoxia (5% O₂) when subjected to dynamic compression.

6.3.1 Cell proliferation and morphology

Cell quantification results in Figure 6.4 show the effect of dynamic compression on DNA production in presence and absence of 1% ZnONP in normoxic and hypoxic conditions for 48 hours. DNA production was greatly enhanced under the influence of mechanical stimulation, particularly for 1% ZnO-POC (hypoxia), Pure-POC (hypoxia), and Pure-

POC (normoxia). However, this was not true in the case of 1% ZnO-POC (normoxia). Both strained and unstrained scaffolds showed that hypoxia-enhanced DNA production and with the combination of dynamic compression demonstrated its beneficial effects on cellular proliferation.

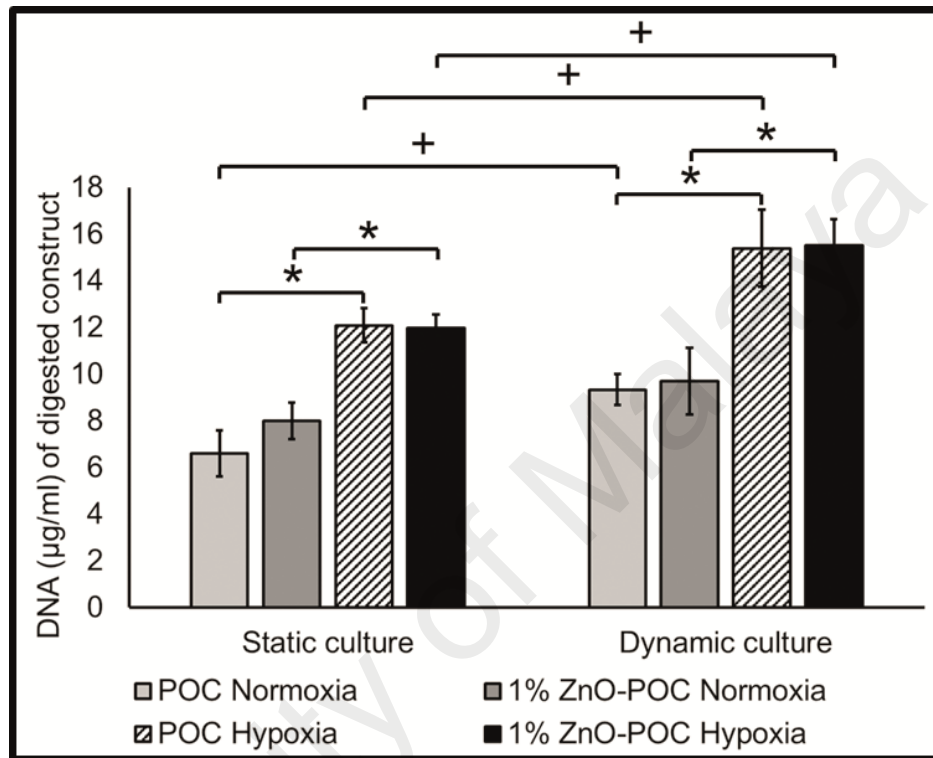


Figure 6.4: Cell quantification through DNA Hoechst fluorescence assay for chondrocytes seeded on pure-POC and 1% ZnO-POC in normoxic (21% O₂) & hypoxic (5% O₂) conditions, under static and dynamic culture regimes. Where ^ shows a significant difference between due to the presence of ZnONP, * shows a significant difference between O₂ tension and + shows a significant difference between static and dynamic culture. p<0.05.

Further qualitative assessment of cell proliferation was carried out using live (green)/dead (red) stains. The number of live and dead cells can be viewed via confocal microscopic images. Figure 6.5 (A-L) indicated that in general, dynamic culture produces more live cells compared to static culture. Closer examination of the insert (Figure 6.5 (B, D, F & H)) of confocal images for cells which were previously cultured in a hypoxic environment

and have also undergone mechanical stimulation have divided, as supported by DNA quantification results in Figure 6.4.

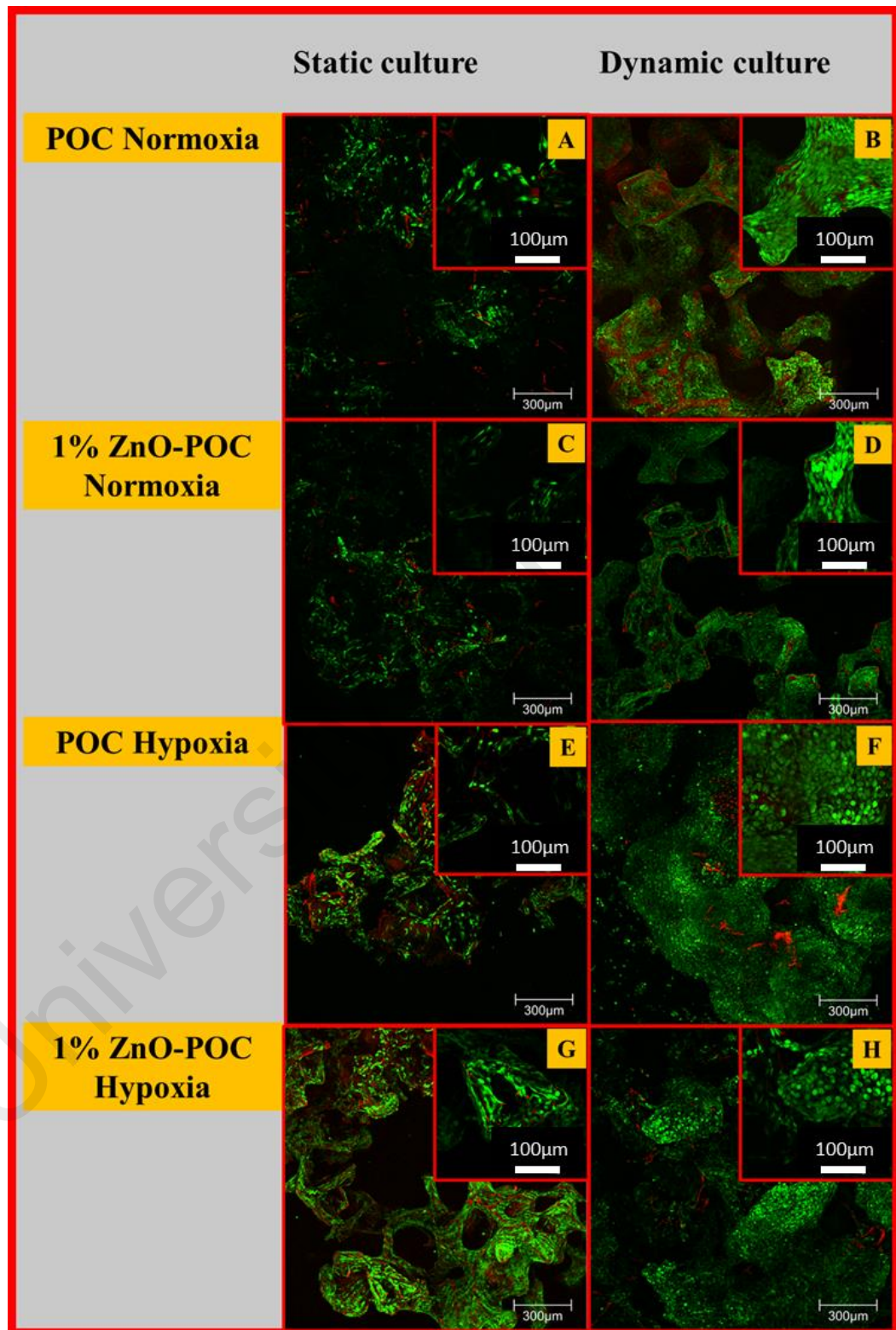


Figure 6.5: Confocal imaging of Chondrocytes (A-H) seeded on Pure-POC and 1% ZnO-POC scaffolds in normoxic (21%O₂) & hypoxic (5%O₂) conditions, under

static and dynamic culture regimes. Outer images are at 10X with a scale bar of 300 μm and their respective inserts are at 40X magnification with a scale bar of 100 μm .

FESEM images (Figure 6.6 (A-H)) also showed that there were more cells in scaffolds which were previously cultured in dynamic environments. Notably, the cells which had undergone dynamic compression tended to keep a rounded morphology, which is typical morphology of chondrocytes. In static culture, cells in scaffolds which contained ZnONP were more rounded and bulged as compared to cells cultured in pure POC.

University of Malaya

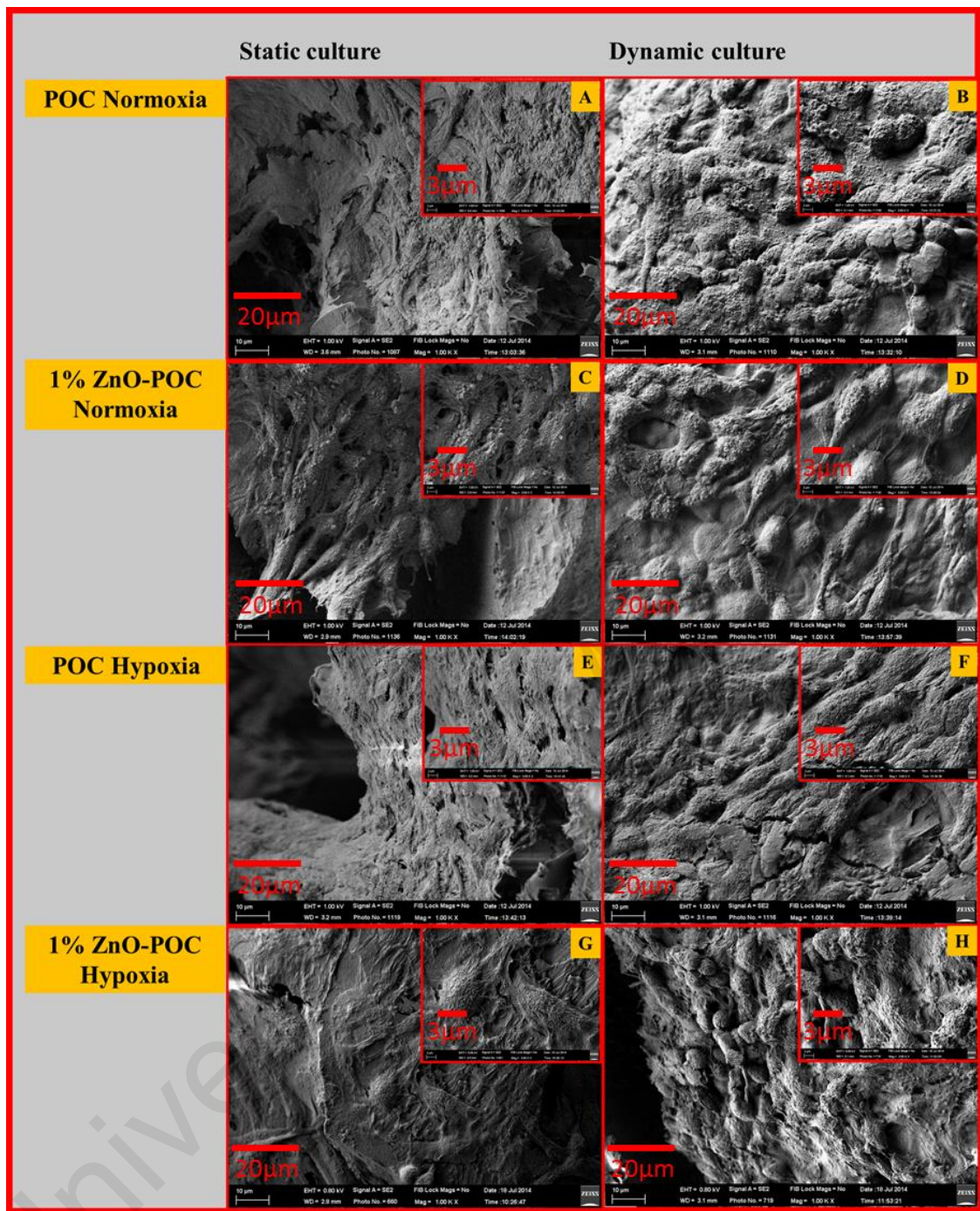


Figure 6.6: SEM imaging of Chondrocytes (A-H) seeded on Pure-POC and 1% ZnO-POC scaffolds in normoxic (21%O₂) & hypoxic (5%O₂) conditions, under static and dynamic culture regimes. Outer images are taken at 1000X magnification, it has a scale bar of 20 μm. Corresponding images in inserts were taken at 3000X magnification having a scale bar of 3 μm.

6.3.2 Proteoglycan synthesis

S-GAG production in the scaffolds was not affected by the presence of dynamic compression, however, the effect of O₂ tension and the incorporation on ZnONP influenced the higher synthesis of S-GAG (Figure 6.7-A). In dynamic culture, there was a higher production of S-GAG in all hypoxic groups. In dynamic culture, when pure POC was compared with 1%ZnO-POC, both in hypoxic condition, the presence of 1%ZnO further enhanced the production of S-GAG. A similar trend is observed in the normoxic groups in a dynamic culture. Static cultures also exhibited similar trend to dynamic culture but did not show a statistically significant effect of ZnONP in the hypoxic group. Dynamic compression showed more distinctive effects of S-GAG released in the medium than in all other groups, except in pure POC culture in normoxic conditions (Figure 6.7-B). Again, hypoxia and ZnONP together or separately have shown a higher production of S-GAG released in the medium in a dynamic culture. The trend of S-GAG release in the medium is identical to S-GAG release from scaffolds in static culture.

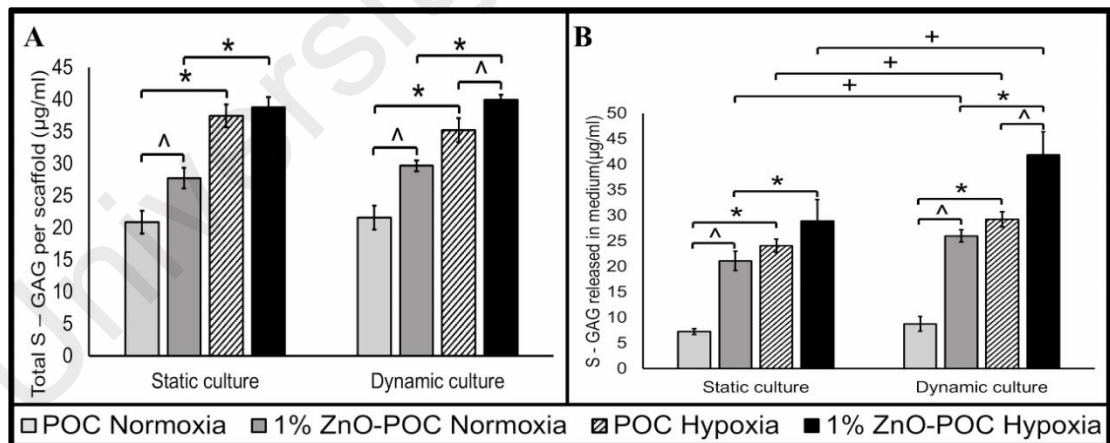


Figure 6.7: DMMB assay for glycosaminoglycans (A) Total S-GAG, measured in digested scaffolds and (B) S-GAG measured in medium via DMMB assay for chondrocytes seeded on pure-POC and 1% ZnO-POC in normoxic (21%O₂) & hypoxic (5%O₂) conditions, under static and dynamic culture regimes. Where ^ shows a significant difference between due to the presence of ZnONP, * shows a

significant difference between O₂ tension and + shows a significant difference between static and dynamic culture. p<0.05.

6.3.3 Gene Expression

The effect of oxygen tension and ZnONP on anabolic (type II collagen and aggrecan) and catabolic (MMP-13) gene expression is presented in Figure 6.8-(A, B & C). In static culture, the effect of hypoxia in increased *COL2A1* (p<0.05) can be seen in the 1% ZnO-POC group only, whereas, in a dynamic culture, the effect of hypoxia and ZnONP can be seen in all groups in the up-regulation of *COL2A1* (p<0.05). Compared to static culture, dynamic culture, in general, has resulted in an up-regulation of *COL2A1* in all groups (p<0.5), except for the pure POC group under normoxia.

The up-regulation of aggrecan expression is greatly affected by O₂ tension and ZnONP in static culture (all groups, p<0.05), and dynamic culture can also further improve the up-regulation of aggrecan (all groups, p<0.05); Figure 6.8-B.

MMP-13 is a well-known cartilage-destructive gene. Hypoxia had an inhibitory effect on *MMP-13* activity both in static and dynamic culture (Figure 6.8-C). Dynamic compression helped in further reducing MMP-13 activity in normoxia for both Pure-POC and 1%ZnO-POC samples, excluding the result from the 1%ZnO-POC group under dynamic culture, in which the level was low both with and without hypoxia. The results demonstrated that hypoxia and dynamic compression both act to reduce the pro-catabolic response. ZnONP also helped to reduce MMP-13 up-regulation for dynamic culture in normoxic conditions.

The HIF-1A gene, which is thought to be one of the major regulators of the hypoxic response, was only present in scaffolds cultured in hypoxic conditions (Figure 6.8-D). It was not affected by the incorporation of ZnONP or mechanical stimulation.

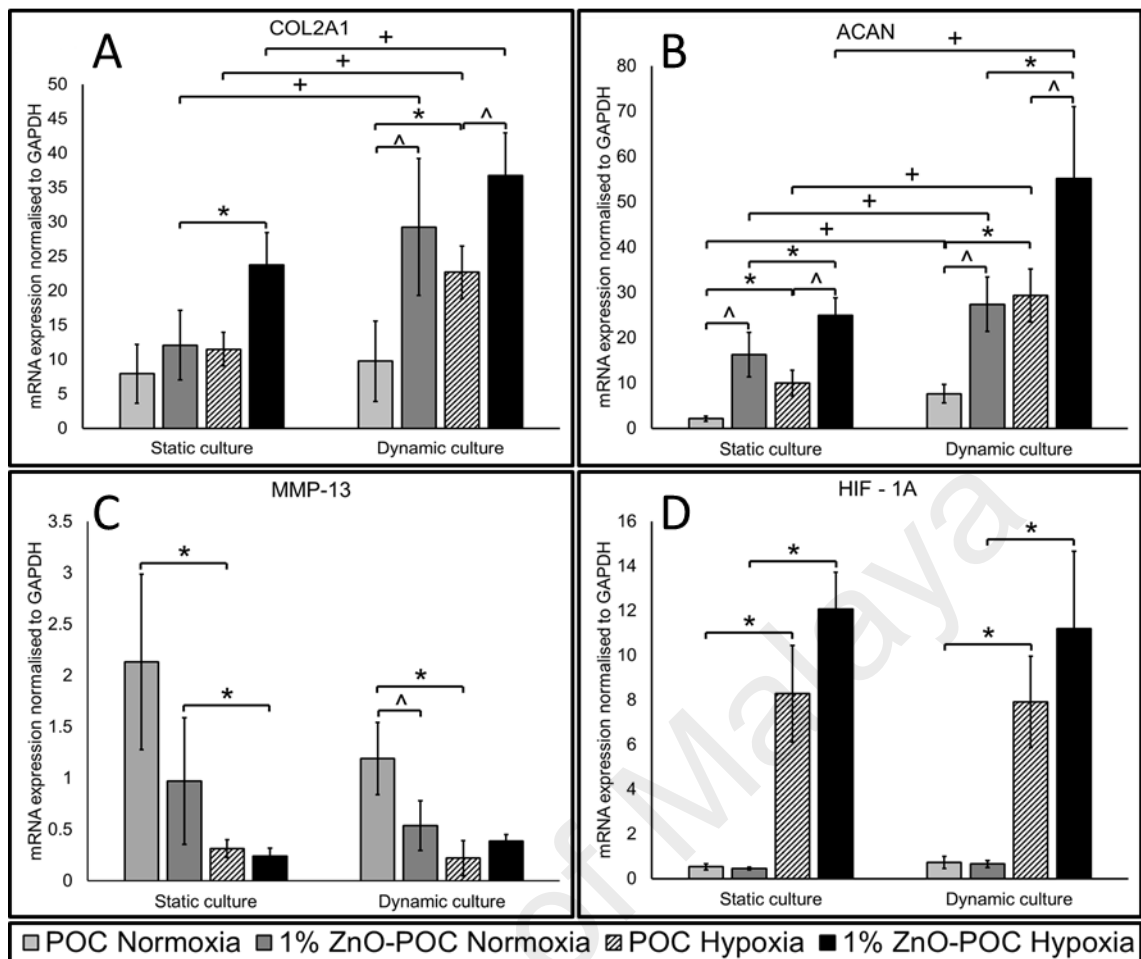


Figure 6.8: (A) *COL2A1*, (B) *ACAN*, (C) *MMP-13* and (D) *HIF-1A*, for chondrocytes seeded on pure-POC and 1% ZnO-POC in normoxic (21%O₂) & hypoxic (5%O₂) conditions, under static and dynamic culture regimes. Where ^ shows a significant difference between due to the presence of ZnONP, * shows a significant difference between O₂ tension and + shows a significant difference between static and dynamic culture. p<0.05.

6.4 Discussion

This study set out to evaluate the feasibility of adding ZnONP to a 3D culture system incorporating mechanical stimulation and hypoxia for chondrocytes. The mechanical stimulation is part of biomimicry, as it is found in the native environment of chondrocytes (Jeon et al., 2012), and has been shown to produce a significant modulation in a matrix formation, cell proliferation, and S-GAG formation by chondrocytes (Grodzinsky et al.,

2000). The use of hypoxia, a further physiological feature of native cartilage (Grimshaw & Mason, 2000), and likewise plays a major role towards *in-vivo* chondrocyte metabolism (Foldager et al., 2011; Schipani et al., 2001).

Whilst the combination of ZnONP and hypoxia has been previously reported (Mirza, Pan-Pan, et al., 2015), it has not been formerly tested in conjunction with mechanical stimulation. Therefore, in the present study, the focus was upon the addition of 1% ZnONP (0% ZnONP = control) to a system comprising native oxygen tension in cartilage (hypoxia, 5% O₂) (normoxia at 21% O₂ = control), with (static culture = control) dynamic compression.

6.4.1 Cell proliferation and morphology

The DNA content demonstrated a highly significant increase due to the hypoxic condition. Furthermore, scaffolds that were dynamically compressed displayed a higher DNA content (Figure 6.4). Upon closer examination of (Figure 6.5-(B, D, F & H)) many 'twinned' chondrocytes can be seen in scaffolds which were previously cultured in dynamic conditions, this indicating that there is an increase in cell proliferation, providing qualitative data in support of the DNA results. Similar results were reported by (Dahlin et al., 2013) where it was concluded that a combination of hypoxia and flow perfusion cultures displayed enhanced DNA content per scaffold. Irrespective of oxygen concentration and the presence of ZnONP, dynamically compressed scaffolds display a more rounded morphology (Figure 6.6-(B, D, F & H)), which is agreeable to phenotypic stability (Villar-Suárez et al., 2004). In separate studies, it was reported that low oxygen tension and flow perfusion is required to maintain cell phenotype and enhance ECM production (Davisson, T. et al., 2002; Murphy & Polak, 2004).

6.4.2 Proteoglycan synthesis

Higher S-GAG formation was observed for scaffolds which incorporate ZnONP when compared to pure-POC in normoxia and hypoxia in a dynamic culture. However, the total S-GAG remained significantly higher among scaffolds that were present in the hypoxic environment (Figure 6.7-A).

Where the S-GAG level in the medium was measured, a similar trend of S-GAG levels in the digested samples was observed. However, the samples which underwent dynamic compression recorded significantly higher levels than those in static conditions, irrespective of oxygen tension or ZnONP incorporation (Figure 6.7-B).

It is postulated that the mechanical loading itself may have triggered leakage of S-GAG from the highly porous POC scaffold. Moreover, the presented results are coherent with another study by Wernike E. et.al, which reported that dynamic compression enhances GAG synthesis (Wernike et al., 2008).

6.4.3 Gene Expression

The gene expression profiles of *COL2A1* and *ACAN* demonstrated enhanced expression due to the incorporation of ZnONP, but this enhanced expression became significant due to dynamic compression (Figure 6.8-(A & B)). Gene expression results suggest that incorporation of ZnONP had a stimulatory effect on *COL2A1* and *ACAN* synthesis, which are the major contributors to extracellular matrix (ECM) (Chen et al., 2014). The increase in gene expression profiles of *COL2A1* and *ACAN* due to dynamic forces was also reported in a separate study which suggested loading duration and strain percentage affect gene expression (Jeon et al., 2012). Overall, the greatest influence on the MMP-13 level was the change in oxygen tension, however, the presence of ZnONP did yield a statistically significant difference in one case under dynamic culture, suggesting a contributory role that may be further clarified in further research (Figure 6.8-C).

Regarding the levels of HIF-1A, a key regulator of hypoxic response, whilst as expected; the HIF-1A levels increased dramatically under hypoxia. Neither the addition of mechanical loading nor ZnONP disrupted the expression of this gene, suggesting that normal hypoxic response is retained in the culture model (Figure 6.8-D).

The mechanism of the Hypoxia Inducible Factor (HIF) protein is illustrated in Figure 6.9. It is understood that the HIF protein is continuously being produced. However, researchers suggest that in the presence of oxygen, this protein is degraded as its hydroxylation takes place by HIF-specific polyhydroxylases which target HIF-alpha subunits (Thoms et al., 2013). In hypoxia, the oxygen concentration is roughly 5%. As hydroxylation requires oxygen to proceed, a lack of oxygen causes the mechanism to diminish substantially, which eventually slows down the degradation process in tissue (Thoms et al., 2013). Previously it had been reported that the cartilage destruction that was induced by interleukin 1 α (IL - 1 α) – an inflammatory cytokine (Kobayashi et al., 2005; Pujol & Loyau, 1987), was inhibited by hypoxia (Thoms et al., 2013).

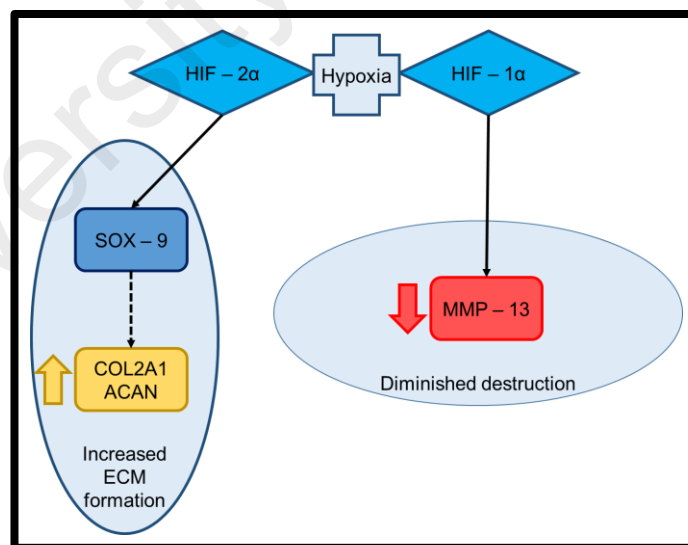


Figure 6.9: Schematic of the possible pathway by which hypoxia inducible factor controls cartilage destruction with the help of its 2 major genes that are up-regulated in hypoxic conditions, based on the work by Thoms *et al.* The schematic is modified from (Thoms et al., 2013).

CHAPTER 7: CONCLUSIONS AND FUTURE DIRECTIONS

7.1 Conclusions

Articular cartilage tissue is made up of a complex network of ECM but only a single cell type, the chondrocyte. Cartilage tissue has a very low capability of self-healing. Cartilage in articulating joints is a vulnerable tissue that is subjected to injuries and degenerative conditions. More than 2 decades have passed since interdisciplinary teams of biologists, engineers, clinicians and materials scientists first studied cartilage behaviour in-vitro and in-vivo. However, till now, there is no single treatment method that outweighs the rest as assured technique to successfully address the cartilage repair dilemma.

The goal of cartilage tissue engineering is to restore smooth movement and load bearing activities as in native articular cartilage. Numerous clinicians, researchers, and scientists have put forward their potential solutions but none have succeeded to be implemented as a single favoured choice all round the world because the limitations of the proposed techniques outweigh their long term benefits.

As discussed in chapter 2, there are several issues that need to be addressed for a successful cartilage tissue engineering strategy. The most important criteria to consider for cartilage tissue engineering are the combination of; (a) cells, (b) scaffold and (c) bio-factors. Together, these are assembled into a tissue construct, which is then implanted to the defect site surgically. This surgical implantation bears the additional risk of infection. The fundamental aim of this thesis was to enhance the understanding of chondrocyte behaviour under a native physical and chemical environment; and to establish concrete evidence for functional antibacterial scaffolds. As highlighted in chapter 1; section 1.4, there were 4 basic objectives of this thesis.

The first objective was to develop a biodegradable scaffold with controlled pore size and porosity mimicking the properties of native articular cartilage. Next objective was to

select and optimise the concentration of nano particles that must be biocompatible and having antibacterial effect while showing no toxicity towards chondrocytes.

A new type of nano-composite scaffold has been produced from citric acid-based polyester and zinc oxide nanoparticles. The scaffolds have been fabricated in two steps: (1) polyesterification synthesis of pre-polymer and mixing with nanoparticles; and (2) production of porous matrix by solvent-casting/particulate-leaching technique. The scaffolds demonstrate elastomeric nature and optimal porosity to be used in cartilage tissue engineering. The current method provides an effective route for production of scaffolds with controlled release of bio-active nanoparticles. The ZnONP have demonstrated strong anti-bacterial properties as evident from the results presented in chapter 4. The antibacterial activity of the reported scaffolds may enhance the clinical outcomes by: (i) reduction of post-operative complications by eliminating the risk of infection from donor; and (ii) reduction of the risk of infection caused by biofilm formation. A multifunctional scaffolds also show a strong potential for cartilage tissue engineering. The concentration of 1 wt% of ZnONP was found to have better performance with chondrocyte proliferation than pure POC, used as control. The 1wt% ZnO-POC nano-composite scaffold has proven to be optimal for seeding with chondrocytes while simultaneously depleting both the gram positive and gram negative bacteria.

The third objective of current thesis was to study the independent and combined effect of Hypoxia and ZnONP on bovine articular chondrocytes (BAC) seeded on POC polymer scaffolds and cultured under 2 different oxygen concentrations; (a) normoxia (21% O₂) and (b) hypoxia (5% O₂). 5% O₂ concentration was selected, as a review of the literature in chapter 2. Section 2.6.2.2 reveals that at a 5% O₂ concentration chondrocytes thrive while lower O₂ concentrations are not feasible and may only be present in abnormal or pathological conditions.

This study highlights the potential for combination of ZnONP and hypoxia, which has demonstrated the ability to promote cartilage synthesis through maintaining chondrocyte morphology when used with POC scaffolds. Incorporation of small proportion of ZnONP have significantly enhanced the chondroprotective behavior of scaffolds. This has been demonstrated particularly in terms of promoting cell proliferation, preserving cell morphology, up-regulating cartilage matrix genes and down-regulating cartilage destructive gene. Further, the presence of ZnONP did not modulate the expression of HIF-1A, indicating a preservation of cartilage homeostasis. This provides an important new route for *in-vitro* cartilage tissue engineering.

Finally, the thesis aims at establishing a relationship between dynamic mechanical stimuli, nanoparticles, and oxygen tension, in chondrocyte seeded on POC polymer scaffolds. In order to understand the underlying mechanism of combining hypoxia, mechanical stimulus and ZnONP, the BAC were seeded on Pure-POC and 1% ZnONP scaffolds and subjected to (a) normoxia (21% O₂) and (b) hypoxia (5% O₂), while simultaneously undergoing a 10% dynamic mechanical compression for 72 hours. Specifically, catabolic gene expression of *MMP-13* was observed to be curtailed in normoxic, and the cartilage matrix specific (*COL2A1 and ACAN*) genes were increased. Differential comparison of groups and controls within the study confirms the benefit of moving from a model without dynamic loading to one including such, yielding a marked increase in cell viability, roundedness of cell morphology, and gene expression even with the presence of ZnONP. ZnONP neither limited nor decreased the previously reported advantages of the use of hypoxia or of mechanical loading in the present model.

In conclusion, all the objectives mentioned in chapter 1, section 1.4 were effectively and efficiently achieved. Furthermore, the hypothesis in chapter 1, section 1.5 stands true, as this thesis successfully demonstrates that chondrocytes proliferated, secreted more extracellular matrix, and showed higher gene expression under a hypoxic environment,

while also showing a strong antibacterial inhibition. The SEM images in figure 5.5 and figure 6.6 reveals that scaffolds incorporated with 1% ZnONP displayed a packed network of interconnecting cells while simultaneously having more rounded morphology. An absence of ZnONP from scaffolds revealed that cells tend to be spindle shaped or elongated like fibroblasts. The combination of hypoxia and the presence of ZnONP in scaffolds was fruitful as it retained cell morphology, which is one of the long awaited predicament to be addressed. Moreover, the inclusion of dynamic mechanical compression enhanced the rounded morphology and elevated cartilage specific matrix genes, while lowering catabolic gene expression.

University of Malaya

7.2 Future Direction

In order to support the current data, future work must target in-vivo studies, as the current thesis is based upon in-vitro models only. Moreover, the current thesis provides the data for one kind of polymer i.e. Poly 1, 8 – Octanediol Citrate. It is suggested that future research must be directed towards establishing non-cytotoxic percentages of ZnONP in other polymers because each polymer has its own degradation and cross-linking properties. Although the current thesis provides a comprehensive account for hypoxic studies, however, only short-term results are provided for dynamic mechanical compression. The reason for this is the limitation of the current bioreactor, which does not provide a sterile environment for long term studies. Hence it is suggested that a new bioreactor should be designed that allows long-term application of dynamic mechanical culture, while maintaining the integrity of culture system.

To obtain qualitative data regarding the performance of scaffolds under hypoxia seeded with BAC, it is suggested that staining and western blotting should also be undertaken to support the existing data.

Lastly, it is suggested that an animal in-vivo model be created for long-term investigation of the chondroprotective response to ZnONP, and its further beneficial effects in wound healing after surgical implantation.

References

- Ab-Rahim, S., Masjudin, T., Selvaratnam, L., & Kamarul, T. Evaluation of Human Autologous Chondrocyte Transplantation Effectiveness in Relation to Rabbit Assessment as an Animal Model.
- Abercrombie, M. (1979). Contact inhibition and malignancy. *Nature*, 281(5729): 259-262.
- Afratis, N., Gialeli, C., Nikitovic, D., Tsegenidis, T., Karousou, E., Theocharis, A. D., Pavão, M. S., Tzanakakis, G. N., & Karamanos, N. K. (2012). Glycosaminoglycans: key players in cancer cell biology and treatment. *Febs Journal*, 279(7): 1177-1197.
- Aigner, T., & Fan, Z. (2003). Anatomy and Biochemistry of Articular Cartilage. In C. Hendrich, U. Nöth & J. Eulert (Eds.), *Cartilage Surgery and Future Perspectives* (pp. 3-7): Springer Berlin Heidelberg.
- Akhtar, M. J., Ahamed, M., Kumar, S., Khan, M. A. M., Ahmad, J., & Alrokayan, S. A. (2012). Zinc oxide nanoparticles selectively induce apoptosis in human cancer cells through reactive oxygen species. *Int J Nanomedicine*, 7: 845-857.
- Aksoy, B., Atakan, N., Aksoy, H. M., Tezel, G. G., Renda, N., Özkara, H. A., & Önder, E. (2010). Effectiveness of topical zinc oxide application on hypertrophic scar development in rabbits. *Burns*, 36(7): 1027-1035.
- Albro, M. B., Nims, R. J., Cigan, A. D., Yeroushalmi, K. J., Shim, J. J., Hung, C. T., & Ateshian, G. A. (2013). Dynamic mechanical compression of devitalized articular cartilage does not activate latent TGF- β . *Journal of Biomechanics*, 46(8): 1433-1439.
- Anower-E-Khuda, M. F., & Kimata, K. (2015). Human Blood Glycosaminoglycans: Isolation and Analysis *Glycosaminoglycans* (pp. 95-103): Springer.
- Appelman, T. P., Mizrahi, J., Elisseeff, J. H., & Seliktar, D. (2011). The influence of biological motifs and dynamic mechanical stimulation in hydrogel scaffold systems on the phenotype of chondrocytes. *Biomaterials*, 32(6): 1508-1516.
- Arima, Y., & Iwata, H. (2007). Effect of wettability and surface functional groups on protein adsorption and cell adhesion using well-defined mixed self-assembled monolayers. *Biomaterials*, 28(20): 3074-3082.
- Ataollahi, F., Pramanik, S., Moradi, A., Dalilottojari, A., Pinguan-Murphy, B., Wan Abas, W. A. B., & Abu Osman, N. A. (2014). Endothelial cell responses in terms of adhesion, proliferation, and morphology to stiffness of polydimethylsiloxane elastomer substrates. *Journal of Biomedical Materials Research Part A*: n/a-n/a.

- Athauda, T., Williams, W., Roberts, K., & Ozer, R. (2013). On the surface roughness and hydrophobicity of dual-size double-layer silica nanoparticles. *Journal of Materials Science*, 48(18): 6115-6120.
- Augustine, R., Dominic, E. A., Reju, I., Kaimal, B., Kalarikkal, N., & Thomas, S. (2014). Investigation of angiogenesis and its mechanism using zinc oxide nanoparticle-loaded electrospun tissue engineering scaffolds. *RSC Advances*, 4(93): 51528-51536.
- Augustine, R., Malik, H., Singhal, D., Mukherjee, A., Malakar, D., Kalarikkal, N., & Thomas, S. (2014). Electrospun polycaprolactone/ZnO nanocomposite membranes as biomaterials with antibacterial and cell adhesion properties. *Journal of Polymer Research*, 21(3): 1-17.
- Azizi, S., Ahmad, M. B., Hussein, M. Z., Ibrahim, N. A., & Namvar, F. (2014). Preparation and properties of poly (vinyl alcohol)/chitosan blend bionanocomposites reinforced with cellulose nanocrystals/ZnO-Ag multifunctional nanosized filler. *Int J Nanomedicine*, 9: 1909.
- Bakhshi, H., Yeganeh, H., & Mehdipour-Ataei, S. (2012). Synthesis and evaluation of antibacterial polyurethane coatings made from soybean oil functionalized with dimethylphenylammonium iodide and hydroxyl groups. *Journal of Biomedical Materials Research Part A*: n/a-n/a.
- Balasundaram, G., Storey, D. M., & Webster, T. J. (2014). Novel nano-rough polymers for cartilage tissue engineering. *Int J Nanomedicine*, 9: 1845-1853.
- Bartlett, W., Skinner, J., Gooding, C., Carrington, R., Flanagan, A., Briggs, T., & Bentley, G. (2005). Autologous chondrocyte implantation versus matrix-induced autologous chondrocyte implantation for osteochondral defects of the knee A PROSPECTIVE, RANDOMISED STUDY. *Journal of Bone & Joint Surgery, British Volume*, 87(5): 640-645.
- Bassleer, C., Rovati, L., & Franchimont, P. (1998). Stimulation of proteoglycan production by glucosamine sulfate in chondrocytes isolated from human osteoarthritic articular cartilage in vitro. *Osteoarthritis and Cartilage*, 6(6): 427-434.
- Benya, P. D., & Shaffer, J. D. (1982). Dedifferentiated chondrocytes reexpress the differentiated collagen phenotype when cultured in agarose gels. *Cell*, 30(1): 215-224.
- Berg-Perier, M., Cederblad, A., & Persson, U. (1992). Ultraviolet radiation and ultra-clean air enclosures in operating rooms. UV-protection, economy, and comfort. *J Arthroplasty*, 7(4): 457-463.

- Betre, H., Ong, S. R., Guilak, F., Chilkoti, A., Fermor, B., & Setton, L. A. (2006). Chondrocytic differentiation of human adipose-derived adult stem cells in elastin-like polypeptide. *Biomaterials*, 27(1): 91-99.
- Beyersmann, D., & Haase, H. (2001). Functions of zinc in signaling, proliferation and differentiation of mammalian cells. *Biometals*, 14(3-4): 331-341.
- Bhattacharjee, M., Coburn, J., Centola, M., Murab, S., Barbero, A., Kaplan, D. L., Martin, I., & Ghosh, S. (2015). Tissue engineering strategies to study cartilage development, degeneration and regeneration. *Advanced Drug Delivery Reviews*, 84: 107-122.
- Bhosale, A. M., & Richardson, J. B. (2008). Articular cartilage: structure, injuries and review of management. *British medical bulletin*, 87(1): 77-95.
- Bian, L., Fong, J. V., Lima, E. G., Stoker, A. M., Ateshian, G. A., Cook, J. L., & Hung, C. T. (2010). Dynamic mechanical loading enhances functional properties of tissue-engineered cartilage using mature canine chondrocytes. *Tissue Engineering Part A*, 16(5): 1781-1790.
- Blaker, J. J., Nazhat, S. N., & Boccaccini, A. R. (2004). Development and characterisation of silver-doped bioactive glass-coated sutures for tissue engineering and wound healing applications. *Biomaterials*, 25(7-8): 1319-1329.
- Bobic, V. (1999). Die Verwendung von autologen Knochen-Knorpel-Transplantaten in der Behandlung von Gelenkknorpelläsionen. *Der Orthopäde*, 28(1): 19-25.
- Boeuf, S., & Richter, W. (2010). Chondrogenesis of mesenchymal stem cells: role of tissue source and inducing factors. *Stem Cell Res Ther*, 1(4): 31.
- Bös, L., Ellermann, A., & aus dem Spring, E.-S. (2000). Ergebnisse und Komplikationen mit dem OATS-Instrumentarium. *Arthroskopie*, 13(3): 99-102.
- Boschetti, F., Pennati, G., Gervaso, F., Peretti, G. M., & Dubini, G. (2004). Biomechanical properties of human articular cartilage under compressive loads. *Biorheology*, 41(3-4): 159-166.
- Bouwmeester, S. J., Beckers, J. M., Kuijer, R., van der Linden, A. J., & Bulstra, S. K. (1997). Long-term results of rib perichondrial grafts for repair of cartilage defects in the human knee. *Int Orthop*, 21(5): 313-317.
- Brand, R. A. (2005). Joint contact stress: a reasonable surrogate for biological processes? *Iowa Orthop J*, 25: 82-94.
- Brézillon, S., Untereiner, V., Lovergne, L., Tadeo, I., Noguera, R., Maquart, F.-X., Wegrowski, Y., & Sockalingum, G. (2014). Glycosaminoglycan profiling in different cell types using infrared spectroscopy and imaging. *Analytical and Bioanalytical Chemistry*, 406(24): 5795-5803.

- Brittberg, M., Lindahl, A., Nilsson, A., Ohlsson, C., Isaksson, O., & Peterson, L. (1994). Treatment of deep cartilage defects in the knee with autologous chondrocyte transplantation. *New England Journal of Medicine*, 331(14): 889-895.
- Brodkin, K. R., García, A. J., & Levenston, M. E. (2004). Chondrocyte phenotypes on different extracellular matrix monolayers. *Biomaterials*, 25(28): 5929-5938.
- Buckwalter, J., & Mankin, H. (1997). Articular cartilage: tissue design and chondrocyte-matrix interactions. *Instructional course lectures*, 47: 477-486.
- Buckwalter, J. A., & Mankin, H. J. (1998a). Articular cartilage repair and transplantation. *Arthritis & Rheumatism*, 41(8): 1331-1342.
- Buckwalter, J. A., & Mankin, H. J. (1998b). Articular cartilage: degeneration and osteoarthritis, repair, regeneration, and transplantation. *Instructional course lectures*, 47: 487-504.
- Buckwalter, J. A., Mankin, H. J., & Grodzinsky, A. J. (2005). Articular cartilage and osteoarthritis. *Instructional Course Lectures-American Academy of Orthopaedic Surgeons*, 54: 465.
- Burg, K. J. L., Porter, S., & Kellam, J. F. (2000). Biomaterial developments for bone tissue engineering. *Biomaterials*, 21(23): 2347-2359.
- Burns, J. L., Ramsey, B. W., & Smith, A. L. (1993). Clinical manifestations and treatment of pulmonary infections in cystic fibrosis. *Adv Pediatr Infect Dis*, 8: 53-66.
- Burrage, P. S., Mix, K. S., & Brinckerhoff, C. E. (2006). Matrix metalloproteinases: role in arthritis. *Front Biosci*, 11(1): 529-543.
- Camarero-Espinosa, S., Rothen-Rutishauser, B., Weder, C., & Foster, E. J. (2016). Directed cell growth in multi-zonal scaffolds for cartilage tissue engineering. *Biomaterials*, 74: 42-52.
- Cannizzaro, C., Tandon, N., Figallo, E., Park, H., Gerecht, S., Radisic, M., Elvassore, N., & Vunjak-Novakovic, G. (2007). Practical aspects of cardiac tissue engineering with electrical stimulation. *Methods Mol Med*, 140: 291-307.
- Caplan, A. I., Elyaderani, M., Mochizuki, Y., Wakitani, S., & Goldberg, V. M. (1997). Principles of cartilage repair and regeneration. *Clin Orthop Relat Res*(342): 254-269.
- Chang, B. P., Akil, H. M., Nasir, R. B. M., Bandara, I., & Rajapakse, S. (2014). The effect of ZnO nanoparticles on the mechanical, tribological and antibacterial properties of ultra-high molecular weight polyethylene. *Journal of Reinforced Plastics and Composites*, 33(7): 674-686.

- Chen, F. H., Rousche, K. T., & Tuan, R. S. (2006). Technology Insight: adult stem cells in cartilage regeneration and tissue engineering. *Nature clinical practice rheumatology*, 2(7): 373-382.
- Chen, J.-L., Duan, L., Zhu, W., Xiong, J., & Wang, D. (2014). Extracellular matrix production in vitro in cartilage tissue engineering. *Journal of Translational Medicine*, 12(1): 88.
- Chen, X., Li, J., Wang, E., Zhao, Q., Kong, Z., & Yuan, X. (2015). Dynamic compression combined with SOX-9 overexpression in rabbit adipose-derived mesenchymal stem cells cultured in a three-dimensional gradual porous PLGA composite scaffold upregulates HIF-1 α expression. *Journal of Biomedical Materials Research Part A*: n/a-n/a.
- Chen, X. C., Wang, R., Zhao, X., Wei, Y. Q., Hu, M., Wang, Y. S., Zhang, X. W., Zhang, R., Zhang, L., Yao, B., Wang, L., Jia, Y. Q., Zeng, T. T., Yang, J. L., Tian, L., Kan, B., Lin, X. J., Lei, S., Deng, H. X., Wen, Y. J., Mao, Y. Q., & Li, J. (2006). Prophylaxis against carcinogenesis in three kinds of unestablished tumor models via IL12-gene-engineered MSCs. *Carcinogenesis*, 27(12): 2434-2441.
- Chen, Z., Chen, J., Wu, L., Li, W., Chen, J., Cheng, H., Pan, J., & Cai, B. (2013). Hyaluronic acid-coated bovine serum albumin nanoparticles loaded with brucine as selective nanovectors for intra-articular injection. *Int J Nanomedicine*, 8: 3843-3853.
- Chilelli, B. J., Mastrocola, M. R., & Gomoll, A. H. Autologous Chondrocyte Implantation: Surgical Technique and Outcomes. *Operative Techniques in Orthopaedics*(0).
- Choi, J. R., Pinguan-Murphy, B., Wan Abas, W. A. B., Noor Azmi, M. A., Omar, S. Z., Chua, K. H., & Wan Safwani, W. K. Z. (2014). Impact of low oxygen tension on stemness, proliferation and differentiation potential of human adipose-derived stem cells. *Biochemical and Biophysical Research Communications*, 448(2): 218-224.
- Chowdhury, T., Bader, D., & Lee, D. (2006). Anti-inflammatory effects of IL-4 and dynamic compression in IL-1 β stimulated chondrocytes. *Biochemical and biophysical research communications*, 339(1): 241-247.
- Chowdhury, T. T., Bader, D. L., & Lee, D. A. (2003). Dynamic compression counteracts IL-1 β -induced release of nitric oxide and PGE₂ by superficial zone chondrocytes cultured in agarose constructs. *Osteoarthritis and Cartilage*, 11(9): 688-696.
- Chung, C., & Burdick, J. A. (2008). Engineering cartilage tissue. *Advanced Drug Delivery Reviews*, 60(2): 243-262.

- Co, C., Vickaryous, M. K., & Koch, T. G. (2014). Membrane culture and reduced oxygen tension enhances cartilage matrix formation from equine cord blood mesenchymal stromal cells in vitro. *Osteoarthritis and Cartilage*, 22(3): 472-480.
- Cohen, N. P., Foster, R. J., & Mow, V. C. (1998). Composition and dynamics of articular cartilage: structure, function, and maintaining healthy state. *Journal of Orthopaedic & Sports Physical Therapy*, 28(4): 203-215.
- Collins, J. A., Moots, R. J., Winstanley, R., Clegg, P. D., & Milner, P. I. (2013). Oxygen and pH-sensitivity of human osteoarthritic chondrocytes in 3-D alginate bead culture system. *Osteoarthritis and Cartilage*, 21(11): 1790-1798.
- Colon, G., Ward, B. C., & Webster, T. J. (2006). Increased osteoblast and decreased Staphylococcus epidermidis functions on nanophase ZnO and TiO₂. *J Biomed Mater Res A*, 78(3): 595-604.
- Costerton, J. W., Stewart, P. S., & Greenberg, E. P. (1999). Bacterial Biofilms: A Common Cause of Persistent Infections. *Science*, 284(5418): 1318-1322.
- Cournil-Henrionnet, C., Huselstein, C., Wang, Y., Galois, L., Mainard, D., Decot, V., Netter, P., Stoltz, J.-F., Muller, S., & Gillet, P. (2008). Phenotypic analysis of cell surface markers and gene expression of human mesenchymal stem cells and chondrocytes during monolayer expansion. *Biorheology*, 45(3): 513.
- Coutts, R. D., Sah, R. L., & Amiel, D. (1997). Effects of growth factors on cartilage repair. *Instructional course lectures*, 46: 487-494.
- Cox Jr, S. T., Hembree Jr, J. H., & McKnight, J. P. (1978). The bactericidal potential of various endodontic materials for primary teeth. *Oral Surgery, Oral Medicine, Oral Pathology*, 45(6): 947-954.
- Dahlin, R. L., Meretoja, V. V., Ni, M., Kasper, F. K., & Mikos, A. G. (2013). Hypoxia and flow perfusion modulate proliferation and gene expression of articular chondrocytes on porous scaffolds. *AIChE Journal*, 59(9): 3158-3166.
- Davies, D. (2003). Understanding biofilm resistance to antibacterial agents. *Nature reviews Drug discovery*, 2(2): 114-122.
- Davisson, T., Kunig, S., Chen, A., Sah, R., & Ratcliffe, A. (2002). Static and dynamic compression modulate matrix metabolism in tissue engineered cartilage. *Journal of Orthopaedic Research*, 20(4): 842-848.
- Davisson, T., Sah, R. L., & Ratcliffe, A. (2002). Perfusion increases cell content and matrix synthesis in chondrocyte three-dimensional cultures. *Tissue Eng*, 8(5): 807-816.
- Demange, M., Minas, T., & Gomoll, A. (2014). Autologous Chondrocyte Implantation After Previous Treatment with Marrow Stimulation Techniques. In P. J. Emans &

L. Peterson (Eds.), *Developing Insights in Cartilage Repair* (pp. 213-225): Springer London.

Démarteau, O., Wendt, D., Braccini, A., Jakob, M., Schäfer, D., Heberer, M., & Martin, I. (2003). Dynamic compression of cartilage constructs engineered from expanded human articular chondrocytes. *Biochem Biophys Res Commun*, 310(2): 580-588.

Denko, N. C., Fontana, L. A., Hudson, K. M., Sutphin, P. D., Raychaudhuri, S., Altman, R., & Giaccia, A. J. (2003). Investigating hypoxic tumor physiology through gene expression patterns. *Oncogene*, 22(37): 5907-5914.

Di Federico, E., Bader, D. L., & Shelton, J. C. (2014). Design and validation of an in vitro loading system for the combined application of cyclic compression and shear to 3D chondrocytes-seeded agarose constructs. *Med Eng Phys*, 36(4): 534-540.

Díaz, E., Puerto, I., & Sandonis, I. (2014). The Effects of Bioactive Nanoparticles on the Degradation of DLGA. *International Journal of Polymeric Materials and Polymeric Biomaterials*, 64(1): 38-46.

Djordjevic, I., Choudhury, N. R., Dutta, N. K., & Kumar, S. (2009). Synthesis and characterization of novel citric acid-based polyester elastomers. *Polymer*, 50(7): 1682-1691.

Djordjevic, I., Choudhury, N. R., Dutta, N. K., Kumar, S., Szili, E. J., & Steele, D. A. (2010). Polyoctanediol citrate/sebacate bioelastomer films: surface morphology, chemistry and functionality. *J Biomater Sci Polym Ed*, 21(2): 237-251.

Djordjevic, I., Szili, E. J., Choudhury, N. R., Dutta, N., Steele, D. A., & Kumar, S. (2010). Osteoblast biocompatibility on poly(octanediol citrate)/sebacate elastomers with controlled wettability. *J Biomater Sci Polym Ed*, 21(8-9): 1039-1050.

Domm, C., Schünke, M., Christesen, K., & Kurz, B. (2002). Redifferentiation of dedifferentiated bovine articular chondrocytes in alginate culture under low oxygen tension. *Osteoarthritis and Cartilage*, 10(1): 13-22.

Doran, P. (2015). Cartilage Tissue Engineering: What Have We Learned in Practice? In P. M. Doran (Ed.), *Cartilage Tissue Engineering* (Vol. 1340, pp. 3-21): Springer New York.

Du, Y., Ge, J., Shao, Y., Ma, P. X., Chen, X., & Lei, B. (2015). Development of silica grafted poly (1, 8-octanediol-co-citrates) hybrid elastomers with highly tunable mechanical properties and biocompatibility. *Journal of Materials Chemistry B*, 3(15): 2986-3000.

Dwivedi, P., Bhat, S., Nayak, V., & Kumar, A. (2014). Study of Different Delivery Modes of Chondroitin Sulfate Using Microspheres and Cryogel Scaffold for Application in Cartilage Tissue Engineering. *International Journal of Polymeric Materials and Polymeric Biomaterials*, 63(16): 859-872.

- Elder, B. D., & Athanasiou, K. A. (2009). Systematic assessment of growth factor treatment on biochemical and biomechanical properties of engineered articular cartilage constructs. *Osteoarthritis and Cartilage*, 17(1): 114-123.
- Elisseeff, J., Anseth, K., Sims, D., McIntosh, W., Randolph, M., & Langer, R. (1999). Transdermal photopolymerization for minimally invasive implantation. *Proc Natl Acad Sci U S A*, 96(6): 3104-3107.
- Espitia, P. J., Soares Nde, F., Teofilo, R. F., Coimbra, J. S., Vitor, D. M., Batista, R. A., Ferreira, S. O., de Andrade, N. J., & Medeiros, E. A. (2013). Physical-mechanical and antimicrobial properties of nanocomposite films with pediocin and ZnO nanoparticles. *Carbohydr Polym*, 94(1): 199-208.
- Eyrich, D., Wiese, H., Maier, G., Skodacek, D., Appel, B., Sarhan, H., Tessmar, J., Staudenmaier, R., Wenzel, M. M., & Goepferich, A. (2007). In vitro and in vivo cartilage engineering using a combination of chondrocyte-seeded long-term stable fibrin gels and polycaprolactone-based polyurethane scaffolds. *Tissue Eng*, 13(9): 2207-2218.
- Farr, J., Cole, B., Dhawan, A., Kercher, J., & Sherman, S. (2011). Clinical Cartilage Restoration: Evolution and Overview. *Clinical Orthopaedics and Related Research®*, 469(10): 2696-2705.
- Fedele, A. O., Whitelaw, M. L., & Peet, D. J. (2002). Regulation of gene expression by the hypoxia-inducible factors. *Mol Interv*, 2(4): 229-243.
- Feng, P., Wei, P., Shuai, C., & Peng, S. (2014). Characterization of Mechanical and Biological Properties of 3-D Scaffolds Reinforced with Zinc Oxide for Bone Tissue Engineering. *PLoS ONE*, 9(1): e87755.
- Fielding, G. A., Bandyopadhyay, A., & Bose, S. (2012). Effects of silica and zinc oxide doping on mechanical and biological properties of 3D printed tricalcium phosphate tissue engineering scaffolds. *Dental Materials*, 28(2): 113-122.
- Filardo, G., Madry, H., Jelic, M., Roffi, A., Cucchiaroni, M., & Kon, E. (2013). Mesenchymal stem cells for the treatment of cartilage lesions: from preclinical findings to clinical application in orthopaedics. *Knee Surgery, Sports Traumatology, Arthroscopy*, 21(8): 1717-1729.
- Foldager, C. B., Nielsen, A. B., Munir, S., Ulrich-Vinther, M., Søballe, K., Bünger, C., & Lind, M. (2011). Combined 3D and hypoxic culture improves cartilage-specific gene expression in human chondrocytes. *Acta Orthopaedica*, 82(2): 234-240.
- Fortier, L. A., Barker, J. U., Strauss, E. J., McCarrel, T. M., & Cole, B. J. (2011). The role of growth factors in cartilage repair. *Clinical Orthopaedics and Related Research®*, 469(10): 2706-2715.

- Fosang, A. J., Last, K., Knäuper, V., Murphy, G., & Neame, P. J. (1996). Degradation of cartilage aggrecan by collagenase-3 (MMP-13). *FEBS Letters*, 380(1–2): 17-20.
- Freed, L., Hollander, A., Martin, I., Barry, J., Langer, R., & Vunjak-Novakovic, G. (1998). Chondrogenesis in a cell-polymer-bioreactor system. *Exp Cell Res*, 240(1): 58-65.
- Friedman, C. D., Costantino, P. D., Takagi, S., & Chow, L. C. (1998). BoneSource hydroxyapatite cement: a novel biomaterial for craniofacial skeletal tissue engineering and reconstruction. *J Biomed Mater Res*, 43(4): 428-432.
- Fu, J., Ji, J., Yuan, W., & Shen, J. (2005). Construction of anti-adhesive and antibacterial multilayer films via layer-by-layer assembly of heparin and chitosan. *Biomaterials*, 26(33): 6684-6692.
- Gallagher, J. T., Spooncer, E., & Dexter, T. (1983). Role of the cellular matrix in haemopoiesis. I. Synthesis of glycosaminoglycans by mouse bone marrow cell cultures. *Journal of cell science*, 63(1): 155-171.
- Gaut, C., & Sugaya, K. (2015). Critical review on the physical and mechanical factors involved in tissue engineering of cartilage. *Regenerative Medicine*(0): 1-15.
- Gawish, S. M., Avci, H., Ramadan, A. M., Mosleh, S., Monticello, R., Breidt, F., & Kotek, R. (2012). Properties of Antibacterial Polypropylene/Nanometal Composite Fibers. *Journal of Biomaterials Science, Polymer Edition*, 23(1-4): 43-61.
- Geilich, B. M. (2013). Reduced adhesion of Staphylococcus aureus to ZnO/PVC nanocomposites. *Int J Nanomedicine*, 8: 1177-1184.
- Genes, N. G., Rowley, J. A., Mooney, D. J., & Bonassar, L. J. (2004). Effect of substrate mechanics on chondrocyte adhesion to modified alginate surfaces. *Archives of biochemistry and biophysics*, 422(2): 161-167.
- Ghadially, F., Thomas, I., Oryschak, A., & Lalonde, J. M. (1977). Long-term results of superficial defects in articular cartilage: A scanning electronmicroscope study. *The Journal of pathology*, 121(4): 213-217.
- Gir, P., Oni, G., Brown, S. A., Mojallal, A., & Rohrich, R. J. (2012). Human adipose stem cells: current clinical applications. *Plastic and reconstructive surgery*, 129(6): 1277-1290.
- Goda, N., Ryan, H. E., Khadivi, B., McNulty, W., Rickert, R. C., & Johnson, R. S. (2003). Hypoxia-inducible factor 1 α is essential for cell cycle arrest during hypoxia. *Molecular and cellular biology*, 23(1): 359-369.
- Goddard, J. M., & Hotchkiss, J. (2007). Polymer surface modification for the attachment of bioactive compounds. *Progress in polymer science*, 32(7): 698-725.

- Godier-Furnémont, A. F., Tiburcy, M., Wagner, E., Dewenter, M., Lämmle, S., El-Armouche, A., Lehnart, S. E., Vunjak-Novakovic, G., & Zimmermann, W.-H. (2015). Physiologic force-frequency response in engineered heart muscle by electromechanical stimulation. *Biomaterials*, *60*: 82-91.
- Goh, Y.-F., Shakir, I., & Hussain, R. (2013). Electrospun fibers for tissue engineering, drug delivery, and wound dressing. *Journal of Materials Science*, *48*(8): 3027-3054.
- Goldring, M. B., Tsuchimochi, K., & Ijiri, K. (2006). The control of chondrogenesis. *Journal of Cellular Biochemistry*, *97*(1): 33-44.
- Gomoll, A. H., & Minas, T. (2014). The quality of healing: Articular cartilage. *Wound Repair and Regeneration*, *22*(S1): 30-38.
- Gooch, K., & Tennant, C. (1997). Chondrocytes. In K. Gooch & C. Tennant (Eds.), *Mechanical Forces: Their Effects on Cells and Tissues* (pp. 79-100): Springer Berlin Heidelberg.
- Gordon, T., Perlstein, B., Houbara, O., Felner, I., Banin, E., & Margel, S. (2011). Synthesis and characterization of zinc/iron oxide composite nanoparticles and their antibacterial properties. *Colloids and Surfaces A: Physicochemical and Engineering Aspects*, *374*(1-3): 1-8.
- Grad, S., Kupcsik, L., Gorna, K., Gogolewski, S., & Alini, M. (2003). The use of biodegradable polyurethane scaffolds for cartilage tissue engineering: potential and limitations. *Biomaterials*, *24*(28): 5163-5171.
- Grande, D. A., Pitman, M. I., Peterson, L., Menche, D., & Klein, M. (1989). The repair of experimentally produced defects in rabbit articular cartilage by autologous chondrocyte transplantation. *Journal of Orthopaedic Research*, *7*(2): 208-218.
- Gray, M. L., Pizzanelli, A. M., Grodzinsky, A. J., & Lee, R. C. (1988). Mechanical and physicochemical determinants of the chondrocyte biosynthetic response. *J Orthop Res*, *6*(6): 777-792.
- Grimshaw, M. J., & Mason, R. M. (2000). Bovine articular chondrocyte function in vitro depends upon oxygen tension. *Osteoarthritis and Cartilage*, *8*(5): 386-392.
- Gristina, A., Naylor, P., & Myrvik, Q. (1989). The Race for the Surface: Microbes, Tissue Cells, and Biomaterials. In L. Switalski, M. Höök & E. Beachey (Eds.), *Molecular Mechanisms of Microbial Adhesion* (pp. 177-211): Springer New York.
- Grodzinsky, A. J., Levenston, M. E., Jin, M., & Frank, E. H. (2000). Cartilage tissue remodeling in response to mechanical forces. *Annu Rev Biomed Eng*, *2*: 691-713.
- Gudas, R., Kalesinskas, R. J., Kimtys, V., Stankevičius, E., Toliušis, V., Bernotavičius, G., & Smailys, A. (2005). A prospective randomized clinical study of mosaic

osteocondral autologous transplantation versus microfracture for the treatment of osteochondral defects in the knee joint in young athletes. *Arthroscopy: The Journal of Arthroscopic & Related Surgery*, 21(9): 1066-1075.

Guigand, M., Vulcain, J.-M., Dautel-Morazin, A., & Bonnaure-Mallet, M. (1997). In vitro study of intradental calcium diffusion induced by two endodontic biomaterials. *J Endod*, 23(6): 387-390.

Guilak, F., Ratcliffe, A., & Mow, V. C. (1995). Chondrocyte deformation and local tissue strain in articular cartilage: a confocal microscopy study. *J Orthop Res*, 13(3): 410-421.

Guo, J., Xie, Z., Tran, R. T., Xie, D., Jin, D., Bai, X., & Yang, J. (2014). Click Chemistry Plays a Dual Role in Biodegradable Polymer Design. *Advanced Materials*, 26(12): 1906-1911.

Guo, Y., Tran, R. T., Xie, D., Wang, Y., Nguyen, D. Y., Gerhard, E., Guo, J., Tang, J., Zhang, Z., Bai, X., & Yang, J. (2015). Citrate-based biphasic scaffolds for the repair of large segmental bone defects. *Journal of Biomedical Materials Research Part A*, 103(2): 772-781.

Gutwein, L., & Webster, T. (2002). Osteoblast and Chondrocyte Proliferation in the Presence of Alumina And Titania Nanoparticles. *Journal of Nanoparticle Research*, 4(3): 231-238.

Gyawali, D., Nair, P., Kim, H. K., & Yang, J. (2013). Citrate-based biodegradable injectable hydrogel composites for orthopedic applications. *Biomaterials science*, 1(1): 52-64.

Haaparanta, A.-M., Järvinen, E., Cengiz, I., Ellä, V., Kokkonen, H., Kiviranta, I., & Kellomäki, M. (2014). Preparation and characterization of collagen/PLA, chitosan/PLA, and collagen/chitosan/PLA hybrid scaffolds for cartilage tissue engineering. *Journal of Materials Science: Materials in Medicine*, 25(4): 1129-1136.

Haase, H., & Rink, L. (2014a). Multiple impacts of zinc on immune function. *Metallomics*, 6(7): 1175-1180.

Haase, H., & Rink, L. (2014b). Zinc signals and immune function. *Biofactors*, 40(1): 27-40.

Hahn, A., Brandes, G., Wagener, P., & Barcikowski, S. (2011). Metal ion release kinetics from nanoparticle silicone composites. *J Control Release*, 154(2): 164-170.

Hall, B. K. (1994). *Mechanisms of Bone Development and Growth*: CRC Press.

Hall, B. K. (2012). *Cartilage VI: Structure, Function, and Biochemistry*: Elsevier Science.

- Hangody, L. (1997). Autogenous osteochondral graft technique for replacing knee cartilage defects in dogs. *Orthopedics*, 5: 175-181.
- Hangody, L., Feczkó, P., Bartha, L., Bodó, G., & Kish, G. (2001). Mosaicplasty for the treatment of articular defects of the knee and ankle. *Clinical orthopaedics and related research*, 391: S328-S336.
- Hansen, U., Schunke, M., Domm, C., Ioannidis, N., Hassenpflug, J., Gehrke, T., & Kurz, B. (2001). Combination of reduced oxygen tension and intermittent hydrostatic pressure: a useful tool in articular cartilage tissue engineering. *J Biomech*, 34(7): 941-949.
- Hardingham, T., Tew, S., & Murdoch, A. (2002). Tissue engineering: chondrocytes and cartilage. *Arthritis res*, 4(Suppl 3): S63-S68.
- Harris, J. D., Siston, R. A., Brophy, R. H., Lattermann, C., Carey, J. L., & Flanigan, D. C. (2011). Failures, re-operations, and complications after autologous chondrocyte implantation – a systematic review. *Osteoarthritis and Cartilage*, 19(7): 779-791.
- Harris, J. D., Siston, R. A., Pan, X., & Flanigan, D. C. (2010). Autologous Chondrocyte Implantation. *The Journal of Bone & Joint Surgery*, 92(12): 2220-2233.
- Hazelwood, K. J., O'Rourke, M., Stamos, V. P., McMillan, R. D., Beigler, D., & Robb, W. J. (2015). Case series report: Early cement–implant interface fixation failure in total knee replacement. *The Knee*.
- Heath, C. A., & Magari, S. R. (1996). Mini-review: Mechanical factors affecting cartilage regeneration in vitro. *Biotechnol Bioeng*, 50(4): 430-437.
- Hege, C., & Schiller, S. (2015). New Bioinspired Materials for Regenerative Medicine. *Current Molecular Biology Reports*, 1(2): 77-86.
- Helliwell, T., Kelly, S., Walsh, H., Klenerman, L., Haines, J., Clark, R., & Roberts, N. (1996). Elemental analysis of femoral bone from patients with fractured neck of femur or osteoarthritis. *Bone*, 18(2): 151-157.
- Hendrich, C., Schütze, N., Barthel, T., Nöth, U., & Eulert, J. (2003). Cartilage injury and repair *Cartilage Surgery and Future Perspectives* (pp. 9-15): Springer.
- Heuer, W., Elter, C., Demling, A., Neumann, A., Suerbaum, S., Hannig, M., Heidenblut, T., Bach, F. W., & Stiesch-Scholz, M. (2007). Analysis of early biofilm formation on oral implants in man. *Journal of Oral Rehabilitation*, 34(5): 377-382.
- Hidalgo-Bastida, L., Barry, J., Everitt, N., Rose, F., Buttery, L., Hall, I., Claycomb, W., & Shakesheff, K. (2007). Cell adhesion and mechanical properties of a flexible scaffold for cardiac tissue engineering. *Acta biomaterialia*, 3(4): 457-462.

- Hjelle, K., Solheim, E., Strand, T., Muri, R., & Brittberg, M. (2002). Articular cartilage defects in 1,000 knee arthroscopies. *Arthroscopy: The Journal of Arthroscopic & Related Surgery*, 18(7): 730-734.
- Ho, E., Courtemanche, C., & Ames, B. N. (2003). Zinc deficiency induces oxidative DNA damage and increases P53 expression in human lung fibroblasts. *Journal of Nutrition*, 133(8): 2543-2548.
- Hoffman, L. R., D'Argenio, D. A., MacCoss, M. J., Zhang, Z., Jones, R. A., & Miller, S. I. (2005). Aminoglycoside antibiotics induce bacterial biofilm formation. *Nature*, 436(7054): 1171-1175.
- Hoiby, N. (1993). Antibiotic therapy for chronic infection of pseudomonas in the lung. *Annu Rev Med*, 44: 1-10.
- Hollinger, J. O., & Battistone, G. C. (1986). Biodegradable bone repair materials. Synthetic polymers and ceramics. *Clin Orthop Relat Res*(207): 290-305.
- Hollister, S. J. (2005). Porous scaffold design for tissue engineering. *Nature materials*, 4(7): 518-524.
- Holmes, B., Fang, X., Zarate, A., Keidar, M., & Zhang, L. G. (2016). Enhanced human bone marrow mesenchymal stem cell chondrogenic differentiation in electrospun constructs with carbon nanomaterials. *Carbon*, 97: 1-13.
- Holmes, R. E. (1979). Bone regeneration within a coralline hydroxyapatite implant. *Plast Reconstr Surg*, 63(5): 626-633.
- Hong, J.-S., Park, M.-K., Kim, M.-S., Lim, J.-H., Park, G.-J., Maeng, E.-H., Shin, J.-H., Kim, Y.-R., Kim, M.-K., Lee, J.-K., Park, J.-A., Kim, J.-C., & Shin, H.-C. (2014). Effect of zinc oxide nanoparticles on dams and embryo–fetal development in rats. *Int J Nanomedicine*, 9(Suppl 2): 145-157.
- Honkanen, V., Pelkonen, P., Mussalo-Rauhamaa, H., Lehto, J., & Westermarck, T. (1989). Serum trace elements in juvenile chronic arthritis. *Clinical Rheumatology*, 8(1): 64-70.
- Hou, Q., Grijpma, D. W., & Feijen, J. (2003). Porous polymeric structures for tissue engineering prepared by a coagulation, compression moulding and salt leaching technique. *Biomaterials*, 24(11): 1937-1947.
- Hubka, K. M., Dahlin, R. L., Meretoja, V. V., Kasper, F. K., & Mikos, A. G. (2014). Enhancing Chondrogenic Phenotype for Cartilage Tissue Engineering: Monoculture and Co-culture of Articular Chondrocytes and Mesenchymal Stem Cells. *Tissue Eng*(ja).

- Hummon, A. B., Lim, S. R., Difilippantonio, M. J., & Ried, T. (2007). Isolation and solubilization of proteins after TRIzol extraction of RNA and DNA from patient material following prolonged storage. *Biotechniques*, 42(4): 467-470, 472.
- Humphreys, J. H., Verstappen, S. M. M., Hyrich, K. L., Chipping, J. R., Marshall, T., & Symmons, D. P. M. (2013). The incidence of rheumatoid arthritis in the UK: comparisons using the 2010 ACR/EULAR classification criteria and the 1987 ACR classification criteria. Results from the Norfolk Arthritis Register. *Annals of the Rheumatic Diseases*, 72(8): 1315-1320.
- Hunter, C. J., Imler, S. M., Malaviya, P., Nerem, R. M., & Levenston, M. E. (2002). Mechanical compression alters gene expression and extracellular matrix synthesis by chondrocytes cultured in collagen I gels. *Biomaterials*, 23(4): 1249-1259.
- Hunziker, E. B. (2002). Articular cartilage repair: basic science and clinical progress. A review of the current status and prospects. *Osteoarthritis Cartilage*, 10(6): 432-463.
- Hunziker, E. B. (2009). The elusive path to cartilage regeneration. *Advanced Materials*, 21(32-33): 3419-3424.
- Husted, H., & Toftgaard Jensen, T. (2002). Clinical outcome after treatment of infected primary total knee arthroplasty. *Acta Orthop Belg*, 68(5): 500-507.
- Ikenoue, T., Trindade, M. C. D., Lee, M. S., Lin, E. Y., Schurman, D. J., Goodman, S. B., & Smith, R. L. (2003). Mechanoregulation of human articular chondrocyte aggrecan and type II collagen expression by intermittent hydrostatic pressure in vitro. *Journal of Orthopaedic Research*, 21(1): 110-116.
- Imazato, S., Russell, R. R. B., & McCabe, J. F. (1995). Antibacterial activity of MDPB polymer incorporated in dental resin. *Journal of Dentistry*, 23(3): 177-181.
- Insall, J. N. (2001). *Surgery of the Knee*: Churchill Livingstone.
- Instructional Course Lectures, The American Academy of Orthopaedic Surgeons - Articular Cartilage. Part I: Tissue Design and Chondrocyte-Matrix Interactions**†. (1997). (Vol. 79).
- Ivan, D., Choudhury, N. R., Dutta, N. K., & Kumar, S. (2009). Synthesis and characterization of novel citric acid-based polyester elastomers. *Polymer*, 50(7): 1682-1691.
- Jakob, R. P., Franz, T., Gautier, E., & Mainil-Varlet, P. (2002). Autologous osteochondral grafting in the knee: indication, results, and reflections. *Clinical orthopaedics and related research*, 401: 170-184.
- Janz, V., Wassilew, G. I., Kribus, M., Trampuz, A., & Perka, C. (2015). Improved identification of polymicrobial infection in total knee arthroplasty through

- sonicate fluid cultures. *Archives of Orthopaedic and Trauma Surgery*, 135(10): 1453-1457.
- Jeon, J. E., Schrobback, K., Hutmacher, D. W., & Klein, T. J. (2012). Dynamic compression improves biosynthesis of human zonal chondrocytes from osteoarthritis patients. *Osteoarthritis and Cartilage*, 20(8): 906-915.
- Jeong, C. G., & Hollister, S. J. (2010). A comparison of the influence of material on in vitro cartilage tissue engineering with PCL, PGS, and POC 3D scaffold architecture seeded with chondrocytes. *Biomaterials*, 31(15): 4304-4312.
- Jeong, C. G., Zhang, H., & Hollister, S. J. (2011). Three-dimensional poly (1, 8-octanediol-co-citrate) scaffold pore shape and permeability effects on subcutaneous in vivo chondrogenesis using primary chondrocytes. *Acta biomaterialia*, 7(2): 505-514.
- Jeuken, R., Roth, A., Peters, R., van Donkelaar, C., Thies, J., van Rhijn, L., & Emans, P. (2016). Polymers in cartilage defect repair of the knee.
- Ji, Y., Wang, X., & Liang, K. (2014). Regulating the mechanical properties of poly(1,8-octanediol citrate) bioelastomer via loading of chitin nanocrystals. *RSC Advances*, 4(78): 41357-41363.
- Jiang, B., Akgun, B., Lam, R. C., Ameer, G. A., & Wertheim, J. A. (2015). A polymer-extracellular matrix composite with improved thromboresistance and recellularization properties. *Acta Biomaterialia*, 18: 50-58.
- Jin, T., Sun, D., Su, J. Y., Zhang, H., & Sue, H. J. (2009). Antimicrobial efficacy of zinc oxide quantum dots against *Listeria monocytogenes*, *Salmonella Enteritidis*, and *Escherichia coli* O157:H7. *J Food Sci*, 74(1): M46-52.
- Johnstone, B., Alini, M., Cucchiarini, M., Dodge, G. R., Eglin, D., Guilak, F., Madry, H., Mata, A., Mauck, R. L., & Semino, C. E. (2013). Tissue engineering for articular cartilage repair--the state of the art. *Eur Cell Mater*, 25(248): e67.
- Jukes, J. M., Both, S. K., Leusink, A., Lotus, M. T., Van Blitterswijk, C. A., & De Boer, J. (2008). Endochondral bone tissue engineering using embryonic stem cells. *Proceedings of the National Academy of Sciences*, 105(19): 6840-6845.
- Jung, C. (2014). Articular Cartilage: Histology and Physiology. In A. A. Shetty, S.-J. Kim, N. Nakamura & M. Brittberg (Eds.), *Techniques in Cartilage Repair Surgery* (pp. 17-21): Springer Berlin Heidelberg.
- Kalashnikova, I., Das, S., & Seal, S. (2015). Nanomaterials for wound healing: scope and advancement. *Nanomedicine*, 10(16): 2593-2612.

- Kamoun, E. A., Chen, X., Mohy Eldin, M. S., & Kenawy, E.-R. S. Crosslinked poly(vinyl alcohol) hydrogels for wound dressing applications: A review of remarkably blended polymers. *Arabian Journal of Chemistry*(0).
- Kang, Y., Yang, J., Khan, S., Anissian, L., & Ameer, G. A. (2006). A new biodegradable polyester elastomer for cartilage tissue engineering. *Journal of Biomedical Materials Research Part A*, 77(2): 331-339.
- Karageorgiou, V., & Kaplan, D. (2005). Porosity of 3D biomaterial scaffolds and osteogenesis. *Biomaterials*, 26(27): 5474-5491.
- Kemppainen, J. M., & Hollister, S. J. (2010). Tailoring the mechanical properties of 3D-designed poly(glycerol sebacate) scaffolds for cartilage applications. *Journal of Biomedical Materials Research - Part A*, 94(1): 9-18.
- Khalil, M. I., Al-Qunaibit, M. M., Al-zahem, A. M., & Labis, J. P. Synthesis and characterization of ZnO nanoparticles by thermal decomposition of a curcumin zinc complex. *Arabian Journal of Chemistry*(0).
- Kirsch, T., Harrison, G., Worch, K. P., & Golub, E. E. (2000). Regulatory Roles of Zinc in Matrix Vesicle-Mediated Mineralization of Growth Plate Cartilage. *Journal of Bone and Mineral Research*, 15(2): 261-270.
- Kisiday, J. D., Jin, M., DiMicco, M. A., Kurz, B., & Grodzinsky, A. J. (2004). Effects of dynamic compressive loading on chondrocyte biosynthesis in self-assembling peptide scaffolds. *Journal of Biomechanics*, 37(5): 595-604.
- Kobayashi, M., Squires, G. R., Mousa, A., Tanzer, M., Zukor, D. J., Antoniou, J., Feige, U., & Poole, A. R. (2005). Role of interleukin-1 and tumor necrosis factor alpha in matrix degradation of human osteoarthritic cartilage. *Arthritis Rheum*, 52(1): 128-135.
- Kock, L., van Donkelaar, C. C., & Ito, K. (2012). Tissue engineering of functional articular cartilage: the current status. *Cell and Tissue Research*, 347(3): 613-627.
- Kołodziejczak-Radzimska, A., & Jesionowski, T. (2014). Zinc oxide—from synthesis to application: a review. *Materials*, 7(4): 2833-2881.
- Kompany, K., Mirza, E. H., Hosseini, S., Pinguan-Murphy, B., & Djordjevic, I. (2014). Polyoctanediol citrate–ZnO composite films: Preparation, characterization and release kinetics of nanoparticles from polymer matrix. *Materials Letters*, 126: 165-168.
- Koyano, Y., Hejna, M., Flechtenmacher, J., Schmid, T. M., Thonar, E. J. M. A., & Mollenhauer, J. (1996). Collagen and Proteoglycan Production by Bovine Fetal and Adult Chondrocytes Under Low Levels of Calcium and Zinc Ions. *Connective Tissue Research*, 34(3): 213-225.

- Kreuz, P., Steinwachs, M., Erggelet, C., Krause, S., Konrad, G., Uhl, M., & Südkamp, N. (2006). Results after microfracture of full-thickness chondral defects in different compartments in the knee. *Osteoarthritis and Cartilage*, 14(11): 1119-1125.
- Kudi, A. C., Umoh, J. U., Eduvie, L. O., & Gefu, J. (1999). Screening of some Nigerian medicinal plants for antibacterial activity. *Journal of Ethnopharmacology*, 67(2): 225-228.
- Kuijjer, R., Jansen, E. J. P., Emans, P. J., Bulstra, S. K., Riesle, J., Pieper, J., Grainger, D. W., & Busscher, H. J. (2007). Assessing infection risk in implanted tissue-engineered devices. *Biomaterials*, 28(34): 5148-5154.
- Kumar, A., Pandey, A. K., Singh, S. S., Shanker, R., & Dhawan, A. (2011). Engineered ZnO and TiO₂ nanoparticles induce oxidative stress and DNA damage leading to reduced viability of *Escherichia coli*. *Free Radical Biology and Medicine*, 51(10): 1872-1881.
- Laachachi, A., Leroy, E., Cochez, M., Ferriol, M., & Cuesta, J. L. (2005). Use of oxide nanoparticles and organoclays to improve thermal stability and fire retardancy of poly (methyl methacrylate). *Polymer Degradation and Stability*, 89(2): 344-352.
- Lam, D., Wong, K. L., Law, P., & Hui, J. H. (2014). Injectable Autologous Bone-Marrow-Derived Mesenchymal Stem Cells for Cartilage Repair: The Singapore Technique *Techniques in Cartilage Repair Surgery* (pp. 205-214): Springer.
- Lang, C., Murgia, C., Leong, M., Tan, L.-W., Perozzi, G., Knight, D., Ruffin, R., & Zalewski, P. (2007). Anti-inflammatory effects of zinc and alterations in zinc transporter mRNA in mouse models of allergic inflammation. *American Journal of Physiology-Lung Cellular and Molecular Physiology*, 292(2): L577-L584.
- Laprell, H., & Petersen, W. (2001). Autologous osteochondral transplantation using the diamond bone-cutting system (DBCS): 6–12 years' follow-up of 35 patients with osteochondral defects at the knee joint. *Archives of Orthopaedic and Trauma Surgery*, 121(5): 248-253.
- Larson, E. M., Doughman, D. J., Gregerson, D. S., & Obritsch, W. F. (1997). A new, simple, nonradioactive, nontoxic in vitro assay to monitor corneal endothelial cell viability. *Invest Ophthalmol Vis Sci*, 38(10): 1929-1933.
- Lawrence, R. C., Felson, D. T., Helmick, C. G., Arnold, L. M., Choi, H., Deyo, R. A., Gabriel, S., Hirsch, R., Hochberg, M. C., Hunder, G. G., Jordan, J. M., Katz, J. N., Kremers, H. M., Wolfe, F., & National Arthritis Data, W. (2008). Estimates of the prevalence of arthritis and other rheumatic conditions in the United States: Part II. *Arthritis & Rheumatism*, 58(1): 26-35.
- Lee, C., Grad, S., Wimmer, M., & Alini, M. (2005). The influence of mechanical stimuli on articular cartilage tissue engineering. *Topics in tissue engineering*, 2: 1-32.

- Lee, D. A., & Bader, D. L. (1997). Compressive strains at physiological frequencies influence the metabolism of chondrocytes seeded in agarose. *Journal of Orthopaedic Research*, 15(2): 181-188.
- Levine, J. P., Bradley, J., Turk, A. E., Ricci, J. L., Benedict, J. J., Steiner, G., Longaker, M. T., & McCarthy, J. G. (1997). Bone morphogenetic protein promotes vascularization and osteoinduction in preformed hydroxyapatite in the rabbit. *Ann Plast Surg*, 39(2): 158-168.
- Li, B., Ma, Y., Wang, S., & Moran, P. M. (2005). Influence of carboxyl group density on neuron cell attachment and differentiation behavior: gradient-guided neurite outgrowth. *Biomaterials*, 26(24): 4956-4963.
- Li, W.-J., Tuli, R., Okafor, C., Derfoul, A., Danielson, K. G., Hall, D. J., & Tuan, R. S. (2005). A three-dimensional nanofibrous scaffold for cartilage tissue engineering using human mesenchymal stem cells. *Biomaterials*, 26(6): 599-609.
- Li, Y., Frank, E. H., Wang, Y., Chubinskaya, S., Huang, H. H., & Grodzinsky, A. J. (2013). Moderate dynamic compression inhibits pro-catabolic response of cartilage to mechanical injury, tumor necrosis factor- α and interleukin-6, but accentuates degradation above a strain threshold. *Osteoarthritis and Cartilage*, 21(12): 1933-1941.
- Lichstein, P., Su, S., Hedlund, H., Suh, G., Maloney, W. J., Goodman, S. B., & Huddleston III, J. I. (2015). Treatment of Periprosthetic Knee Infection With a Two-stage Protocol Using Static Spacers. *Clinical Orthopaedics and Related Research*: 1-6.
- Lichte, P., Pape, H. C., Pufe, T., Kobbe, P., & Fischer, H. (2011). Scaffolds for bone healing: Concepts, materials and evidence. *Injury*, 42(6): 569-573.
- Liedtke, J., & Vahjen, W. (2012). In vitro antibacterial activity of zinc oxide on a broad range of reference strains of intestinal origin. *Veterinary Microbiology*, 160(1-2): 251-255.
- Liu, L., Ercan, B., Sun, L., Ziemer, K. S., & Webster, T. J. (2015). Understanding the Role of Polymer Surface Nanoscale Topography on Inhibiting Bacteria Adhesion and Growth. *ACS Biomaterials Science & Engineering*.
- Liu, X., & Ma, P. (2004). Polymeric Scaffolds for Bone Tissue Engineering. *Annals of Biomedical Engineering*, 32(3): 477-486.
- Liu, Y., He, L., Mustapha, A., Li, H., Hu, Z., & Lin, M. (2009). Antibacterial activities of zinc oxide nanoparticles against Escherichia coli O157: H7. *Journal of applied microbiology*, 107(4): 1193-1201.
- Luo, L., Thorpe, S. D., Buckley, C. T., & Kelly, D. J. (2015). The effects of dynamic compression on the development of cartilage grafts engineered using bone

marrow and infrapatellar fat pad derived stem cells. *Biomedical Materials*, 10(5): 055011.

Luo, Y.-B., Li, W.-D., Wang, X.-L., Xu, D.-Y., & Wang, Y.-Z. (2009). Preparation and properties of nanocomposites based on poly(lactic acid) and functionalized TiO₂. *Acta Materialia*, 57(11): 3182-3191.

MacDonald, R. S. (2000). The Role of Zinc in Growth and Cell Proliferation. *The Journal of Nutrition*, 130(5): 1500S-1508S.

Mackie, E. J., Thesleff, I., & Chiquet-Ehrismann, R. (1987). Tenascin is associated with chondrogenic and osteogenic differentiation in vivo and promotes chondrogenesis in vitro. *The Journal of cell biology*, 105(6): 2569-2579.

Madeira, C., Santhagunam, A., Salgueiro, J. B., & Cabral, J. M. (2015). Advanced cell therapies for articular cartilage regeneration. *Trends in Biotechnology*, 33(1): 35-42.

Madej, W., van Caam, A., Blaney Davidson, E. N., van der Kraan, P. M., & Buma, P. (2014). Physiological and excessive mechanical compression of articular cartilage activates Smad2/3P signaling. *Osteoarthritis and Cartilage*, 22(7): 1018-1025.

Malda, J., Martens, D. E., Tramper, J., van Blitterswijk, C. A., & Riesle, J. (2003). Cartilage tissue engineering: controversy in the effect of oxygen. *Crit Rev Biotechnol*, 23(3): 175-194.

Malda, J., van Blitterswijk, C. A., van Geffen, M., Martens, D. E., Tramper, J., & Riesle, J. (2004). Low oxygen tension stimulates the redifferentiation of dedifferentiated adult human nasal chondrocytes. *Osteoarthritis Cartilage*, 12(4): 306-313.

Marcacci, M., Filardo, G., & Kon, E. (2013). Treatment of cartilage lesions: What works and why? *Injury*, 44: S11-S15.

Marlovits, S., Zeller, P., Singer, P., Resinger, C., & Vecsei, V. (2006). Cartilage repair: generations of autologous chondrocyte transplantation. *Eur J Radiol*, 57(1): 24-31.

Mathur, D., Pereira, W. C., & Anand, A. (2012). Emergence of chondrogenic progenitor stem cells in transplantation biology—prospects and drawbacks. *Journal of Cellular Biochemistry*, 113(2): 397-403.

McMahon, L., O'Brien, F., & Prendergast, P. (2008). Biomechanics and mechanobiology in osteochondral tissues.

Meinig, R. P., Buesing, C. M., Helm, J., & Gogolewski, S. (1997). Regeneration of diaphyseal bone defects using resorbable poly(L/DL-lactide) and poly(D-lactide) membranes in the Yucatan pig model. *J Orthop Trauma*, 11(8): 551-558.

- Memarzadeh, K., Sharili, A. S., Huang, J., Rawlinson, S. C. F., & Allaker, R. P. (2014). Nanoparticulate zinc oxide as a coating material for orthopedic and dental implants. *Journal of Biomedical Materials Research Part A*: n/a-n/a.
- Meng, Z. X., Zheng, W., Ding, M. H., Zhou, H. M., Chen, X. Q., Chen, J. C., Liu, M. K., & Zheng, Y. F. (2011). Fabrication and characterization of elastomeric polyester/carbon nanotubes nanocomposites for biomedical application. *J Nanosci Nanotechnol*, *11*(4): 3126-3133.
- Meretoja, V. V., Dahlin, R. L., Wright, S., Kasper, F. K., & Mikos, A. G. (2013). The effect of hypoxia on the chondrogenic differentiation of co-cultured articular chondrocytes and mesenchymal stem cells in scaffolds. *Biomaterials*, *34*(17): 4266-4273.
- Messner, K., & Gillquist, J. (1996). Cartilage repair: a critical review. *Acta Orthopaedica*, *67*(5): 523-529.
- Meyer, E. G., Buckley, C. T., Thorpe, S. D., & Kelly, D. J. (2010). Low oxygen tension is a more potent promoter of chondrogenic differentiation than dynamic compression. *J Biomech*, *43*(13): 2516-2523.
- Mierzecki, A., Strecker, D., & Radomska, K. (2011). A pilot study on zinc levels in patients with rheumatoid arthritis. *Biol Trace Elem Res*, *143*(2): 854-862.
- Milanino, R., Frigo, A., Bambara, L. M., Marrella, M., Moretti, U., Pasqualicchio, M., Biasi, D., Gasperini, R., Mainenti, L., & Velo, G. P. (1993). Copper and zinc status in rheumatoid arthritis: studies of plasma, erythrocytes, and urine, and their relationship to disease activity markers and pharmacological treatment. *Clin Exp Rheumatol*, *11*(3): 271-281.
- Millward-Sadler, S. J., Wright, M. O., Davies, L. W., Nuki, G., & Salter, D. M. (2000). Mechanotransduction via integrins and interleukin-4 results in altered aggrecan and matrix metalloproteinase 3 gene expression in normal, but not osteoarthritic, human articular chondrocytes. *Arthritis & Rheumatism*, *43*(9): 2091-2099.
- Minas, T. (1999). The role of cartilage repair techniques, including chondrocyte transplantation, in focal chondral knee damage. *Instructional course lectures*, *48*: 629-643.
- Minas, T., & Nehrer, S. (1997). Current concepts in the treatment of articular cartilage defects. *Orthopedics*, *20*(6): 525-538.
- Mirza, E. H., Pan-Pan, C., Wan Ibrahim, W. M. A. B., Djordjevic, I., & Pinguan-Murphy, B. (2015). Chondroprotective effect of zinc oxide nanoparticles in conjunction with hypoxia on bovine cartilage-matrix synthesis. *Journal of Biomedical Materials Research Part A*, *103*(11): 3554 - 3563.

- Mirza, E. H., Wan Ibrahim, W. M. A. B., Pinguan-Murphy, B., & Djordjevic, I. (2015). Polyoctanediol Citrate-Zinc Oxide Nano-Composite Multifunctional Tissue Engineering Scaffolds with Anti-Bacterial Properties. *Digest Journal of Nanomaterials and Biostructures*, 10(2): 415-428.
- Mithoefer, K., McAdams, T., Williams, R. J., Kreuz, P. C., & Mandelbaum, B. R. (2009). Clinical efficacy of the microfracture technique for articular cartilage repair in the knee an evidence-based systematic analysis. *The American journal of sports medicine*, 37(10): 2053-2063.
- Moezzi, A., McDonagh, A. M., & Cortie, M. B. (2012). Zinc oxide particles: Synthesis, properties and applications. *Chemical Engineering Journal*, 185–186(0): 1-22.
- Moorer, W. R., & Genet, J. M. (1982). Antibacterial activity of gutta-percha cones attributed to the zinc oxide component. *Oral Surg Oral Med Oral Pathol*, 53(5): 508-517.
- Moradi, A., Dalilottojari, A., Pinguan-Murphy, B., & Djordjevic, I. Fabrication and characterization of elastomeric scaffolds comprised of a citric acid-based polyester / hydroxyapatite microcomposite. *Materials & Design*, 50(0): 446-450.
- Morel, V., Merçay, A., & Quinn, T. M. (2005). Prestrain decreases cartilage susceptibility to injury by ramp compression in vitro. *Osteoarthritis and Cartilage*, 13(11): 964-970.
- Morrier, J. J., Suchett-Kaye, G., Nguyen, D., Rocca, J. P., Blanc-Benon, J., & Barsotti, O. (1998). Antimicrobial activity of amalgams, alloys and their elements and phases. *Dental Materials*, 14(2): 150-157.
- Moutos, F. T., Freed, L. E., & Guilak, F. (2007). A biomimetic three-dimensional woven composite scaffold for functional tissue engineering of cartilage. *Nature materials*, 6(2): 162-167.
- Mueller, M. B., & Tuan, R. S. (2008). Functional characterization of hypertrophy in chondrogenesis of human mesenchymal stem cells. *Arthritis & Rheumatism*, 58(5): 1377-1388.
- Munir, S., Foldager, C., Lind, M., Zachar, V., Søballe, K., & Koch, T. (2014). Hypoxia enhances chondrogenic differentiation of human adipose tissue-derived stromal cells in scaffold-free and scaffold systems. *Cell and Tissue Research*, 355(1): 89-102.
- Murphy, C. L., & Polak, J. M. (2004). Control of human articular chondrocyte differentiation by reduced oxygen tension. *J Cell Physiol*, 199(3): 451-459.
- Murphy, C. L., & Sambanis, A. (2001). Effect of oxygen tension and alginate encapsulation on restoration of the differentiated phenotype of passaged chondrocytes. *Tissue Eng*, 7(6): 791-803.

- Murphy, L., & Helmick, C. G. (2012). The impact of osteoarthritis in the United States: a population-health perspective. *AJN The American Journal of Nursing*, 112(3): S13-S19.
- Murray, I. R., Benke, M. T., & Mandelbaum, B. R. (2015). Management of knee articular cartilage injuries in athletes: chondroprotection, chondrofacilitation, and resurfacing. *Knee Surgery, Sports Traumatology, Arthroscopy*: 1-10.
- Na, K., Kim, S., Sun, B., Woo, D., Chung, H.-M., & Park, K.-H. (2007). Blended construct consisting of thermo-reversible hydrogels and heparinized nanoparticles for increasing the proliferation activity of the rabbit chondrocyte in vivo test. *Biotechnology Letters*, 29(10): 1447-1452.
- Network, N. Y. O. D. (2012). from <http://www.donatelifeny.org/about-donation/data/#Data> US1
- Ng, L. J., Tam, P. P., & Cheah, K. S. (1993). Preferential expression of alternatively spliced mRNAs encoding type II procollagen with a cysteine-rich amino-peptide in differentiating cartilage and nonchondrogenic tissues during early mouse development. *Developmental biology*, 159(2): 403-417.
- Nicoll, S. B., Wedrychowska, A., Smith, N. R., & Bhatnagar, R. S. (2001). Modulation of proteoglycan and collagen profiles in human dermal fibroblasts by high density micromass culture and treatment with lactic acid suggests change to a chondrogenic phenotype. *Connect Tissue Res*, 42(1): 59-69.
- Nielsen, T. H., Arenholt-Bindslev, D., Kilian, M., & Philipsen, H. P. (1993). Chelate root filling cements: biological properties. *J Endod*, 19(1): 17-21.
- Niemeyer, P., Pestka, J. M., Kreuz, P. C., Erggelet, C., Schmal, H., Suedkamp, N. P., & Steinwachs, M. (2008). Characteristic Complications After Autologous Chondrocyte Implantation for Cartilage Defects of the Knee Joint. *The American journal of sports medicine*, 36(11): 2091-2099.
- Nyman, J. S., Leng, H., Neil Dong, X., & Wang, X. (2009). Differences in the mechanical behavior of cortical bone between compression and tension when subjected to progressive loading. *Journal of the Mechanical Behavior of Biomedical Materials*, 2(6): 613-619.
- O'Driscoll, S. W. (1998). The healing and regeneration of articular cartilage. *J Bone Joint Surg Am*, 80(12): 1795-1812.
- Oberlender, S. A., & Tuan, R. S. (1994). Expression and functional involvement of N-cadherin in embryonic limb chondrogenesis. *Development*, 120(1): 177-187.
- Odell, E., & Pertl, C. (1995). Zinc as a growth factor for *Aspergillus* sp. and the antifungal effects of root canal sealants. *Oral Surg Oral Med Oral Pathol Oral Radiol Endod*, 79(1): 82-87.

- Outerbridge, H., Outerbridge, A., & Outerbridge, R. (1995). The use of a lateral patellar autologous graft for the repair of a large osteochondral defect in the knee. *The Journal of Bone & Joint Surgery*, 77(1): 65-72.
- Paladini, F., Pollini, M., Talà, A., Alifano, P., & Sannino, A. (2012). Efficacy of silver treated catheters for haemodialysis in preventing bacterial adhesion. *Journal of Materials Science: Materials in Medicine*, 23(8): 1983-1990.
- Palukuru, U. P., McGoverin, C. M., & Pleshko, N. (2014). Assessment of hyaline cartilage matrix composition using near infrared spectroscopy. *Matrix Biology*, 38(0): 3-11.
- Panadero, J. A., Lanceros-Mendez, S., & Ribelles, J. L. G. (2016). Differentiation of mesenchymal stem cells for cartilage tissue engineering: Individual and synergetic effects of three-dimensional environment and mechanical loading. *Acta Biomaterialia*, 33: 1 - 12.
- Park, H., & Lee, K. Y. (2014). Cartilage regeneration using biodegradable oxidized alginate/hyaluronate hydrogels. *Journal of Biomedical Materials Research Part A*, 102(12): 4519-4525.
- Parker, E., Vessillier, S., Pingguan-Murphy, B., Abas, W., Bader, D. L., & Chowdhury, T. T. (2013). Low oxygen tension increased fibronectin fragment induced catabolic activities--response prevented with biomechanical signals. *Arthritis Res Ther*, 15(5): R163.
- Pascon, E. A., & Spangberg, L. S. (1990). In vitro cytotoxicity of root canal filling materials: 1. Gutta-percha. *J Endod*, 16(9): 429-433.
- Pavithra, D., & Doble, M. (2008). Biofilm formation, bacterial adhesion and host response on polymeric implants—issues and prevention. *BIOMEDICAL MATERIALS*, 3.
- Pawlowski, K. S., Wawro, D., & Roland, P. S. (2005). Bacterial biofilm formation on a human cochlear implant. *Otol Neurotol*, 26(5): 972-975.
- Pelttari, K., Steck, E., & Richter, W. (2008). The use of mesenchymal stem cells for chondrogenesis. *Injury*, 39(1, Supplement): 58-65.
- Peretti, G. M., Randolph, M. A., Villa, M. T., Buragas, M. S., & Yaremchuk, M. J. (2000). Cell-based tissue-engineered allogeneic implant for cartilage repair. *Tissue Eng*, 6(5): 567-576.
- Peter, S. J., Miller, M. J., Yasko, A. W., Yaszemski, M. J., & Mikos, A. G. (1998). Polymer concepts in tissue engineering. *J Biomed Mater Res*, 43(4): 422-427.

- Peterson, L., Minas, T., Brittberg, M., Nilsson, A., Sjögren-Jansson, E., & Lindahl, A. (2000). Two-to 9-year outcome after autologous chondrocyte transplantation of the knee. *Clinical orthopaedics and related research*, 374: 212-234.
- Pi, Y., Zhang, X., Shao, Z., Zhao, F., Hu, X., & Ao, Y. (2015). Intra-articular delivery of anti-Hif-2 α siRNA by chondrocyte-homing nanoparticles to prevent cartilage degeneration in arthritic mice. *Gene therapy*.
- Pingguan-Murphy, B., & Nawi, I. (2012). Upregulation of matrix synthesis in chondrocyte-seeded agarose following sustained bi-axial cyclic loading. *Clinics*, 67(8): 939-944.
- Piscoya, J. L., Fermor, B., Kraus, V. B., Stabler, T. V., & Guilak, F. (2005). The influence of mechanical compression on the induction of osteoarthritis-related biomarkers in articular cartilage explants. *Osteoarthritis and Cartilage*, 13(12): 1092-1099.
- Poole, C. A. (1997). Review. Articular cartilage chondrons: form, function and failure. *Journal of anatomy*, 191(01): 1-13.
- Pooyan, P., Brewster, L., Tannenbaum, R., & Garmestani, H. (2015). Design and Integration of a Nanohybrid Functional Biomaterial with Enhanced Mechanical and Thermal Properties *Integrated Systems: Innovations and Applications* (pp. 55-67): Springer.
- Portocarrero, G., Collins, G., & Livingston Arinze, T. (2013). Challenges in cartilage tissue engineering. *J Tissue Sci Eng*, 4(1): e120.
- Portron, S., Hivernaud, V., Merceron, C., Lesoeur, J., Masson, M., Gauthier, O., Vinatier, C., Beck, L., & Guicheux, J. (2015). Inverse Regulation of Early and Late Chondrogenic Differentiation by Oxygen Tension Provides Cues for Stem Cell-Based Cartilage Tissue Engineering. *Cellular Physiology and Biochemistry*, 35(3): 841-857.
- Prasad, A. S. (2008). Clinical, immunological, anti-inflammatory and antioxidant roles of zinc. *Experimental Gerontology*, 43(5): 370-377.
- Prasad, A. S. (2014). Zinc is an antioxidant and anti-inflammatory agent: Its role in human health. *Frontiers in Nutrition*, 1.
- Prasad, A. S., Beck, F. W. J., Bao, B., Fitzgerald, J. T., Snell, D. C., Steinberg, J. D., & Cardozo, L. J. (2007). Zinc supplementation decreases incidence of infections in the elderly: Effect of zinc on generation of cytokines and oxidative stress. *American Journal of Clinical Nutrition*, 85(3): 837-844.
- Prasad, A. S., Halsted, J. A., & Nadimi, M. (1961). Syndrome of iron deficiency anemia, hepatosplenomegaly, hypogonadism, dwarfism and geophagia. *The American Journal of Medicine*, 31(4): 532-546.

- Pujol, J. P., & Loyau, G. (1987). Interleukin-1 and osteoarthritis. *Life Sci*, 41(10): 1187-1198.
- Qiu, H., Yang, J., Kodali, P., Koh, J., & Ameer, G. A. (2006). A citric acid-based hydroxyapatite composite for orthopedic implants. *Biomaterials*, 27(34): 5845-5854.
- Raffi, M., Hussain, F., Bhatti, T., Akhter, J., Hameed, A., & Hasan, M. (2008). Antibacterial characterization of silver nanoparticles against E. coli ATCC-15224. *Journal of Materials Science and Technology*, 24(2): 192-196.
- Reddy, K. M., Feris, K., Bell, J., Wingett, D. G., Hanley, C., & Punnoose, A. (2007). Selective toxicity of zinc oxide nanoparticles to prokaryotic and eukaryotic systems. *Applied physics letters*, 90(21): 213902.
- Redman, S., Oldfield, S., & Archer, C. (2005). Current strategies for articular cartilage repair. *Eur Cell Mater*, 9(23-32): 23-32.
- Regina, V. R., Søhoel, H., Lokanathan, A. R., Bischoff, C., Kingshott, P., Revsbech, N. P., & Meyer, R. L. (2012). Entrapment of Subtilisin in Ceramic Sol–Gel Coating for Antifouling Applications. *ACS Applied Materials & Interfaces*, 4(11): 5915-5921.
- Ren, K., He, C., Xiao, C., Li, G., & Chen, X. (2015). Injectable glycopolyptide hydrogels as biomimetic scaffolds for cartilage tissue engineering. *Biomaterials*, 51: 238-249.
- Rink, L., & Haase, H. (2007). Zinc homeostasis and immunity. *Trends in Immunology*, 28(1): 1-4.
- Robins, J. C., Akeno, N., Mukherjee, A., Dalal, R. R., Aronow, B. J., Koopman, P., & Clemens, T. L. (2005). Hypoxia induces chondrocyte-specific gene expression in mesenchymal cells in association with transcriptional activation of Sox9. *Bone*, 37(3): 313-322.
- Romanos, G. E., Delgado-Ruiz, R. A., Gómez-Moreno, G., López-López, P. J., Mate Sanchez de Val, J. E., & Calvo-Guirado, J. L. (2015). Role of mechanical compression on bone regeneration around a particulate bone graft material: an experimental study in rabbit calvaria. *Clinical oral implants research*.
- Rosenberg, K., Olsson, H., Mörgelin, M., & Heinegård, D. (1998). Cartilage Oligomeric Matrix Protein Shows High Affinity Zinc-dependent Interaction with Triple Helical Collagen. *Journal of Biological Chemistry*, 273(32): 20397-20403.
- Rosenberg, L., Choi, H. U., Tang, L. H., Pal, S., Johnson, T., Lyons, D. A., & Laue, T. M. (1991). Proteoglycans of bovine articular cartilage. The effects of divalent cations on the biochemical properties of link protein. *Journal of Biological Chemistry*, 266(11): 7016-7024.

- Ryan, J. A., Eisner, E. A., DuRaine, G., You, Z., & Reddi, A. H. (2009). Mechanical compression of articular cartilage induces chondrocyte proliferation and inhibits proteoglycan synthesis by activation of the ERK pathway: implications for tissue engineering and regenerative medicine. *J Tissue Eng Regen Med*, 3(2): 107-116.
- Saini, S., & Wick, T. M. (2004). Effect of low oxygen tension on tissue-engineered cartilage construct development in the concentric cylinder bioreactor. *Tissue Eng*, 10(5-6): 825-832.
- Salinas, A. J., Shrutti, S., Malavasi, G., Menabue, L., & Vallet-Regí, M. (2011). Substitutions of cerium, gallium and zinc in ordered mesoporous bioactive glasses. *Acta Biomaterialia*, 7(9): 3452-3458.
- Salvati, E. A., Robinson, R. P., Zeno, S. M., Koslin, B. L., Brause, B. D., & Wilson, P. D., Jr. (1982). Infection rates after 3175 total hip and total knee replacements performed with and without a horizontal unidirectional filtered air-flow system. *J Bone Joint Surg Am*, 64(4): 525-535.
- Sanchez-Adams, J., Leddy, H., McNulty, A., O'Connor, C., & Guilak, F. (2014). The Mechanobiology of Articular Cartilage: Bearing the Burden of Osteoarthritis. *Current Rheumatology Reports*, 16(10): 1-9.
- Sauer, G. R., Smith, D. M., Cahalane, M., Wu, L. N. Y., & Wuthier, R. E. (2003). Intracellular zinc fluxes associated with apoptosis in growth plate chondrocytes. *Journal of Cellular Biochemistry*, 88(5): 954-969.
- Schätti, O., Gallo, L., & Torzilli, P. (2015). Mechanobiological response of articular cartilage subjected to simultaneous compression and sliding. *Osteoarthritis and Cartilage*, 23: A270-A271.
- Schipani, E., Ryan, H. E., Didrickson, S., Kobayashi, T., Knight, M., & Johnson, R. S. (2001). Hypoxia in cartilage: HIF-1 α is essential for chondrocyte growth arrest and survival. *Genes & development*, 15(21): 2865-2876.
- Schulze-Tanzil, G. (2015). Polymer-Assisted Cartilage and Tendon Repair. In H. Zreiqat, C. R. Dunstan & V. Rosen (Eds.), *A Tissue Regeneration Approach to Bone and Cartilage Repair* (pp. 229-254): Springer International Publishing.
- Schulze-Tanzil, G., Mobasheri, A., de Souza, P., John, T., & Shakibaei, M. (2004). Loss of chondrogenic potential in dedifferentiated chondrocytes correlates with deficient Shc–Erk interaction and apoptosis. *Osteoarthritis and cartilage*, 12(6): 448-458.
- Seifarth, C., Csaki, C., & Shakibaei, M. (2009). Anabolic actions of IGF-I and TGF- β 1 on Interleukin-1 β -treated human articular chondrocytes: Evaluation in two and three dimensional cultures. *Histol Histopathol*, 24: 1245-1262.

- Seo, H.-J., Cho, Y.-E., Kim, T., Shin, H.-I., & Kwun, I.-S. (2010). Zinc may increase bone formation through stimulating cell proliferation, alkaline phosphatase activity and collagen synthesis in osteoblastic MC3T3-E1 cells. *Nutrition research and practice*, 4(5): 356-361.
- Serrano, M. C., Chung, E. J., & Ameer, G. A. (2010). Advances and Applications of Biodegradable Elastomers in Regenerative Medicine. *Advanced Functional Materials*, 20(2): 192-208.
- Serrano, M. C., Vavra, A. K., Jen, M., Hogg, M. E., Murar, J., Martinez, J., Keefer, L. K., Ameer, G. A., & Kibbe, M. R. (2011). Poly(diol-co-citrate)s as Novel Elastomeric Perivascular Wraps for the Reduction of Neointimal Hyperplasia. *Macromolecular Bioscience*, 11(5): 700-709.
- Sharma, A. K., Hota, P. V., Matoka, D. J., Fuller, N. J., Jandali, D., Thaker, H., Ameer, G. A., & Cheng, E. Y. (2010). Urinary bladder smooth muscle regeneration utilizing bone marrow derived mesenchymal stem cell seeded elastomeric poly (1, 8-octanediol-co-citrate) based thin films. *Biomaterials*, 31(24): 6207-6217.
- Shi, R., Zhang, Z., Liu, Q., Han, Y., Zhang, L., Chen, D., & Tian, W. (2007). Characterization of citric acid/glycerol co-plasticized thermoplastic starch prepared by melt blending. *Carbohydr Polym*, 69(4): 748-755.
- Shi, S., Jiang, W., Zhao, T., Aifantis, K. E., Wang, H., Lin, L., Fan, Y., Feng, Q., Cui, F. z., & Li, X. (2015). The application of nanomaterials in controlled drug delivery for bone regeneration. *Journal of Biomedical Materials Research Part A*, 103(12): 3978-3992.
- Shi, Y., Xiong, D., Peng, Y., & Wang, N. (2016). Effects of polymerization degree on recovery behavior of PVA/PVP hydrogels as potential articular cartilage prosthesis after fatigue test. *Express Polymer Letters*, 10(2).
- Shirazi, H. S., Forooshani, P. K., Pingguan-Murphy, B., & Djordjevic, I. (2014). Processing and characterization of elastomeric polycaprolactone triol–citrate coatings for biomedical applications. *Progress in Organic Coatings*, 77(4): 821-829.
- Singhal, D., Psaltis, A. J., Foreman, A., & Wormald, P. J. (2010). The impact of biofilms on outcomes after endoscopic sinus surgery. *Am J Rhinol Allergy*, 24(3): 169-174.
- Sirelkhatim, A., Mahmud, S., Seeni, A., Kaus, N. H. M., Ann, L. C., Bakhori, S. K. M., Hasan, H., & Mohamad, D. (2015). Review on zinc oxide nanoparticles: antibacterial activity and toxicity mechanism. *Nano-Micro Letters*, 7(3): 219-242.
- Skoog, S. A., Bayati, M. R., Petrochenko, P. E., Stafslie, S., Daniels, J., Cilz, N., Comstock, D. J., Elam, J. W., & Narayan, R. J. (2012). Antibacterial activity of zinc oxide-coated nanoporous alumina. *Materials Science and Engineering: B*, 177(12): 992-998.

- Spiller, K. L., Maher, S. A., & Lowman, A. M. (2011). Hydrogels for the repair of articular cartilage defects. *Tissue engineering part B: reviews*, 17(4): 281-299.
- Stashak, T. S., Farstvedt, E., & Othic, A. (2004). Update on wound dressings: Indications and best use. *Clinical Techniques in Equine Practice*, 3(2): 148-163.
- Steinert, A., Ghivizzani, S., Rethwilm, A., Tuan, R., Evans, C., & Nöth, U. (2007). Major biological obstacles for persistent cell-based regeneration of articular cartilage. *Arthritis research & therapy*, 9(3): 1-15.
- Stewart, M., Welter, J. F., & Goldberg, V. M. (2004). Effect of hydroxyapatite/tricalcium-phosphate coating on osseointegration of plasma-sprayed titanium alloy implants. *Journal of Biomedical Materials Research Part A*, 69(1): 1-10.
- Sun, D., Chen, Y., Tran, R. T., Xu, S., Xie, D., Jia, C., Wang, Y., Guo, Y., Zhang, Z., Guo, J., Yang, J., Jin, D., & Bai, X. (2014). Citric Acid-based Hydroxyapatite Composite Scaffolds Enhance Calvarial Regeneration. *Scientific Reports*, 4: 6912.
- Sun, T., Higham, M., Layton, C., Haycock, J., Short, R., & MacNeil, S. (2004). Developments in xenobiotic-free culture of human keratinocytes for clinical use. *Wound repair and regeneration*, 12(6): 626-634.
- Sunzel, B., Söderberg, T. A., Johansson, A., Hallmans, G., & Gref, R. (1997). The protective effect of zinc on rosin and resin acid toxicity in human polymorphonuclear leukocytes and human gingival fibroblasts in vitro. *Journal of Biomedical Materials Research*, 37(1): 20-28.
- Taccola, L., Raffa, V., Riggio, C., Vittorio, O., Iorio, M. C., Vanacore, R., Pietrabissa, A., & Cuschieri, A. (2011). Zinc oxide nanoparticles as selective killers of proliferating cells. *Int. J. Nanomed*, 6: 1129-1140.
- Takahashi, Y., Takahashi, S., Shiga, Y., Yoshimi, T., & Miura, T. (2000). Hypoxic induction of prolyl 4-hydroxylase α (I) in cultured cells. *Journal of Biological Chemistry*, 275(19): 14139-14146.
- Takai, Y., Miyoshi, J., Ikeda, W., & Ogita, H. (2008). Nectins and nectin-like molecules: roles in contact inhibition of cell movement and proliferation. *Nature Reviews Molecular Cell Biology*, 9(8): 603-615.
- Tang, E., Cheng, G., & Ma, X. (2006). Preparation of nano-ZnO/PMMA composite particles via grafting of the copolymer onto the surface of zinc oxide nanoparticles. *Powder Technology*, 161(3): 209-214.
- Tang, J., Guo, J., Li, Z., Yang, C., Xie, D., Chen, J., Li, S., Li, S., Kim, G. B., & Bai, X. (2015). A fast degradable citrate-based bone scaffold promotes spinal fusion. *Journal of Materials Chemistry B*, 3(27): 5569-5576.

- Taylor, G. J., Leeming, J. P., & Bannister, G. C. (1993). Effect of antiseptics, ultraviolet light and lavage on airborne bacteria in a model wound. *J Bone Joint Surg Br*, 75(5): 724-730.
- Temenoff, J. S., & Mikos, A. G. (2000). Review: tissue engineering for regeneration of articular cartilage. *Biomaterials*, 21(5): 431-440.
- Thadavirul, N., Pavasant, P., & Supaphol, P. (2014). Improvement of dual-leached polycaprolactone porous scaffolds by incorporating with hydroxyapatite for bone tissue regeneration. *Journal of Biomaterials Science, Polymer Edition*: 1-23.
- Thambyah, A., Goh, J. C., & De, S. D. (2005). Contact stresses in the knee joint in deep flexion. *Med Eng Phys*, 27(4): 329-335.
- Theis, K. A., Murphy, L., Hootman, J. M., Helmick, C. G., & Yelin, E. (2007). Prevalence and correlates of arthritis-attributable work limitation in the US population among persons ages 18–64: 2002 National Health Interview Survey Data. *Arthritis Care & Research*, 57(3): 355-363.
- Thoms, B. L., Dudek, K. A., Lafont, J. E., & Murphy, C. L. (2013). Hypoxia Promotes the Production and Inhibits the Destruction of Human Articular Cartilage. *Arthritis & Rheumatism*, 65(5): 1302-1312.
- Thorpe, S. D., Buckley, C. T., Vinardell, T., O'Brien, F. J., Campbell, V. A., & Kelly, D. J. (2010). The response of bone marrow-derived mesenchymal stem cells to dynamic compression following TGF- β 3 induced chondrogenic differentiation. *Annals of Biomedical Engineering*, 38(9): 2896-2909.
- Toledano, M., Yamauti, M., Osorio, E., & Osorio, R. (2012). Zinc-Inhibited MMP-Mediated Collagen Degradation after Different Dentine Demineralization Procedures. *Caries Research*, 46(3): 201-207.
- Torabinejad, M., Hong, C. U., Ford, T. R. P., & Kettering, J. D. (1995). Antibacterial effects of some root end filling materials. *J Endod*, 21(8): 403-406.
- Trampuz, A., & Zimmerli, W. (2006). Diagnosis and treatment of infections associated with fracture-fixation devices. *Injury*, 37(2, Supplement): S59-S66.
- Tran, P., Biswas, D., & O'Connor, A. (2014). Simple one-step method to produce titanium dioxide–polycaprolactone composite films with increased hydrophilicity, enhanced cellular interaction and improved degradation for skin tissue engineering. *Journal of Materials Science*, 49(18): 6373-6382.
- Tran, R. T., Wang, L., Zhang, C., Huang, M., Tang, W., Zhang, C., Zhang, Z., Jin, D., Banik, B., Brown, J. L., Xie, Z., Bai, X., & Yang, J. (2014). Synthesis and characterization of biomimetic citrate-based biodegradable composites. *Journal of Biomedical Materials Research Part A*, 102(8): 2521-2532.

- Tran, R. T., Yang, J., & Ameer, G. A. (2015). Citrate-Based Biomaterials and Their Applications in Regenerative Engineering. *Annual Review of Materials Research*(0).
- Tsuchida, S., Arai, Y., Takahashi, K. A., Kishida, T., Terauchi, R., Honjo, K., Nakagawa, S., Inoue, H., Ikoma, K., Ueshima, K., Matsuki, T., Mazda, O., & Kubo, T. (2014). HIF-1 α -induced HSP70 regulates anabolic responses in articular chondrocytes under hypoxic conditions. *Journal of Orthopaedic Research*, 32(8): 975-980.
- Urban, J. P. (1994). The chondrocyte: a cell under pressure. *Br J Rheumatol*, 33(10): 901-908.
- Vafaei, S., Borca-Tasciuc, T., Podowski, M. Z., Purkayastha, A., Ramanath, G., & Ajayan, P. M. (2006). Effect of nanoparticles on sessile droplet contact angle. *Nanotechnology*, 17(10): 2523-2527.
- Vahdati, A., & Wagner, D. R. (2013). Implant size and mechanical properties influence the failure of the adhesive bond between cartilage implants and native tissue in a finite element analysis. *J Biomech*, 46(9): 1554-1560.
- Van de Putte, K. A., & Urist, M. R. (1965). Osteogenesis in the interior of intramuscular implants of decalcified bone matrix. *Clin Orthop Relat Res*, 43: 257-270.
- Vandeputte, K. A., & Urist, M. R. (1965). EXPERIMENTAL MINERALIZATION OF COLLAGEN SPONGE AND DECALCIFIED BONE. *Clin Orthop Relat Res*, 40: 48-56.
- Varaprasad, K., Raghavendra, G. M., Jayaramudu, T., & Seo, J. (2016). Nano zinc oxide–sodium alginate antibacterial cellulose fibres. *Carbohydr Polym*, 135: 349-355.
- Vavken, P., & Samartzis, D. (2010). Effectiveness of autologous chondrocyte implantation in cartilage repair of the knee: a systematic review of controlled trials. *Osteoarthritis and Cartilage*, 18(6): 857-863.
- Villar-Suárez, V., Calles-Venal, I., Bravo, I. G., Fernández-Álvarez, J. G., Fernández-Caso, M., & Villar-Lacilla, J. M. (2004). Differential Behavior Between Isolated and Aggregated Rabbit Auricular Chondrocytes on Plastic Surfaces. *Journal of Biomedicine and Biotechnology*, 2004(2): 86-92.
- Vitale-Brovarone, C., Miola, M., Balagna, C., & Verné, E. (2008). 3D-glass–ceramic scaffolds with antibacterial properties for bone grafting. *Chemical Engineering Journal*, 137(1): 129-136.
- von Keudell, A., Canseco, J. A., & Gomoll, A. H. (2013). Deleterious Effects of Diluted Povidone–Iodine on Articular Cartilage. *The Journal of Arthroplasty*, 28(6): 918-921.

- von Keudell, A., Han, R., Bryant, T., & Minas, T. (2016). Autologous Chondrocyte Implantation to Isolated Patella Cartilage Defects Two-to 15-Year Follow-up. *Cartilage*: 1947603516654944.
- Wallace, R., Brown, A. P., Brydson, R., Wegner, K., & Milne, S. J. (2013). Synthesis of ZnO nanoparticles by flame spray pyrolysis and characterisation protocol. *Journal of Materials Science*, 48(18): 6393-6403.
- Wang, M., Sampson, E., Jin, H., Li, J., Ke, Q., Im, H.-J., & Chen, D. (2013). MMP13 is a critical target gene during the progression of osteoarthritis. *Arthritis Res Ther*, 15(1): R5.
- Wang, Y., Ameer, G. A., Sheppard, B. J., & Langer, R. (2002). A tough biodegradable elastomer. *Nat Biotechnol*, 20(6): 602-606.
- Webb, A. R., Yang, J., & Ameer, G. A. (2004). Biodegradable polyester elastomers in tissue engineering. *Expert opinion on biological therapy*, 4(6): 801-812.
- Wernike, E., Li, Z., Alini, M., & Grad, S. (2008). Effect of reduced oxygen tension and long-term mechanical stimulation on chondrocyte-polymer constructs. *Cell and tissue research*, 331(2): 473-483.
- Westmoreland, N., & Hoekstra, W. G. (1969). Pathological Defects in the Epiphyseal Cartilage of Zinc-deficient Chicks. *The Journal of Nutrition*, 98(1): 76-82.
- Widelitz, R. B., Jiang, T. X., Murray, B. A., & Chuong, C. M. (1993). Adhesion molecules in skeletogenesis: II. Neural cell adhesion molecules mediate precartilaginous mesenchymal condensations and enhance chondrogenesis. *J Cell Physiol*, 156(2): 399-411.
- Wirth, C. J., & Rudert, M. (1996). Techniques of cartilage growth enhancement: a review of the literature. *Arthroscopy: The Journal of Arthroscopic & Related Surgery*, 12(3): 300-308.
- Woodfield, T. B. F., Malda, J., de Wijn, J., Péters, F., Riesle, J., & van Blitterswijk, C. A. (2004). Design of porous scaffolds for cartilage tissue engineering using a three-dimensional fiber-deposition technique. *Biomaterials*, 25(18): 4149-4161.
- Wu, L., & Ding, J. (2004). In vitro degradation of three-dimensional porous poly(D,L-lactide-co-glycolide) scaffolds for tissue engineering. *Biomaterials*, 25(27): 5821-5830.
- Yang, J., Webb, A. R., & Ameer, G. A. (2004). Novel Citric Acid-Based Biodegradable Elastomers for Tissue Engineering. *Advanced Materials*, 16(6): 511-516.
- Yang, J., Webb, A. R., Pickerill, S. J., Hageman, G., & Ameer, G. A. (2006). Synthesis and evaluation of poly(diols citrate) biodegradable elastomers. *Biomaterials*, 27(9): 1889-1898.

- Yang, S., Zhang, Y., Yu, J., Zhen, Z., Huang, T., Tang, Q., Chu, P. K., Qi, L., & Lv, H. (2014). Antibacterial and mechanical properties of honeycomb ceramic materials incorporated with silver and zinc. *Materials & Design*, 59(0): 461-465.
- Yang, W., Both, S. K., van Osch, G., Wang, Y., Jansen, J., & Yang, F. (2014). Performance of different three-dimensional scaffolds for in vivo endochondral bone generation. *Bone Regeneration: From Intramembranous to Endochondral Pathway*: 81.
- Yeo, Q. Y., Lye, D. C., & Sathappan Sathappan Sathappan, F. O. (2015). Can Intra-Articular Therapies Prior to Total Knee Arthroplasty Increase the Risk of Periprosthetic Infection? *Med J Malaysia*, 70(1): 55.
- Yodmuang, S., Gadjanski, I., Chao, P.-h. G., & Vunjak-Novakovic, G. (2013). Transient hypoxia improves matrix properties in tissue engineered cartilage. *Journal of Orthopaedic Research*, 31(4): 544-553.
- Yodmuang, S., Marolt, D., Marcos-Campos, I., Gadjanski, I., & Vunjak-Novakovic, G. (2015). Synergistic Effects of Hypoxia and Morphogenetic Factors on Early Chondrogenic Commitment of Human Embryonic Stem Cells in Embryoid Body Culture. *Stem Cell Reviews and Reports*, 11(2): 228-241.
- Yodmuang, S., McNamara, S. L., Nover, A. B., Mandal, B. B., Agarwal, M., Kelly, T.-A. N., Chao, P.-h. G., Hung, C., Kaplan, D. L., & Vunjak-Novakovic, G. (2015). Silk microfiber-reinforced silk hydrogel composites for functional cartilage tissue repair. *Acta biomaterialia*, 11: 27-36.
- Yoo, H. S., Lee, E. A., Yoon, J. J., & Park, T. G. (2005). Hyaluronic acid modified biodegradable scaffolds for cartilage tissue engineering. *Biomaterials*, 26(14): 1925-1933.
- Yoon, Y.-M., Kim, S.-J., Oh, C.-D., Ju, J.-W., Song, W. K., Yoo, Y. J., Huh, T.-L., & Chun, J.-S. (2002). Maintenance of differentiated phenotype of articular chondrocytes by protein kinase C and extracellular signal-regulated protein kinase. *Journal of Biological Chemistry*, 277(10): 8412-8420.
- Zak, A. K., Majid, W. H. A., Darroudi, M., & Yousefi, R. (2011). Synthesis and characterization of ZnO nanoparticles prepared in gelatin media. *Materials Letters*, 65(1): 70-73.
- Zeimaran, E., Pourshahrestani, S., Pingguan-Murphy, B., Kadri, N., Rothan, H., Yusof, R., Towler, M., & Djordjevic, I. (2015). Fabrication and characterization of poly(octanediol citrate)/gallium-containing bioglass microcomposite scaffolds. *Journal of Materials Science*, 50(5): 2189-2201.
- Zhang, L., Jiang, Y., Ding, Y., Povey, M., & York, D. (2007). Investigation into the antibacterial behaviour of suspensions of ZnO nanoparticles (ZnO nanofluids). *Journal of Nanoparticle Research*, 9(3): 479-489.

- Zhang, L., Long, Y., Chen, Z., & Wan, M. (2004). The Effect of Hydrogen Bonding on Self-Assembled Polyaniline Nanostructures. *Advanced Functional Materials*, 14(7): 693-698.
- Zhang, R., & Ma, P. X. (1999). Poly(alpha-hydroxyl acids)/hydroxyapatite porous composites for bone-tissue engineering. I. Preparation and morphology. *J Biomed Mater Res*, 44(4): 446-455.
- Zhang, X. Q., Tang, H., Hoshi, R., De Laporte, L., Qiu, H., Xu, X., Shea, L. D., & Ameer, G. A. (2009). Sustained transgene expression via citric acid-based polyester elastomers. *Biomaterials*, 30(13): 2632-2641.
- Zhao, X.-Y., Sun, L., Wang, M.-Z., Sun, Z.-Y., & Xie, J. (2014). Review of crosslinked and non-crosslinked copolyesters for tissue engineering and drug delivery. *Polymer International*, 63(3): 393-401.
- Zhou, C., Zheng, H., Seol, D., Yu, Y., & Martin, J. A. (2014). Gene expression profiles reveal that chondrogenic progenitor cells and synovial cells are closely related. *Journal of Orthopaedic Research*, 32(8): 981-988.
- Zhou, S., Cui, Z., & Urban, J. P. G. (2004). Factors influencing the oxygen concentration gradient from the synovial surface of articular cartilage to the cartilage–bone interface: A modeling study. *Arthritis & Rheumatism*, 50(12): 3915-3924.
- Zhu, X., Cui, W., Li, X., & Jin, Y. (2008). Electrospun Fibrous Mats with High Porosity as Potential Scaffolds for Skin Tissue Engineering. *Biomacromolecules*, 9(7): 1795-1801.
- Zoli, A., Altomonte, L., Caricchio, R., Galossi, A., Mirone, L., Ruffini, M. P., & Magaró, M. (1998). Serum zinc and copper in active rheumatoid arthritis: Correlation with interleukin 1 β and tumour necrosis factor α . *Clinical Rheumatology*, 17(5): 378-382.
- Zuscik, M. J., Hilton, M. J., Zhang, X., Chen, D., & O'Keefe, R. J. (2008). Regulation of chondrogenesis and chondrocyte differentiation by stress. *The Journal of clinical investigation*, 118(2): 429.

List of Publications

Accepted Publications

1. Kompany, K., Mirza, E. H., Hosseini, S., Pinguan-Murphy, B., & Djordjevic, I. (2014). Polyoctanediol citrate–ZnO composite films: Preparation, characterization and release kinetics of nanoparticles from polymer matrix. *Materials Letters*, 126, 165-168.
2. Mirza, E. H., Pan-Pan, C., Wan Ibrahim, W. M. A. B., Djordjevic, I., & Pinguan-Murphy, B. (2015). Chondroprotective effect of zinc oxide nanoparticles in conjunction with hypoxia on bovine cartilage-matrix synthesis. *Journal of Biomedical Materials Research Part A*, 103(11), 3554 - 3563. doi: 10.1002/jbm.a.35495
3. Mirza, E. H., Wan Ibrahim, W. M. A. B., Pinguan-Murphy, B., & Djordjevic, I. (2015). Polyoctanediol Citrate-Zinc Oxide Nano-Composite Multifunctional Tissue Engineering Scaffolds with Anti-Bacterial Properties. *Digest Journal of Nanomaterials and Biostructures*, 10(2), 415-428.

Under Review

1. The effect of Zinc Oxide on Bovine Chondrocytes in three-dimensional culture, under mechanical loading in hypoxic conditions. Eraj Humayun Mirza, Wan Mohd Azhar bin Wan Ibrahim and Belinda Pinguan-Murphy (Applied Sciences)